Accuracy of Sampling Methods in Morphometric Studies of the Sural Nerve in Man

Zhao Cai

Department of Neurology, Royal Adelaide Hospital
Department of Medicine, University of Adelaide

and

Neuropathology Laboratory
Division of Tissue Pathology
Institute of Medical and Veterinary Science
Adelaide, South Australia

THESIS SUBMITTED TO THE UNIVERSITY OF ADELAIDE FOR THE MASTER DEGREE OF MEDICAL SCIENCE

1997

TABLE OF CONTENTS

Declaration

This work contains no material which has been accepted for the award of any other degree or diploma in any university or other tertiary institution and, to the best of my knowledge and belief, contains no material previously published or written by another person, except where due reference has been made in the text.

I give consent to this copy of my thesis, when deposited in the University Library, being available for loan and photocopying.

Zhao Cai

December, 1997

Acknowledgments

I express my warmest thanks to Professor Philip D. Thompson and Dr. Peter C. Blumbergs for their providing me with the opportunity to study in Adelaide, and for their tireless supervision throughout the year. Their continual interest and encouragement were truly inspirational and quite contagious and I extend my sincere gratitude for the stimulation and advice they have provided.

Special thanks to Dr. N. Fazzalari, Dr. P. Smith, Mr. I. Parkinson and Mr. J. Swift for their considerable support of my morphometric studies.

Thank you to Dr. Grace Scott and Dr. Barbara Koscyza for their kind help.

I also acknowledge Dr. Tom Kimber, Dr. Jason Warren for their helpful support.

I am greatly indebted to Kathy Cash for her invaluable time and patience in teaching me many valuable laboratory techniques and for assistance in the technical aspects of sural nerve biopsies.

I also acknowledge the entire Neuropathology Lab including Helen Wainwright, Jim Manavis, Penny Leaney and Bernice Gutschmidt for their support and assistance with matters technical. Thank you also to Margeret Elemer.

I fondly acknowledge the neverending support, friendship and positive energy of my room-mates, Corinna Van Den Heuvel, Nathan Judd, and Samantha Smith. It has been a privilege to work in such a pleasant environment with such terrific people.

I must thank my family and close friends for their valuable support over this year. Special thanks to my elder brother and sister-in-law for providing a solid foundation upon which I can stand. Thank you to my wife for her genuine support.

Abbreviations

Da	axonal diameter
DaSD	1 standard deviation of axonal diameter
Dm	thickness of the myelin sheath
Ds	fibre diameter or segmental diameter; total diameter of a segment of myelinated fibre on cross section
DsSD	1 standard deviation of fibre diameter
g-ratio	quotient axonal diameter/fibre diameter
K-S	Kolmogorov-Smirnov goodness-of-fit test
mDa	mean axonal diameter
mDs	mean fibre diameter
MF	myelinated fibre
MFD	myelinated fibre density; the number of myelinated fibres per unit area
MFDSD	1 standard deviation of myelinated fibre density
mMFD	mean myelinated fibre density
NMF	number of myelinated fibres
TFA	transverse fascicular area
TNMF	total number of myelinated fibres
TTFA	total transverse fascicular area
Wilcox.	Wilcoxon Rank-Sum test

Chapter 1: Summary

A variety of sampling methods are used in quantitative studies of myelinated sural nerve fibres, however there is no consensus as to which method is most accurate. This study compares whole fascicular sampling and systematic sampling of myelinated fibres with evaluation of the total myelinated nerve fibre population.

Two control and eighteen pathological sural nerves showing varying degrees of demyelination/remyelination and axonal degeneration were examined. The fascicular area, number of myelinated fibres, myelinated fibre density, fibre diameter and axonal diameter were measured in each fascicle of all the nerves using 1 micron plastic cross sections stained with osmium tetroxide. Each fascicle was divided into measuring frames, and the number and size of myelinated fibres in each frame (field) counted using the Quantimet 500MC computer-assisted image analysis system (Leica-Cambridge, UK). Frequency distributions of myelinated fibre density and size were calculated. The mean values and frequency distributions of fibre density, fibre diameter and axonal diameter of each sample were compared to the whole population by the Wilcoxon Rank-Sum test and Kolmogorov-Smirnov goodness-of-fit test.

Fascicular sampling of the two control sural nerves (14 fascicles) showed that 8 fascicles had different myelinated fibre density ($P<0.05$), and 8 fascicles had different fibre diameter and/or axonal diameter ($P<0.05$) when compared to the whole population. In the 18 pathological nerves there were 168 fascicles. When compared to the whole population, 61 fascicles had different myelinated fibre density ($P<0.05$), and 90 fascicles had different fibre diameter and/or axonal diameter ($P<0.05$). There was no relationship between the

myelinated fibre density of each fascicle and the fascicle diameter or area in either control and pathological sural nerves.

It is concluded that morphometric study of myelinated fibres of one or part of a fascicle cannot accurately represent the whole myelinated fibre population in the sural nerve. Systematic sampling of one third to half of the total transverse fascicular area in control and pathological sural nerves did not accurately depict the fibre diameter or axonal diameter of the whole myelinated fibre population. The myelinated fibre density derived from systematic sampling was more accurate than that derived from fascicular sampling. The spatial distribution of the number and size of myelinated fibres within and between fascicles is heterogeneous in the sural nerve. It is necessary to quantitate more than half the area of every fascicle to acquire accurate data about myelinated fibres that is representative of the whole myelinated fibre population.

CHAPTER 2: INTRODUCTION

2.1 GENERAL INTRODUCTION

Pathological studies of peripheral nerves are used widely in the investigation of peripheral nerve disorders (Dyck and Lofgren 1968, Dyck *et al.* 1993, Dyck *et al.* 1996, Thomas 1970a, Thomas *et al.* 1997), and other neurological diseases (King 1994). Quantitative studies of nerve fibre morphology are used to supplement the information obtained by qualitative histological assessment (Dyck *et al.* 1993). Morphometric studies are particularly useful in assessment of the myelinated nerve fibre population, aiding in the recognition of loss or alterations in size (atrophy or enlargement) of myelinated fibres (Dyck *et al.* 1993, Thomas *et al.* 1993). Pathological studies are usually undertaken on sural nerve, and occasionally on radial, anterior tibial, or superficial peroneal nerve biopsies. More morphometric data is available for the sural nerve than for any other nerve (Behse 1990, Dyck *et al.* 1993, Friede and Beuche 1985a, Ferriere *et al.* 1985, Jacobs and Love 1985, O'Sullivan and Swallow 1968, Thomas *et al.* 1993, Tohgi *et al.* 1977b).

The following discourse is a review of the basic anatomical features of peripheral nerves, and of quantitation of myelinated fibres in transverse sections of peripheral nerve, with special emphasis on the sural nerve.

2.2 ANATOMY OF PERIPHERAL NERVES

The peripheral nerves consist of nerve fibres, supporting cells, blood vessels and collagenous connective tissue, all enclosed within continuous connective tissue sheaths (Thomas *et al.* 1992, 1993, 1997).

2.2.1 NERVE FIBRES

i) Myelinated and Unmyelinated Fibres

Nerve fibres are usually categorized as myelinated and unmyelinated nerve fibres according to their relationship to Schwann cells (King *et al.* 1994, Ross *et al.* 1995, Thomas *et al.* 1992, Thomas *et al.* 1993, Thomas *et al.* 1997). Myelinated axons lie singly within a chain of Schwann cells, each of which contributes to the myelin sheath around the axon. Unmyelinated nerve fibres consist of one or more axons invaginated in a Schwann cell

Myelinated fibres (MF)

Normal myelinated nerve fibres range in size from 1-22μm in the adult and comprise 20%-25% of all nerve fibres. The thickness of myelin varies according to the fibre type and in the sural nerve range from 0.2-6.0μm. Myelinated fibres first appear in the fetal sural nerve at 21 weeks with numbers increasing to 25,000MF/mm^2 at 36 weeks (Shield *et al.* 1986).

In transverse section, a myelinated fibre shows two main concentric zones: an outer Schwann cell zone and an inner axon zone. The Schwann cell zone consists of three parts: the outer (abaxonal) and inner (adaxonal) cytoplasmic compartments and between them the myelin compartment (Thomas *et al.* 1993). The myelin compartment is usually used as a marker for recognition and quantitation of myelinated fibres. Most researchers agree that myelinated fibres are near cylindrical (Dyck *et al.* 1993, Thomas *et al.* 1993, Thomas *et al.* 1997). The transverse contour of myelinated axons is boomerang in shape in the region of Schwann cell nuclei, crenated in the paranode, and circular or near circular in the region between paranode and Schwann cell nucleus region (Karnes *et al.* 1977).

In longitudinal sections and teased fibres, the myelin sheath is segmented as each Schwann cell wraps only a short segment of axon. The junction where two adjacent Schwann cells meet is devoid of myelin sheath, and only covered by basal lamina. This site is called the

node of Ranvier (1875). The segments ensheathed by myelin are the internodes. The region adjacent to the node of Ranvier is called a paranode. A node of Ranvier and its two bordering paranodes constitute a Paranode-Node-Paranode (PNP) region.

Myelin sheath

The structure of the myelin sheath

On electron microscopy, the myelin sheath surrounding the axon is composed of multiple layers of Schwann cell membrane wrapped concentrically around the axon. During development, the process of myelination is initiated by an increase in the length of the mesaxon connecting the periaxonal space to the surface of the Schwann cell. The thin layer of cytoplasm between the pairs of membranes is extruded to produce the radially repeating structure of alternate dense and less dense lines characteristic of myelin in electron micrographs (Thomas *et al.* 1997). The dense lines are derived from the cytoplasmic aspect of each pair of membranes, and the less dense lines from the apposed outer surface of each pair of membranes. There is a small extracellular space separating the less dense line which appears as an intervening lucent gap in electron micrographs.

The thickness of the myelin sheath

The thickness of the myelin sheath is related to both the axonal diameter and the length of the internode. Larger myelinated fibres usually have a thicker myelin sheath (Beuche and Friede 1985, Thomas *et al.* 1993, Thomas *et al.* 1997).

Schmidt-Lanterman clefts

Myelin is interrupted at intervals by the presence of oblique clefts at an angle of about 9^0 to the long axis of the sheath termed the Schmidt-Lanterman clefts (Hall and Williams 1970). The Schmidt-Lanterman clefts provide a pathway for protoplasmic connections between the inner and outer compartments of the Schwann cell. The pathway may be the route by which metabolic materials pass between these two parts of the Schwann cell, and onwards to the axon (Ghabriel and Allt 1981, Hall and Williams 1971, Krishnan and Singer 1973, Mugnaini

et al. 1977). The Schmidt-Lanterman clefts may be involved in the longitudinal growth and metabolic maintenance of myelin (Celio 1976, Thomas *et al.* 1993). The clefts probably provide elasticity in the myelin sheaths, so that the internodes are able to elongate (Friede and Samorajski 1969). The number of Schmidt-Lanterman clefts increases with increasing fibre diameter and thickness of the myelin sheath. The number of Schmidt-Lanterman clefts is greater in regenerating and remyelinating fibres than in normal fibres (Behse *et al.* 1990, Buchthal *et al.* 1987, Friede and Samorajski 1967, Hiscoe 1947, Thomas *et al.* 1993, Thomas *et al.* 1997).

Biochemistry of myelin

Lipids and proteins are the two principal components of the myelin (Mezei 1993, Thomas *et al.* 1997). Sphingomyelin, cerebroside and sulfatide are the main components of myelin lipids in both central and peripheral nervous system (PNS). Peripheral nerve myelin contains a larger proportion of sphingomyelin and less cerebroside and sulfatide than central nerve myelin. In some animals the ganglioside LM1 (sialosyllactoneotetraosylceramide) is a characteristic component of myelin in the PNS (Mezei 1993, Thomas *et al.* 1997). The major components of myelin proteins in PNS are P_0, myelin basic proteins (MBPs), peripheral myelin protein 22 (PMP22), and myelin-associated glycoprotein (MAG). P_0 is an integral membrane protein of the myelin sheath of 28KD, which contributes 50% of the total myelin protein and consists of an extracellular immunoglobulin-like domain, a single transmembrane domain and an intracellular cytoplasmic domain. P_0 protein plays an important role in myelin compaction and stabilizing the major dense line of the myelin (Ding and Brunden 1994, D'Urso *et al.* 1990, Lemke and Axel 1985, Mezei 1987, Poduslo 1946). MBPs are a series of highly charged molecules of 12-20KD, located in the major dense line and account for 15-20% of the protein content of PNS myelin (Greenfield *et al.* 1982). PMP22 is a 22KD protein that is localized to compact myelin, and contributes 2-5% of PNS myelin protein. PMP22 is membrane associated and has a complex structure consisting of

four transmembrane domains, two extracellular loops, one intracellular loop and two short intracellular tails (Pareek *et al.* 1993, Thomas *et al.* 1997). MAG comprises approximately 0.1% of the total myelin proteins in the PNS, and is localized to the external and periaxonal layers of the myelin sheath, and non-compact myelin at the Schmidt-Lanterman clefts and paranodal terminal loop (Brady and Quarles 1988, Lai *et al.* 1987, Martini 1994). Two major functions have been postulated for MAG: maintenance of the structural integrity of periaxonal regions of the myelin sheath, particularly the 12 to 14nm Schwann cell-cytoplasmic periaxonal collar, and mediation of intercellular interactions (Martini and Schachner 1988, Trapp 1988, Trapp *et al.* 1984).

Internodes

Each internode consists of three main parts: a central stereotyped internodal (STIN) region and two paranodal regions. The paranodal regions of an internode are dilated, the distal one slightly more so than the proximal one, forming the paranodal bulbs. The length of the node of Ranvier is approximately 1μm. The internodal length ranges from 200μm to 1500μm. The STIN forms about 95% of the whole internodal length, and each of the paranodal regions form about 2-3% of the whole internodal length. The length of internode is related to axon diameter (Behse 1990, Friede *et al.* 1981, Thomas *et al.* 1993, Thomas *et al.* 1997, Williams and Kashef 1968, Williams and Wendell-Smith 1971).

Myelinated fibre axons

The axon consists of a relatively firm gelatinous cord of neuronal cytoplasm, enclosed by the axolemma. The axon is separated from the adaxonal Schwann cell membrane by a narrow extracellular gap, the periaxonal space or the adaxonal space (Thomas *et al.* 1993, Waxman 1985). The axoplasm consists of a fluid cytosol and formed elements. The formed elements consist of neurofilaments, microtubules (neurotubules), mitochondria, axoplasmic (endoplasmic) reticulum, dense bodies, multivesicular bodies, membranous cisterns and tubes, membranous bound vesicles, the cytoskeleton, and granular material.

Formed elements are most numerous and elaborate in the peranodal regions. The size of the axon is by conventiona measured in the STIN region and ranges of 1 to 20μm diameter in mammalian peripheral nerves. In normal human sural nerve, the myelinated axon diameter is usually less than 12μm (Bardosi *et al.* 1987, Friede and Beuche 1985a). The axon is smaller in the paranodal region than in the STIN region (Thomas *et al.* 1993, Thomas *et al.* 1997).

Unmyelinated fibres (UFs)

Unmyelinated axons are also enveloped by Schwann cells. One or more unmyelinated axons may be enclosed by a single invagination of the Schwann cell surface membrane (Thomas *et al.* 1993). Due to the small size, UFs are better studied by electron microscopy. In human sural nerves, the daimeter of unmyelinated axons ranges from 0.2 to 3.5μm with a unimodal frequency distribution of fibre diameter (Aguayo *et al.* 1971, Dyck and Lambert 1969, Dyck *et al.* 1971c, Jacobs and Love 1985, Ochoa and Mair 1969a, Ochoa and Mair 1969b, Weller 1967).

Schwann cell-axon relationships

All axons are enclosed by Schwann cells. As discussed in sections **2.6.7** and **2.6.8** (see pp37-40) the thickness of myelin sheaths and the number of myelin lamellae are linearly related to the axonal diameter (Behse 1990, Ferriere *et al.* 1985, Friede and Beuche 1985a, Friede and Beuche 1985b, Schröder *et al.* 1978). Close reciprocal relationships exist between Schwann cells and axons. Both send signals and trophic substances to promote mutual growth, survival and differentiation (Mezei 1993).

Axonal regulation of Schwann cell

Axonal factors regulate Schwann cell proliferation. During maturation and in adult life, all Schwann cells are related to axons in normal nerves (Aguayo *et al.* 1976). Schwann cells without axons are rarely found. Axons are mitogenic for Schwann cells in tissue culture (Wood and Bunge 1975), and axonal degeneration, demyelination and axonal regenerating sprouts can stimulate the proliferation of Schwann cells (Griffin *et al.* 1990, Pellegrino and Spencer 1985). Axonal contact is necessary for survival of Schwann cells. Schwann cells cannot survive after the axons are lost, and will atrophy and gradually disappear (Roytta and Salonen 1988, Thomas 1948, Weinberg and Spencer 1978). Some properties of axons, such as axonal diameter and specific axolemmal molecules, act as signals to stimulate myelination in development and axonal regeneration (Griffin *et al.* 1993, Voyvodic *et al.* 1989, Weinberg and Spencer 1976). After Schwann cells lose contact with axons, delayed re-contact with axons can result in Schwann cells that are less able to respond to axonal signals to form myelin (Li *et al.* 1997). Axonal contact is necessary for the Schwann cells to synthesize basal lamina (Bunge *et al.* 1980, 1982). The maintenance of the myelin sheath is influenced by the axon (Griffin *et al.* 1993), and the volume of the myelin is regulated by the axonal diameter and the internodal length (Friede and Bischhausen 1982, Smith *et al.* 1982).

Schwann cell influence on axons

Schwann cells exert a profound influence on axons. Close intercellular contact between myelinating Schwann cells and axons is necessary for maintaining axon size and function. Segmental demyelination of myelinated fibres may decrease local neurofilament phosphorylation, axonal diameter and axonal transport, and increase local neurofilament density (Dewaegh *et al.* 1992).

After nerve transection, Schwann cells commence synthesis of nerve growth factor (NGF) and nerve growth factor receptor (NGF-R) (Heumann *et al.* 1987, Johnson *et al.* 1988,

Taniuchi *et al.* 1988). Schwann cells undergo a series of mitoses and begin to divide (Clemence *et al.* 1989, Pellegrino *et al.* 1986, Pellegrino and Spencer 1985). The proliferating Schwann cells and the regenerating axonal sprouts enclosed by the old basal lamella form the Bands of Büngner through which axons regenerate and extend distally. The old basal lamina is very slowly broken down into fragments (Griffin *et al.* 1993), and during this period axons regenerate and induce the Schwann cell to form new basal lamina.

Cell adhesion molecules (CAMs) in axon-Schwann cell interactions

The intimate relationships between axons and Schwann cells are mediated by specific proteins, termed cell adhesion molecules (CAMs) (Griffin *et al.* 1993, Salzer 1995). These proteins are located on the apposed plasma membranes of the periaxonal space or in the extracellualr matrix (Burgoon *et al.* 1991, Martini and Schachner 1986, Mirsky *et al.* 1986, Trapp *et al.* 1989, Trapp and Quarles 1982). Abnormal CAMs can disrupt the structure of periaxonal space (Yu and Bunge 1975) and interfere with axon ensheathment, nerve fibre growth, and Schwann cell proliferation and differentiation (DeWaegh *et al.* 1992, Einheber *et al.* 1993, Letourneau *et al.* 1990, Letourneau *et al.* 1991, Marchionni *et al.* 1993, Sadoul *et al.* 1990, Sobue and Pleasure 1985). CAMs may be divided into three major families (Salzer 1995): (1) A family of proteins showing significant sequence and structural homology to the immunoglobulins, termed the immunoglobulin gene superfamily (Ig-CAM) (Salzer and Colman 1989, Williams and Barclay 1988); (2) A family of calcium-dependent adhesion molecules, the cadherins (Takeichi 1991); (3) A family of heterodimeric receptors, the integrins (Albelda and Buck 1990, Hynes 1992, Reichardt and Tomaselli 1991). Usually representative proteins of the three families are present in a single cell simultaneously (Rutishauser and Jessell 1988) and these are involved in the interactions between cells.

ii) Classification of Peripheral Nerve Fibres According to Their Diameter, Function and Conduction Velocity

According to diameter, peripheral nerve fibres can be divided into three groups: A, B and C (Boyd and Davey 1968, Ochoa 1976, Thomas *et al.* 1997, Weller and Cervós-Navarro 1978).

Group A

Nerve fibres in group A range from 1-20μm in diameter and include somatic afferent and efferent myelinated fibres. Group A fibres can be subdivided according to their size and function into afferent groups, I, II and III, and efferent groups, α, β and γ. In the adult cat Group I fibres range from 10 to 20μm in diameter, have a conduction velocity of 50-100m/s and carry impulses from muscle spindles and tendon organs. Group II fibres range from 5-15μm with conduction velocities of 20-70m/s and carry impulses from secondary sensory endings on the intrafusal muscle fibres within muscle spindles and cutaneous sensory fibres. Group III fibres range from 1-7μm in diameter, with conduction velocities of 5-30m/s, and include the fibres responsible for nociception and some aspects of cutaneous sensibility. The efferent α-fibres (diameter 9-20μm, conduction velocity 50-100m/s) are exclusively skeletomotor; the β-fibres (diameter 9-15μm, conduction velocity 50-85m/s) are both skeletomotor and fusimotor; and the γ-fibres (diameter 4.5-8.5μm, conduction velocity 20-40m/s) are exclusively fusimotor.

Group B

Nerve fibres in group B are generally less than 3μm in diameter and include myelinated preganglionic fibres of the autonomic nervous system which conduct impulses at 3-15m/s.

Group C

Fibres in group C have a range of 0.2-1.5μm in diameter and include postganglionic autonomic efferent fibres which conduct impulses at 0.3-1.6m/s.

2.2.2 CONNECTIVE TISSUES

The connective tissue components of a peripheral nerve can be divided into three parts: endoneurium, perineurium and epineurium (Ross *et al.* 1995,Thomas *et al.* 1992, Thomas *et al.* 1993, Thomas *et al.* 1997).

Endoneurium

The endoneurium is mainly composed of collagen fibrils and fibroblasts. The interstices between the fibres of peripheral nerves are packed with collagen fibrils in a mucopolysaccharide ground substance. The collagen fibrils connect the nerve fibres to form fibre bundles. Most of the fibrils run longitudinally in parallel with nerve fibres, and have relatively uniform diameter in the range 30-65nm. Fibroblasts are the principle cellular constituents of the endoneurium. On cross section, fibroblasts lie free between the endoneurial collagen. They are believed to be responsible for the production of the major part of the extracellular endoneurial connective tissue. Sometimes, a few mast cells and macrophages are also found in the endoneurium in control nerves. They are related to the immune system of the peripheral nervous system (Thomas *et al.* 1993, 1997).

Perineurium

The perineurium is the concentric connective tissue which surrounds the endoneurium and its contained nerve fibres to form nerve fascicles. Perineurium consists of layers of sheets of extremely flattened, squamous-like cells, inter-leaved by thin layers of fine collagen fibrils aligned parallel to the axis of the nerve, and serves as a semipermeable barrier. The collagen fibrils range from 40-80nm in diameter. Occasionally, elastic fibrils are present in the perineurium, and fibroblasts and mast cells are found in the outer layers. The thickness of the perineurium is related to the diameter of the contained nerve fascicle (Gamble and Eames 1964, Ross *et al.* 1995, Thomas 1963, Thomas and Jones 1967, Thomas *et al.* 1993, Thomas *et al.* 1997, Tohgi *et al.* 1977b).

Epineurium

The epineurium is the outermost layer of the peripheral nerve sheath, consisting of massed collagen fibrils with a longitudinal or shallow spiral orientation, interspersed with occasional elastic fibres, fibroblasts, mast cells, and the small arteries veins which supply and drain the endoneurial capillary plexus. The collagen fibrils in the epineurium bind the fascicles together and are larger than those in the endoneurium and perineurium, and range from 60 to 100nm in diameter. The epineurium can be divided into two parts: the outer layers of the epineurium (epifascicular epineurium) which form the outermost tissue of the nerve trunk, and the inner layers (interfascicular epineurium) which extend between the fascicles. The epineurium has a protective function in cushioning the fascicles against damage by compression (Ross *et al.* 1995, Thomas *et al.* 1993, Thomas *et al.* 1997).

2.2.3 VASCULATURE OF PERIPHERAL NERVES

Small arteries and veins ramify and branch in the epineurium. The arteries penetrate the perineurium at an oblique angle, then divide into capillaries to supply the endoneurial capillary plexus (Ross *et al.* 1995, Thomas *et al.* 1992, Thomas *et al.* 1993).

2.3 PATHOLOGICAL ANATOMY OF PERIPHERAL NERVES

Disorders of the peripheral nervous system can also be classified into those that primarily affect nerve fibres, and those that primarily affect connective tissues or blood vessels with secondary effects on the nerve fibres (Dyck *et al.* 1993, Thomas *et al.* 1997). According to the location of damage, peripheral neuropathies can be divided in to neuronopathies, axonopathies, and demyelinating neuropathies (Dyck *et al.* 1993, King *et al.* 1994, Ross *et al.* 1995, Thomas *et al.* 1997).

2.3.1 DEMYELINATING NEUROPATHIES

Segmental Demyelination

Demyelination in peripheral nerves usually displays segmental loss of myelin sheaths. Loss of myelin may be limited to the region of paranode (paranodal segmental demyelination) or of internode (internodal segmental demyelination) (Dyck *et al.* 1993). The mechanism of demyelination varies, depending on the disease process, and can be divided into primary and secondary types of demyelination (Dyck *et al.* 1993, King 1994, Thomas *et al.* 1992, Thomas *et al.* 1997).

Primary segmental demyelination

Primary segmental demyelination is caused by abnormalities affecting the Schwann cells or the myelin. The axon is relatively normal. Demyelination of this type affects internodes on a random basis (Dyck *et al.* 1993, King *et al.* 1994, Thomas *et al.* 1992, Thomas *et al.* 1997). The mechanism of demyelination varies according to the disease process. In the Guillain-Barré syndrome, myelin is actively stripped off axons by macrophages, whereas in experimental lysolecithin demyelination there is detergent related dissolution of myelin (Carpenter 1972, Lampert 1969, Prineas 1972, Wisniewski *et al.* 1969).

Secondary segmental demyelination

This type of demyelination is secondary to pathological change involving the axon (Dyck *et al.* 1993, King *et al.* 1994, Esiri 1995, Thomas *et al.* 1997). In secondary demyelination, individual fibres may have multiple consecutive internodes affected (clustered demyelination) while neighbouring fibres remain unaffected (Dyck *et al.* 1993, Esiri 1995, King 1994, Thomas *et al.* 1992, Thomas *et al.* 1997). Secondary demyelination was first recognized in studies of uraemic neuropathy (Dyck *et al.* 1971a, Thomas *et al.* 1971). Secondary demyelination may be due to axonal atrophy as shown in the animal model of permanent axotomy (Dyck *et al.* 1981a, Dyck *et al.* 1985). Enlargement of the axon can also cause secondary demyelination, such as in giant axonal neuropathy (Spencer and

Schaumburg 1977) and polyglucosan neuropathy (Yoshikawa *et al.* 1990). In some neuropathies, secondary demyelination is probably induced by axonal degeneration without obvious change of axonal caliber (Engelstad *et al.* 1997, Gabreëls-Festen *et al.* 1992, Llewelyn *et al.* 1991). In human neuropathies, the secondary type of segmental demyelination is more common than the primary type (Dyck *et al.* 1993).

Features that both primary and secondary demyelination have in common include (1) paranodal or internodal demyelination, (2) remyelination, (3) small myelin breakdown products, (4) intact axons, and (5) normal ultrastructural features of axons. In secondary demyelination: (1) the axons are smaller or larger than they should be considering myelin thickness, (2) demyelination and remyelination affects especially fibres showing severe axonal attenuation, and (3) demyelination and remyelination are clustered on individual fibres and not randomly distributed (Dyck *et al.* 1993, Thomas *et al.* 1997).

2.3.2 REMYELINATION

After demyelination, the Schwann cells divide and surround the denuded axon to form new myelin. The destroyed myelin sheaths are replaced by myelin supplied by two or more Schwann cells, rather than a single one as originally. Therefore, the resultant remyelinated segments are of varying length, but all usually shorter than the original unless only paranodal widening has occurred (Esiri 1995, King 1994, Thomas *et al.* 1992, Thomas *et al.* 1997). The remyelinating myelin sheath will be initially disproportionately thin compared with the relatively normal axonal calibre. Repeated attempts at remyelination in chronic demyelinating diseases eventually result in Schwann cell hyperplasia and the formation of concentric Schwann cell processes known as 'onion bulbs'. The affected nerve becomes enlarged or hypertrophic as a result (Dyck *et al.* 1993, Esiri 1995, King 1994, Thomas *et al.* 1992, Thomas *et al.* 1997).

2.3.3 AXONAL DEGENERATION

The primary pathological change is axonal damage. It can be divided into the following subgroups (Dyck *et al.* 1993, Thomas *et al.* 1997).

Wallerian degeneration

An axon cut off from its parent cell body undergoes Wallerian degeneration. The distal axon develops irregular swellings and break into fragments which eventually become absorbed. The myelin sheath around the axon is destroyed and digested.

'Dying-back' axonopathy

The axonal damage is manifest first and most severely at the distal ends, and degeneration typically progresses in a distal-proximal direction.

Axonal sequestration

During a slowly evolving axonal degeneration, prominent axon-Schwann cell networks develop. These are related to the ingrowth of processes from adaxonal Schwann cell which branch and enclose multiple small compartments of the axon.

2.3.4 AXONAL ATROPHY, MYELIN REMODELLING, AND SECONDARY DEMYELINATION

Axonal atrophy

Axonal atrophy is usually due to chronic neuronal injury (Dyck *et al.* 1993, Thomas *et al.* 1992), and has been identified in uraemic neuropathy (Dyck *et al.* 1971a, Thomas 1971), and Friedreich's ataxia (Dyck *et al.* 1971b). In Friedreich's ataxia progressive axonal atrophy may lead to axonal degeneration which occasionally can be demonstrated in sural nerve biopsies and appears to be a final event in this type of axonal atrophy (Dyck *et al.* 1971b). After axon section, the proximal axon retracts, and the axonal diameter decreases (atrophies) over the course of the ensuing 3 months. If satisfactory regeneration takes

place, the axonal diameter recovers; if regeneration does not occur, axonal atrophy progresses, and demyelination associated with such axonal atrophy occurs later (Aitken and Thomas 1962, Cragg and Thomas 1961, Dyck *et al.* 1981a, Dyck *et al.* 1985). Therefore, axonal atrophy may result in eventual axonal degeneration, and disappearance of the axon.

Myelin remodelling

The length of internodes remain relatively unchanged in healthy adults. When an axon atrophies, a type of myelin remodelling occurs, in which the myelin spiral length becomes smaller than it was, and the length of internodes increases (Dyck *et al.* 1981a).

Secondary demyelination due to axonal atrophy

Segmental demyelination is commonly associated with axonal loss (Dyck *et al.* 1971a, Dyck *et al.* 1971b, Hopkins 1970, Thomas *et al.* 1971). Dyck and co-workers (1971a, 1971b) found that in uraemic neuropathy and Friedreich's ataxia, which are thought to be primary neuronopathies, (1) axons were attenuated relative to the amount of myelin, (2) the axonal atrophy was accompanied by demyelination and remyelination, (3) fibres with segmental demyelination and/or remyelination had small axons relative to the thickness of myelin in noninvolved internodes. They speculated that progressive axonal atrophy leads sequentially to myelin wrinkling, nodal lengthening and myelin breakdown and remyelination. These cellular events of axonal atrophy and secondary segmental demyelination are illustrated in the figure 2.3-1, and have been shown to occur in an animal model of axonal atrophy and secondary segmental demyelination and remyelination (Dyck *et al.* 1981a, Dyck *et al.* 1985).

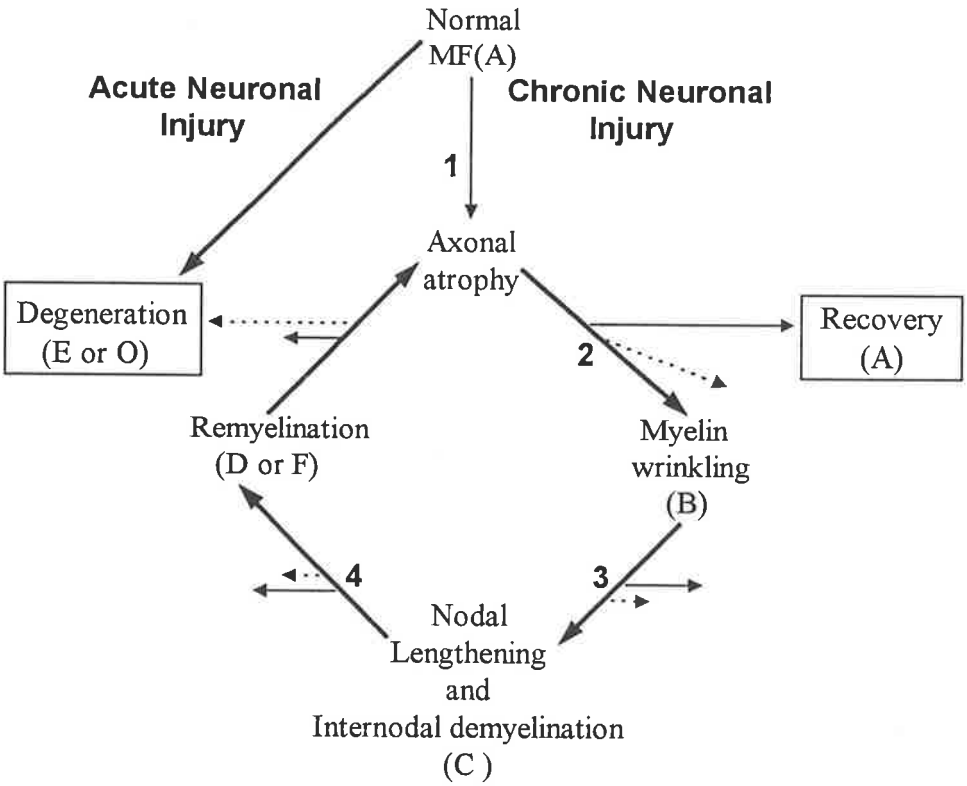

Figure 2.3-1: The proposed cellular events in chronic neuronal injury (cell body, axon, or both) of various types leading to **axonal atrophy** and **secondary segmental demyelination** (From: Dyck *et al.* 1981a)

2.3.5 AXONAL REGENERATION

Soon after focal nerve injury, regenerative events usually occur (Dyck *et al.* 1993, King 1994, Thomas *et al.* 1992, Thomas *et al.* 1997). Regenerating axonal sprouts arise from interrupted axons, grow along the Büngner bands, and may become myelinated when they attain an appropriate size. In cross sections, several myelinated sprouts from one fibre usually remain closely associated, forming a regenerative cluster.

2.3.6 MIXED PATTERNS OF AXONAL DEGENERATION AND SEGMENTAL DEMYELINATION

As mentioned above, axonal degeneration can induce segmental demyelination. Conversely, segmental demyelination also can induce axonal damage (Dyck *et al.* 1993). On the other hand, the causal factors may damage myelin and axon simultaneously, and segmental demyelination and axonal degeneration concur. Mixed patterns of segmental demyelination

and axonal degeneration are frequently found in sural nerve biopsies and it may be difficult to determine which is the primary injury.

2.4 SITE OF NERVE BIOPSY

As a general rule, nerve biopsies have been limited to distal nerves that meet six criteria: (1) the nerve is affected by the neuropathic process, (2) the nerve is constant in its location and is readily accessible, (3) either a pure sensory or a pure motor nerve, (4) long enough so that 6 to 10cm of the nerve can be removed, (5) located where entrapment and pressure are not common, and (6) suitable for conduction velocity studies in vitro (Dyck and Lofgren 1966, Dyck and Lofgren 1968, Thomas 1970a). The sural nerve meets all six criteria (Dyck *et al.* 1993). The sural nerve is commonly biopsied at the level of the lateral malleolus (Behse 1990, Cash and Blumbergs 1994, Dyck *et al.* 1993, King 1994, and Thomas 1970a) because distal to this level, it divides into smaller branches (Behse 1990, Dyck *et al.* 1993) and the pathological neuropathic changes are often more pronounced at this than at other levels (Dyck *et al.* 1971a). Biopsies of the sural nerve taken at the level of midcalf or lower midcalf can also conveniently be combined with muscle biopsy of the gastrocnemius (Gabreëls-Festen *et al.* 1992, Ferriere *et al.* 1985, Schröder *et al.* 1978, Younger *et al.* 1996). However, the disadvantages of this approach are that it may be more traumatic and associated with greater neurological deficits. Quantitative morphometric studies of normal control sural nerves have been performed on tissue obtained from necropsies, amputations or patients with minimal evidence of peripheral neuropathy (Behse 1990, Friede and Beuche 1985a, Ferriere *et al.* 1985, Jacobs *et al.* 1985, O'Sullivan and Swallow 1968, Schröder *et al.* 1978, Swallow 1966, Tohgi *et al.* 1977b). A fascicular biopsy is recommended by some in order to minimize resultant sensory deficit (Dyck and Lofgren 1966, King 1994, Thomas 1970a) and avoid the risk of 'trophic' ulceration (Llewelyn *et al.* 1991). However, Pollock

et al. (1983) followed patients for five or more years after both types of sural nerve biopsy and found no advantage of fascicular over whole-nerve removal with respect to sensory loss. They concluded that whole nerve biopsy was surgically simpler and allowed for more comprehensive evaluation. Since the shape of MFs is susceptible to change, it is necessary to obtain nerve tissue as soon as possible after death or amputation. The commonest artifacts, seen in nerves removed more than 12 hours after death, were swelling and electron-lucency of endothelial and Schwann cell cytoplasm (Jacobs and Love 1985). In our studies, sural nerves obtained 18-24 hours after death were found to be unsuitable for quantitation due to artifactual splitting of the myelin sheaths.

2.5 TISSUE PREPARATION

2.5.1 FIXATION AND EMBEDDING

During tissue preparation, shrinkage is unavoidable. The fascicular area and myelinated fibre shape are sensitive to fixative osmolarity (Dyck *et al.* 1980). Fixation by immersion in isosmolar 2.5% glutaraldehyde solution and isosmolar osmium tetroxide followed by embedding in epoxy resin are considered to be the most suitable for morphometric study as this minimizes the shrinkage of the fascicular area and the distortion of the shapes of MFs (Dyck *et al.* 1980). When fixed in formol-saline, formol-calcium, Flemming's solution, or hypersosmolar glutaraldehyde solution, the nerve fascicles undergo severe shrinkage, and the shapes of fascicles and nerve fibres are distorted severely (Behse 1990, Dyck *et al.* 1980, Thomas 1970a, Tohgi *et al.* 1977b). Paraffin-embedded sections are not suitable for quantitative studies due to extensive shrinkage, severe distortion of fibre shape, and the thickness of sections.

2.5.2 THICKNESS OF TRANSVERSE SECTION

For light microscopy (LM), 0.5-1.5 μm plastic (epoxy) embedded cross-sections are commonly used for morphological and morphometric study (Cash and Blumbergs 1994, Dyck *et al.* 1993, Schellens *et al.* 1993). Thick sections, such as 5μm (Behse 1990), may result in fibres with spuriously thick myelin sheaths and thin axons (Dyck *et al.* 1993). Thin sections (40-80nm) are often used for electron microscopy (EM) (Behse 1990, Dyck *et al.* 1993, Schellens *et al.* 1993).

2.5.3 STAINING

In order to enhance visualization of the myelin for LM, toluidine blue (methylene blue), paraphenylenediamine, thionin and acridine orange are commonly used to stain specimens (Behse 1990, Cash and Blumbergs 1994, Dyck and Lofgren 1968, Llewelyn *et al.* 1991, Schellens *et al.* 1993, Thomas 1970a, Vita *et al.*1992). For EM, thin sections are often double stained with uranyl acetate and lead citrate.

2.6 MORPHOMETRIC STUDIES

Information on sex and left-right side differences in human peripheral nerves is sparse. Schellens et al (1993) indicated that there was no significant sex dependency in the values for fascicular area, fibre density and number of MFs in control sural nerves at the level of midcalf. In phrenic nerves, the number of MFs and the size of MFs were similar on both sides (Bradley *et al.* 1987). O'Sullivan and Swallow (1968) found that there was no obvious difference between sexes in the mean values of myelinated fibre density in tibial and sural nerves. The most comprehensive data was obtained by Saxod *et al.* (1995) who measured the total number of myelinated fibres (TNMF), total transverse fascicular area (TTFA) and myelinated fibre density (MFD) of seventeen pairs of the sensory portion of the

superficial peroneal nerves (Table 2.6-1). Fascicular area and total number of myelinated fibres are greater on the right side, but the left and right MFD does not differ significantly.

Table 2.6-1: Left and Right Comparison of TNMF, TTFA and MFD

sensory portion of peroneal nerve (n=17)	left (mean±SD)	right (mean±SD)	P value (*t* test) (paired two samples)
TNMF (#/nerve)	1312±719*	1856±897*	0.027*
TTFA (mm^2)	0.166±0.094*	0.258±0.159*	0.014*
MFD (#/mm^2)	8175±2058*	7715±1691*	0.303*

Abbreviations for table 2.6-1

*: data calculated from the raw data in the literature (Saxod *et al.* 1985)

TNMF: total number of myelinated fibres per nerve

TTFA: total transverse fascicular area per nerve

MFD: myelinated fibre density (the number of myelinated fibres per square millimeter)

SD: 1 standard deviation

2.6.1 THE NUMBER AND SIZE OF FASCICLES

The number of fascicles ranges between 3 and 18 per sural nerve, and is not related to age and gender (Behse 1990, Dyck *et al.* 1984, Dyck *et al.* 1993, Schellens *et al.* 1993). At the level of the lateral malleolus, the sural nerve usually contains 5-10 fascicles (Jacobs and Love 1985). O'Sullivan and Swallow (1968) found 230 fascicles in 27 control sural nerves. Among the 230 fascicles, 13 had a diameter less than 100μm, and the average diameter of the other 217 fascicles was 0.333±0.11mm (mean±SD), ranging from 0.056 to 0.742mm. Jacobs and Love found that the smallest fascicle in 27 control nerves was 300μm^2 in cross-sectional area, and the largest varied from 0.03-0.06mm^2 during the first few months of life to 0.06-0.19mm^2 in adults. Walsh (1971) found that the fascicular area of individual fascicles ranged from 0.02 to 0.46mm^2 in 3 control sural nerves. Swallow (1966) found that age had no effect on either the number or size of the constituent fascicles of the anterior tibial nerves.

2.6.2 TOTAL TRANSVERSE FASCICULAR AREA (TTFA)

Behse (1990) measured 10 control sural nerves at the level of the ankle and found that TTFA, distributed in 7-18 fascicles, ranged from 0.65-1.26mm^2. Schellens *et al.* (1993) found that at the level of midcalf the mean TTFA was 0.73mm^2 in sural nerves with 3-4 fascicles, and 0.74mm^2 in nerves with 5-10 fascicles. Schellens *et al.* (1993) found that TTFA increased with age in sural nerves, whereas Swallow (1966) found that the TTFA of anterior tibial nerves was not related to age. Fascicular area is sensitive to fixative osomolarity. This was displayed by Dyck *et al.* (1980) who found a 10% shrinkage in fascicular area in sural nerves that had been immersion fixed in isosmolar glutaraldehyde solution and osmium tetroxide, as compared to cryostat sections. These researchers also showed a 43% shrinkage in area following fixation by hyperosmolar glutaraldehyde and osmium. Fascicular area may increase in chronic relapsing polyneuritis (Prineas and McLeod 1976). TTFA is greatly increased in hypertrophic neuropathies such as hereditary motor and sensory neuropathy (type I and III), Refsum's disease and chronic inflammatory demyelinating polyneuropathy (Dyck and Lambert 1966, Dyck *et al.* 1993, Gabreëls *et al.* 1995, Thomas *et al.* 1997, Webster *et al.* 1967). Hypertrophic changes have been produced in a variety of experimental demyelinating neuropathies and axonal neuropathies, including lead neuropathy, recurrent compression and experimental allergic neuritis (Dyck 1969, Lampert and Schochet 1968, Nichols *et al.* 1968, Pollard *et al.* 1975, Thomas 1970b) (Table 2.6-2).

Table 2.6-2: changes of TTFA in some diseases

Author(s)	Disease	Age	Nerve	NN	TTFA(mm^2)	Control
Behse *et al.* 1972	HNLPP	8-44	S	6	1.16±0.36*	0.9±0.3
Dyck *et al.* (1986)	diabetic neuropathy	19-73	T	14	6.5±3.1	6.4±2.9
			S	14	0.8±0.2	1.1±0.7
			P	14	3.5±1.3	3.2±1.3
Gabreëls-Festen et al 1995	CMT1A with 17p11.2-p12 duplication	3-26	S	11	217%±88% of age related controls*	0.61 (2-5ys) 0.72 (6-10ys)
	CMT1A with PMP22 point mutation	4-17	S	3	433%±35% of age related controls*	0.87 (11-30ys)
Webster et al 1967	CNP with onion bulbs	9-65	S	5	1.1-2.9	1.0-1.2 (n=2)
Ohnishi *et al.* 1977	ELN (3 months)		P (m)		0.212±0.023	0.144±0.017
			P (k)		0.190±0.055	0.132±0.008
			S (m)		0.056±0.016	0.049±0.009
			S (K)		0.047±0.004	0.037±0.005
	ELN (6 months)		P (m)		0.345±0.184	0.154±0.013
			P (k)		0.381±0.213	0.153±0.023
			S (m)		0.081±0.016	0.046±0.011
			S (K)		0.055±0.014	0.033±0.004
Nichols *et al.* 1968	EHN		P		0.14	0.23

Abbreviations for table 2.6-2

HNLPP: hereditary neuropathy with liability to pressure palsies

EHN: experimental hypertrophic neuropathy in Sprague-Dawley rats 3 days after nerve crush

CMT1A: Charcot-Marie-Tooth disease type 1a (HMSN1a)

ELN: experimental lead neuropathy in Sprague-Dawley rats

S: sural nerve; (m)= at the level of midcalf; (k)= at the level of knee

P: peroneal nerve; (m)= at the level of midcalf; (k)= at the level of knee

T: tibial nerve

NN: number of nerves

* calculated from the raw data in the literature

2.6.3 TOTAL NUMBER OF MYELINATED FIBRES (TNMF)

At the level of the lateral malleolus the total number of MFs per sural nerve is usually in the range of 4500–12000 in adult under 65 years (Behse 1990, Jacobs and Love 1985, Thomas and Ochoa 1984). This may decrease to about 3300 after the age of 65 (Jacobs and Love 1985), or less in very old age (Behse 1990). According to many researchers (Behse 1990,

Jacobs and Love 1985, Tohgi *et al.* 1977b), the number of MFs in the sural nerve decreases with age after 30 years. But, Schellens *et al.* (1993) reported that the total number of MFs, with a range of 3630 to 16300 at midcalf level from 0 to 69 years, did not correlate with age, and that the relative composition of large and small fibres remained constant over age. In childhood, the range of the total number of MFs is 3360 to 6920 at ankle level up to 10 years (Jacobs and Love 1985), or 2300 to 8500 at midcalf level up to 17 years (Ferriere *et al.* 1985). In an amputated control leg, Behse (1990) found that at ankle level the sural nerve contained about 40% less MFs than did its two uniting branches at the calf 20cm proximal to the ankle.

Loss of myelinated fibres is one of the most prominent changes in many peripheral nerve disorders, such as amyotrophic lateral sclerosis (Atsumi and Miyatake 1987, Bradley *et al.* 1983) and diabetic neuropathy (Dyck *et al.* 1986a, Dyck *et al.* 1986b, Llewelyn *et al.* 1991). If loss of MFs is more severe in distal than in proximal regions, it probably indicates a "dying back" change (Dyck *et al.* 1971a, Dyck *et al.* 1993).

2.6.4 MYELINATED FIBRE DENSITY (MFD)

Estimations of MFD vary considerably between researchers because endoneurial area shrinkage may be different due to different methods of tissue preparation (Behse 1990, Dyck *et al.* 1980, Tohgi *et al.* 1977b). Severe shrinkage of fascicular area caused by hyperosmolar fixative or paraffin embedding gives rise to an increased MFD (Dyck *et al.* 1980, Tohgi *et al.* 1977b). Table 2.6-3 displays the changes in MFD produced by different methods of tissue preparation in control sural nerves.

Myelinated fibres appear in fetal sural nerves at 15-16 weeks, rising to 25000/mm^2 at 36 weeks (Shield *et al.* 1986). MFD of sural nerves is greatest during the first few years of

life, thereafter decreasing with age (Dyck *et al.* 1986b, Jacobs and Love 1985, Ferriere *et al.* 1985, O'Sullivan and Swallow 1968, Schellens *et al.* 1993, Tohgi *et al.* 1977b). Based on fibre diameter distribution, Tohgi *et al.* (1977b) calculated MFDs of small and large fibres respectively, and found: (a) the average small fibre density decreased rapidly from the age of 1 week (26300mm^2) to the second decade (9560/mm^2) and continued to decrease with age, reaching an average of 9730/mm^2 for the eighth decade, 74% of that for the second decade; (b) large fibre density increased from 3 months of age, reached the maximum average in the third decade (6480/mm^2), and thereafter decreased with age, reaching an average of 3480/mm^2 for the ninth decade, 54% of that of the third decade. Age-related decrease of MFD is also found in laboratory and domestic animals (Griffiths and Duncan 1988). In contrast, Saxod *et al.* (1985) did not find a correlation between MFD and age in human superficial peroneal nerve. Dyck *et al.* (1982) measured MFD in the sural nerve both at the midcalf and ankle level, and found that MFD decreased from proximal to distal region.

Table 2.6-3: Method of tissue preparation and corresponding MFD in control sural nerves

Author(s)	Fixative(s)	Embed.	Age(yr)	NN	MFD
Behse *et al.* 1972	2%Glu+1%OT	Epon	15-59	6	7000±1600 (mean±SD)
Dyck *et al.* 1971	10%Formalin	Paraffin	7-10	3	11242-14373
			14-66	6	7157-10450
Ferriere *et al.* 1985*	2.5%Glu	Epon 812	0-17	9	10300±3700 (mean±SD)
Gabreëls-Festen *et al.* 1992	2%Glu+2%OT	Epon 812	2-5	5	14170 (mean)
			6-10	11	13180 (mean)
			11-20	5	10530 (mean)
			21-30	7	9640 (mean)
			31-50	5	9760 (mean)
Hamida *et al.* 1987	Glu#+2%OT	Epon	9-18	3	11836±7452 (mean±SD)
			22-28	4	13351±3015 (mean±SD)
			32-56	8	10257±1398 (mean±SD)
Jacobs and Love 1985	3%Glu+1%OT	Araldite	0-10	13	9400-25890
			21-69	14	7460-10190
Llewelyn *et al.* 1991**	3%Glu+1%OT	Araldite	28-55	5	7172-11571
Matsummuro *et al.* 1994	3%Glu	Epon		6	8353±1476 (mean±SD)
O'Sullivan and Swallow 1968	Flemming	Paraffin	17-39	9	6130±1110 (mean±SD)
			40-59	10	5780±900 (mean±SD)
			60-80	8	4780±1080 (mean±SD)
Schellens *et al.* 1993*		Epon	0-69	51	6000-22000
Tohgi *et al.* 1977b		Paraffin	11-20	4	15750±4340 (mean±SD)
			21-30	12	15390±2920 (mean±SD)
			31-40	12	12100±2830 (mean±SD)
			41-50	15	13300±3160 (mean±SD)
			51-60	7	11170±1350 (mean±SD)
			61-70	11	11200±4700 (mean±SD)
			71-80	7	9730±4040 (mean±SD)
			81-88	4	12500±2380 (mean±SD)

Abbreviations for table 2.6-3: * midcalf level; ** fascicular biopsy; # mixture glutaraldehyde-paraformaldehyde in a phosphate buffer; Glu= glutaraldehyde; OT= osmium tetroxide; Flemming= Flemming's solution; Embed.= embedding medium; NN= number of nerves.

2.6.5 FIBRE DIAMETER (Ds)

On cross section, the outer diameter of myelin usually serves as the fibre diameter (segmental diameter of the total fibre on cross section), the inner diameter of myelin sheath usually serves as axonal diameter, as shown in figure 2.6-1. Dm is the thickness of myelin sheath.

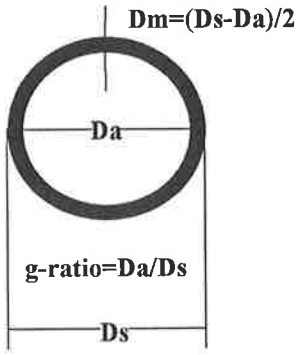

Figure 2.6-1: diagram of a MF on transverse section showing Ds, Da, Dm and g-ratio

Myelinated nerve fibres in human peripheral nerve trunks range in diameter between 1 and 22μm (Thomas *et al.* 1993). In control sural nerves, fibre diameters usually range from 1 to 18 μm. In the foetus and at birth, the frequency distribution of Ds is unimodal (Behse 1990, Ferriere *et al.* 1985, Friede and Beuche 1985a, Schröder *et al.* 1975, Shield *et al.* 1986, Tohgi *et al.* 1977b,). It becomes bimodal by the 3rd month (Ferriere *et al.* 1985), 7th month (Tohgi *et al.* 1977b), or 6th–12th month (Friede and Beuche 1985a), and reaches adult values by 2.5–3 (Tohgi *et al.* 1977b), 5 (Gutrecht and Dyck 1970), 8 years of age (Behse 1990) or 14 years of age (Schröder *et al.* 1975). In adulthood it has a bimodal distribution with the first or lower peak corresponding to type A-III fibres and the second or upper peak corresponding to type A-II fibres (Auer 1994, Behse 1990, Dyck *et al.* 1982, Ferriere *et al.* 1985, Jacobs and Love 1985, Schellens *et al.* 1993, O'Sullivan and Swallow 1968). Table 2.6-4 shows the range of Ds and positions of diameter peaks in adulthood according to different authors. Different methods of tissue processing, primary parameter measurement, and secondary parameter calculation probably account for the wide variance in results reported by different investigators.

Table 2.6-4: Range of fibre diameter and positions of two peaks

Author(s)	Embedding Medium	Range of Ds (μm)	lower peak (μm)	upper peak (μm)
Auer 1994	Epon	1-18	3-4	9-10
Behse 1990	Epon	1-18	5-6	13-14
Dyck et al. 1982	Epon	1-14	3-5	9-12
Ferriere et al. 1985*	Epon	1-14	2-3	8-9
Friede and Beuche 1985	Araldite	1-14	3-4	6-9
Jacobs and Love 1985	Araldite	1-12	3-5	9-11
O'Sullivan and Swallow 1968	Paraffin	1-16	3-6	9-13
Schellens et al. 1993*	Epon	1-17	3-6	9-14

*midcalf level

The composition of MFs is different between different species, different nerves, and even between different levels of the same nerve (Dyck *et al.* 1982). However, the positions of the two peaks of Ds of sural nerve at ankle and midcalf level are similar (Behse 1990, Dyck *et al.* 1982). It is inferred that the myelinated fibre diameter in sural nerve attenuates 1-2 μm from the level of ankle to the border of the foot because the distal sural nerve conduction velocity from the lateral border of the foot to the lateral malleolus is slower than at midcalf (Behse 1990). The examination of the MF size spectrum can demonstrate selective loss of particular groups of nerve fibres in pathological conditions.

With advancing age, the sural nerve loses its fibres, with the loss being predominantly in large size fibres (O'Sullivan and Swallow 1968, Tohgi *et al.* 1977b). This phenomenon is also found in anterior tibial and radial nerves (O'Sullivan and Swallow 1968, Swallow 1966). In peripheral neuropathies, the loss of MFs can be divided into three types according to fibre size: (1) selective loss of large fibres, (2) selective loss of small fibres, (3) loss of both large and small fibres, or general loss of MFs. General loss of MFs can be found in many peripheral neuropathies or neurological disorders, such as diabetic autonomic

and painful sensory neuropathy (Llewelyn *et al.* 1991). Nerves from patients with motor neuron disease (Atsumi and Miyatake 1987, Bradley *et al.* 1983, Hamida *et al.* 1987), Friedreich's ataxia (Dyck *et al.* 1971b), experimental organophosphate neuropathy (Cavanagh 1964), and ischaemic neuropathy (Garven *et al.* 1962) show selective loss of large fibres. Selective loss of small fibres occurs in amyloid neuropathy (Dyck and Lambert 1969), Fabry's disease (Kocen and Thomas 1970a) and painful diabetic neuropathy (Brown *et al.* 1976, Said *et al.* 1983). In amyotrophic lateral sclerosis, the total number of large fibres and mean fibre diameter of total MFs in hypoglossal nerves were both reduced, corresponding to the grading of the muscular atrophy of the tongue. Also the duration of bulbar symptoms was inversely proportional to the large myelinated fibre densities (Atsumi and Miyatake 1987). Depletion of a class of MFs may be associated with selective sensory loss in peripheral neuropathy (Dyck *et al.* 1971b). The different types of diabetic neuropathy may show selective loss of large fibres, small fibres, or general loss of both large and small fibres (Archer *et al.* 1983, Behse *et al.* 1977, Brown *et al.* 1976, Dyck et al 1986b, Llewelyn *et al.* 1991, Said *et al.* 1983). But in the studies of diabetic symmetrical distal polyneuropathy, Dyck *et al.* (1986a, 1986b) concluded that selective loss of small or large MFs are probably extremes of normal distribution and not different disorders. Selective loss of large MFs is more common than selective loss of small MFs.

2.6.6 AXONAL DIAMETER (Da)

Axonal diameter is determined by genetic and developmental factors, including the synthesis, assembly, and transport of neurofilament proteins (Hoffman and Griffin 1993, Ochs and Brimijoin 1993). In control human sural nerves, it ranges from 0.5μm to 7.5μm (Behse 1990), from 1μm to 9μm (Jacobs and Love 1985), from 1μm to 12μm (Bardosi *et al.* 1987, Friede and Beuche 1985a). In the adult, its frequency distribution is also bimodal, corresponding roughly to that of Ds (Behse 1990, Friede and Beuche 1985a, Tohgi *et al.*

1977b). Axonal diameter may be altered by various neurologic disorders and neuropathies (Dyck *et al.* 1993). It also can be decreased acutely by a shift of fluid, as in hyperglycemic hyperosmolar coma or fixation in hyperosmolar fixative (Dyck *et al.* 1980, Dyck *et al.* 1981b). Table 2.6-4 shows the changes of TNMF, MFD, and MF composition in some neuropathies.

Table 2.6-5: Changes of TNMF, MFD, and MF composition in diseased nerves

Author(s)	Disease	Age	Nerve	NN	TNMF	Control	MFD(/mm^2)	Control	Small Fibres	Control
Behse *et al.* 1972	HNLLP	8-44	S	6	7926±4718	6200±1090	5700-10600	7000±1600	77.1%-93.4%[a](Ds<8μm)	71.3[a] (mean)
Atsumi and Miyatake 1987	ALS	28-68	XII	13	5206±1340	9920±448			34.7%±11.9%[a,b](Ds<4.5μm)	16.4%±4.5%[a,b](mean±SD)
Bradley *et al.* 1983	ALS	44-73	Phr(1)	11	2388±919	2993±475			1778±703 (Ds<8μm)	1218±383
			Phr(2)	11	2303±551	3141±143			1682±347	1491±479
			Phr(3)	11	2113±589	3339±365			1541±448	1370±483
			Phr(4)	11	2026±1023	3179±330			1526±811	1347±256
			S(B)	6	5868±1730				4479±1201	
			S(P)	4	5834±741	8279±2083			4143±466	6087±1707
Hamida *et al.* 1987	Classical ALS	35-57	S	9	7243±1102	9920±488				
	Juvenile ALS	10-30	S	7	10686±1306	10257±1398				
	Early onset ALS	21-39	S	4	7941±1259	13351±3015				
Bardosi *et al.* 1987	PNP in IMLD	2-30m	S	4			5700-8100	8500(n=1)	70%[a] (mean, Da<5μm)	72%[a] (mean)
	PNP in JMLD	3-10	S	2			7100-10000	9300(n=1)	72%[a] (mean)	68%[a] (mean)
	PNP in AMLD	adult	S	3			2700-6200	7400(n=1)	67%[a] (mean)	71%[a] (mean)
Thomas *et al.* 1971	Uraemic NP	19-48	S	6			3812±2283[a]	6130±1110		
Gabreëls-Festen *et al.* 1995	CMT1A(1)	3-26	S	12			31%±18%[b,c]	*		
	CMT1A(1)	4-30	S	4			17%±2%[b,c]	*		

Continued in next page

Author(s)	Disease	Age	Nerve	NN	TNMF	Control	MFD(/mm^2)	Control	Small Fibres	Control
Dyck *et al.* 1986a	NID without PVD	23-78	S	3	7%-53%[b]	10000±5000	39%[b](mean)	11000±3000	81%[b] (mean, Ds<6.5μm)	6000(mean)
	NID with PVD			3	6%-14%[b]		14%[b](mean)		97%[b] (mean)	
	IDDM without PVD			1	13%[b]		18%[b]		94%[b]	
	IDDM with PVD			3	7-28%[b]		22%[b](mean)		95%[b] (mean)	
Llewelyn *et al.* 1991	IDD with SAN(1)	23-39	S	10			737-3135	7172-11571	49%-100%[a] (Ds<7μm)	53%-67%[a]
	IDD with SAN(2)	8-32	S	4			1073-3242		49%-97%[a]	
	IDD with PSN	18-54	S	5			2684-6920		56%-76%[a]	
Nukada *et al.* 1983	HMSN type I	13-51	S	10			1767(mean)	8853(mean)	1319 (mean, <6.5μm)	5546(mean, /mm^2)
Matsummuro *et al.* 1994	CIDP	15-76	S	9			5357±1414[b]	8353±1476	2767±1416[b](<5.5μm)	3720±652(/mm^2)
Thomas *et al.* 1987	CDPN with MCNSD	19-44	S	6			2556±2062[b]	7500-10000	1907±1584[b] (/mm^2, <7μm)	
Prineas and Mcleod 1976	CRP	3-68	S	21			4405±1605[B]	4570±890		
							(1885-7931)	(3810-6420)		

For abbreviations see next page.

Abbreviations for table 2.6-5

[a] percentage of total number

[b] calculated from the raw data in the literature

[c] percentage of age-related control

* mean of age-related controls: 14170 (2-5years), 13180 (6-10years), 10530 (11-20years), 9640 (21-30years)

NN: number of nerves

HNLLP: hereditary neuropathy with liability to pressure palsies

ALS: amyotrophic lateral sclerosis

PNP in IMLD: peripheral neuropathy in late infantile metachromatic leucodystrophy

PNP in JMLD: peripheral neuropathy in juvenile metachromatic leucodystrophy

PNP in AMLD: peripheral neuropathy in adult metachromatic leucodystrophy

Uremic NP: uremic neuropathy

CMT1A(1): Charcot-Marie-Tooth disease type 1A (HMSN type Ia) with 17p11.2-p12 duplication

CMA1A(2): Charcot-Marie-Tooth disease type1A (HMSN type Ia) with PMP22 point mutation

HMSN type I: hereditary motor and sensory neuropathy type I

IDD with SAN(1): insulin-dependent diabetes with severe autonomic neuropathy and an accompany painless sensory neuropathy

IDD with SAN(2): insulin-dependent diabetes with severe autonomic neuropathy and a chronic painful sensory neuropathy

IDD with PSN: insulin-dependent diabetes with chronic or acute painful sensory neuropathy and no autonomic neuropathy

IDD with PVD: insulin-dependent diabetic neuropathy with peripheral vascular disease

IDD without PVD: insulin-dependent diabetic neuropathy without peripheral vascular disease

NID with PVD: non-insulin-dependent diabetic neuropathy with peripheral vascular disease

NID without PVD: non-insulin-dependent diabetic neuropathy without peripheral vascular disease

S: sural nerve

XII: hypoglossal nerve

Phre(1) to Phre(4): four levels of phrenic nerve from proximal to distal

CIDP: chronic inflammatory demyelinating polyneuropathy

CDPN with MCNSD: chronic demyelinating peripheral neuropathy associated with multifocal central nervous system demyelination

2.6.7 THICKNESS OF MYELIN SHEATH (Dm)

Dm ranges from 0.2 to 6 μm (Behse 1990, Jacobs and Love 1985, Ferriere *et al.* 1985) in control sural nerves. Its distribution is bimodal in adults (Behse 1990). In the foetus, the thickness of the myelin sheath increases gradually with the growth of the myelinated fibres (Shield *et al.* 1986). From birth, Dm increases with advancing age till it reaches the adult value at the age of 14 years (Schröder *et al.* 1978).

The thickness of myelin sheaths has attracted a great deal of attention. There is a positive linear relationship between myelin sheath thickness and fibre size (Ferriere *et al.* 1985, Jacobs and Love 1985, King 1994, Schröder *et al.* 1978). This relationship may be between Dm and Ds (Jacobs and Love 1985), or between Dm and Da (Ferriere *et al.* 1985, King 1994, Schröder *et al.* 1978). Behse (1990) and Friede and Beuche (1985) showed that the relationship between Dm and Da is different in type-III and type-II fibres. The relationship between Dm and fibre calibre (Ds or Da) changed with age (Ferriere *et al.* 1985, Jacobs and Love 1985, Schröder *et al.* 1978). In the development the axon diameter increases till 5 years of age whereas the thickness of myelin sheath increases continuously but more slowly than that of the axon until 14 years of age. This asynchronous development of myelin and axon accounts for the change of the relationship between Dm and Ds or Da with ageing (Schröder *et al.* 1978).

Ultrastructural morphometric studies support a positive relationship between myelin thickness and the size of axon (Arbuthnott *et al.* 1980, Boyd and Kalu 1973, Friede 1972, Friede and Samorajski 1967). The myelin sheath consists of a number of myelin lamellae with a radial periodicity of 12–17nm in fixed nerve, and 17–18nm in unfixed nerve (King 1994, Thomas *et al.* 1993). The number of myelin lamellae is linearly related to axonal circumference (Arbuthnott *et al.* 1980, Boyd and Kalu 1973, Dyck *et al.* 1971a, Dyck *et al.*

1971c, Friede and Samorajski 1967). In the mouse, there was one lamella for every 0.24μm increase in axon circumference (Friede and Samorajski 1967). In the cat, Arbuthnott *et al.* (1980) found that the equation m=0.103s–0.26 (m: the thickness of the myelin sheath; s: axonal perimeter) was an accurate representation of group II, III and γ fibre. In the development of peripheral nerves, retardation of axon growth retarded myelin sheath growth, and acceleration of axon growth accelerated myelin sheath growth (Friede 1972).

Dyck and co-workers found (1971a, 1971b) that around the atrophic axons in uraemic and Friedreich's ataxic neuropathies the number and periodicity of myelin lamellae remained relatively constantly. The number and periodicity of myelin lamellae also remained unchanged in axonal enlargement due to polyglucosan disease despite an increase in the myelin sheath spiral length (Yoshikawa, *et al.* 1990). In experimental axonal atrophy, the myelin lamellar number also remained unchanged (O'Neil *et al.* 1984, O'Neil and Gilliatt 1987). Dyck *et al.* (1971b) found no correlation between the axonal circumference and the number of myelin lamellae in the sural nerves from patients with Déjérine-Sottas hypertrophic neuropathy although the number of myelin lamellae per fibre was less than that of control fibres of the same axonal size (Dyck *et al.* 1970).

Morphometric approaches have been used to assess axonal atrophy or shrinkage in various experimental and human neuropathies (Dyck *et al.* 1971a, Dyck *et al.* 1971b, Dyck *et al.* 1980, Dyck *et al.* 1981a, Dyck *et al.* 1981b, Dyck *et al.* 1985, Dyck *et al.* 1993, Engelstad *et al.* 1997, Gabreëls-Festen *et al.* 1992, Gabreëls-Festen *et al.* 1995, Jakobsen 1976, Llewelyn *et al.* 1991). Is it possible to distinguish primary from secondary demyelination by morphometric methods? This question is complicated, and needs more study.

2.6.8 G-RATIO

The g-ratio is the quotient of axonal diameter/fibre diameter (Schmitt and Bear 1937), and ranges from 0.4 to 0.9 in human sural nerve (Behse 1990, Friede and Beuche 1985a). The relationship between the g-ratio and fibre size is complicated. Sunderland and Roche (1958) found that the g-ratio increased continuously with increase of fibre diameter, but Buchthal and Rosenfalck (1966) found, on the contrary, that the g-ratio was decreased in the largest fibre groups. Behse (1990) and Friede and Beuche (1985) found that the g-ratio increased with fibre diameter in a parabolic fashion, and that the small fibres had a larger mean g-ratio than the large fibres. According to Behse (1990) about two thirds of large fibres in the control sural nerve had a g-ratio around 0.6. These conflicting results may be due to different morphometric methodologies and different sample size. In childhood, the g-ratio decreases with age (Friede and Beuche 1985a) due to the asynchronous development of myelin and axon (Schröder *et al.* 1978).

The g-ratio, as well as myelin thickness, are often used to detect axonal atrophy and secondary demyelination (Engelstad *et al.* 1997, Gabreëls-Festen *et al.* 1992, Gabreëls-Festen *et al* 1995, Llewelyn *et al.* 1991, Schröder *et al.* 1978). Previous reports on g-ratios in peripheral nerve diseases are summarized in table 2.6-6.

Table 2.6-6: G-ratio in peripheral nerve disease

Author(s)	Disease	age(ys)	Nerve	NN	G-ratio	Control
Bardosi *et al.* 1987	PNP in IMLD	2-30m	sural	4	0.85±0.06	0.78±0.05
	PNP in JMLD	3-10	sural	2	0.82±0.06	0.74±0.08
	PNP in AMLD	adult	sural	3	0.77±0.07	0.73±0.08
Gabreëls-Festen *et al.*	CMA1A(1)	3-5	sural	3	0.57±0.02*	
1995		6-30	sural	9	0.56±0.05*	
	CMA1A(2)	4	sural	1	0.97	0.73 (2-5ys)
		9-30	sural	3	0.80±0.08*	0.66 (6-30ys)

Abbreviations for table 2.6-6 see next page.

Abbreviations for table 2.6-6

*calculated from the raw data in the literature

NN: number of nerves

PNP in IMLD: peripheral neuropathy in late infantile metachromatic leucodystrophy

PNP in JMLD: peripheral neuropathy in juvenile metachromatic leucodystrophy

PNP in AMLD: peripheral neuropathy in adult metachromatic leucodystrophy

CMA1A(1): Charcot-Marie-Tooth disease type 1A (HMSN type Ia) with 17p11.2-p12 duplication

CMA1A(2): Charcot-Marie-Tooth disease type1A (HMSN type Ia) with PMP22 point mutation

2.7 QUANTITATING METHODS

Manual-mechanical measurement on enlargement photomicrographs

This method was time-consuming and inaccurate, and for these reasons is of historical interest only (Espir and Harding 1961, Dyck *et al.* 1993)

Digitizing methods

The development of digitizing tablets and microprocessors allowed peripheral nerves to be quantified using either enlarged photomicrographs or camera lucida drawings (Behse 1990, Cavallari *et al.* 1989, Dyck *et al.* 1993, Ewart *et al.* 1989, Fraher 1980, Lipski and Martin-Body 1987, Hahn *et al.* 1987, Gago *et al.* 1988, Naus *et al.* 1987, Tohgi *et al.* 1977b). However, digitizing methods still required manual attention to individual nerve fibres with the possibility of operator bias during measurement.

Computer-assisted image analysis system

The development of computer and image analysis systems allows automatic morphometric assessment of myelinated nerve fibres. Zimmerman *et al.* (1980) developed the first system based on computerized image analysis. Vita *et al.* (1992) and Auer (1994) developed systems that can recognize, enumerate, and evaluate the sizes and shapes of transverse nerve fibre profiles automatically.

The hardware components of a computer-assisted image analysis system consist principally of a personal computer with hard disk drive and mouse, video camera, image monitor, light microscope with variotube and C-mount adaptor for video-camera, and cables for connecting monitor to computer (Auer 1994, Cavallari *et al.* 1989, Torch *et al.* 1989b, Vita *et al.* 1992, Zimmerman *et al.* 1980).

The software for myelinated fibre quantitation in peripheral nerves is variable according to researcher or company, but the mechanism of myelinated fibre morphometry is similar—based on operator-interactive selection of colour value limits. Through the light microscope and a variotube, the image of endoneurium is magnified onto a video camera. Every measuring frame is divided into many Myelinated fibre is conducted as a function of pixel brightness. Each point of the analysed image is coded into 256 grey-scale levels. On fixed and stained nerve sections, myelin sheaths appear as dark objects on a bright background and consequently pixels whose grey-level values are less than the threshold value chosen by the operator are considered to belong to myelin sheaths. Conversely, the remaining pixels, whose grey-level values are greater than this threshold value, are considered as non-myelin structures. The original image is then transformed to a binary image (or logic mask) of the myelin sheath. Inversion of the image generates a logic mask of the axon, and this inversion leads to the construction of a logic mask for the myelinated fibre. The myelin sheath masks, fibre masks and the corresponding axon masks are extracted one by one from the fibre binary image and the measurements of the myelin sheath area, fibre area, axon area, the inner and the outer perimeter of the myelin sheath are made on the myelin sheath binary masks, fibre binary masks and the axon binary masks, respectively. Data are stored on disk for further calculation. Operator-interaction is necessary for the available image analysis system to eliminate large Schwann cell nuclei, dust particles and stain crystals, erase dark degenerated fibres, separate touching fibres and

correct the profiles of fibres with pale myelin sheaths. Judgement is according to histological criteria on video screen (Auer 1994, Cavallari *et al.* 1989, Torch *et al.* 1989b, Vita *et al.* 1992, Zimmerman *et al.* 1980, Leica Quantimet 500MC User Manual, Leica Quantimet 600 User Manual).

Computer imaging has a number of advantages in determining the number, size, shape, and distribution of MFs and their components: it is speedy, measures the perimeter and area precisely, automatically quantifies on average not less than 85% MFs in each measuring frame, excludes operator bias, and eliminates the step of photographic processing (Auer 1994, Dyck *et al.* 1993, Vita *et al.* 1992).

However, no completely automatic method is currently available because some problems have yet to be resolved.

(1) Operator intervention is still necessary in order to eliminate unwanted structures, such as Schwann cell nuclei and stain particles (Auer 1994, Vita *et al.* 1992). This difficulty can be resolved by quantifying MFs in specimens only after osmium tetroxide postfixation without further staining. Dyck and Lofgren (1968) first fixed the specimen in glutaraldehyde, postfixed with 1% buffered osmium tetroxide, and then examined the specimen using phase contrast microscopy. But phase contrast microscope needs a relatively thick (1.5μm) section, and this may result in fibres spurious thick myelin sheaths and thin axon as mentioned above.

(2) Manual movement of the microscope stage is necessary to alter the measuring frame. Using an automatic microscopic stage would partly overcome this problem. However, this would require the computer to have the ability to recognize the perineurium, know when to change frames, and know when to end quantifying. These technical difficulties are still to be overcome.

(3) The problem of Schmidt-Lanterman clefts. The Schmidt-Lanterman cleft is part of the normal structure of a myelinated fibre (Thomas *et al.* 1993). The number of these clefts is directly related to the myelin thickness or fibre diameter (Buchthal *et al.* 1987, Friede and Samorajski 1969, Ghabriel and Allt 1979, Ghabriel and Allt 1980). In human sural nerves, Schmidt-Lanterman clefts amount to nearly 50% of the internode length in large fibres and up to 6% in small fibres (Buchthal *et al.* 1987). In previous morphometric studies investigators manually excluded fibres cut through the Schmidt-Lanterman cleft when considering fibre calibers and relative thickness of the myelin sheath (Behse 1990, Llewelyn et al 1991), or considered them as 'double-sheathed' fibres (Torch *et al.* 1989). Auer (1994) and Vita *et al.* (1992) did not address the question of how to deal with such fibres using automatic methods of quantitation. With the Quantimet 500MC (Leica-Cambridge, UK), the clefts were usually so small in normal sural nerve that the computerized image analyzer mistook them as part of the myelin sheath. However, in diseased nerves, especially in some severe axonal atrophic nerves, the width of the clefts became larger and clearer, and the image analyzer sometimes considered one fibre cut through a wide Schmidt-Lanterman cleft to be two concentric fibres.

(4) How to deal with degenerating fibres? Both the myelin and axons of degenerating fibres appear as dark structure. Vita *et al.* (1992) manually erased these fibres. Other researchers have not discussed how they dealt with these fibres.

(5) The methods of Auer (1994) and Vita (1992) require manual separation of fibres that are close to each other, especially clusters of regenerating fibres. Otherwise fibres that touch each other are measured as distorted larger fibre(s).

(6) When using the method of Auer (1994), the measured perimeter of some diseased nerve fibres may be larger than they should be because the image system also includes in its measurement clefts and myelin sheath folds.

(7) Automatic methods still lose 10%–15% fibres, including fibres cut through the node of Ranvier and some pale fibres (Auer 1994, Dyck *et al.* 1993, Vita 1992, Zimmerman *et al.* 1980) which may be regenerating or remyelinating fibres.

Calculation of fibre and axonal diameter

On a transverse section, the most common parameters used to depict the size of MFs are the segmental fibre diameter (Ds) and the axonal diameter (Da). In the *in vivo* state, the shape of MFs in transverse section is assumed near-circular, and myelin is semi liquid (Dyck *et al.* 1993, King 1994). Distortions of nerve fibres occur during the processing of samples (Behse 1990, Dyck *et al.* 1980, Karnes *et al.* 1977). During quantitation, many primary parameters can be measured directly from each individual MF, such as: the long axis (longest distance across the fibre), the short axis (greatest distance across the fibre at right angles to the long axis or the distance across the center of the fibre at right angles to the long axis), the perimeters of the outer edge and inner edge of myelin sheath, the area of myelin sheath, the area of axon, and the area of the total fibre on cross section (Auer 1994, Behse 1990, Cavallari *et al.* 1989, Dyck *et al.* 1993, Karnes *et al.* 1977, Vita *et al.* 1992). In earlier studies, the long axis, the short axis, and the arithmetic or geometric mean of the long and the short axis were used to represent fibre caliber (Behse 1990, Blight and Decrescito 1986, Cavallari *et al.* 1989, Chaia *et al.* 1987, Dunn *et al.* 1975, Karnes 1977, Mackinnon *et al.* 1986, Tomanek and Tipton 1967). These parameters are no longer employed to represent the fibre diameter as they are inaccurate (Karnes *et al.* 1977, Dyck *et al.* 1993). Currently, three kinds of methods are commonly used to calculate Ds and Da. They are shown in table 2.7-1. These methods are all based on primary parameters which are directly measured using a digitizer or image system.

Table 2.7-1. Three methods of calculating fibre and axonal diameter

Method	Formula	Author
(1) area-equivalent circle	(a) $Ds = 2\sqrt{\mathbf{As}/\pi}$	Vita *et al.* (1992)
	$Da = 2\sqrt{\mathbf{Aa}/\pi}$	
	(b) $Da = 2\sqrt{\mathbf{Aa}/\pi}$	Zimmerman *et al.* (1980)
	$Ds = Da + 2\mathbf{Dm}$	Dyck and Karnes (1981)
	Advantage: Diameters derived from area measurements show the greatest precision and accuracy, with the least bias (Karnes *et al.* 1977).	
	Disadvantage: The above equations were derived using 2% Glutaraldehyde solution fixed nerves, and there was no comparison with fresh or cryostat sections, or between different methods of fixation to assess whether there is any difference in the degrees of shrinkage between myelin sheaths and axoplasm. **Dm** is not uniform on cross section, especially in nerves showing pathological changes.	
(2) perimeter-equivalent circle	(a) $Ds = \mathbf{Ps}/\pi$	Friede and Beuche (1985)
	$Da = \mathbf{Pa}/\pi$	Torch *et al.* (1989)
	(b) $Da = \mathbf{Pa}/\pi$	
	$Ds = Da + Dm^*$	Llewelyn *et al.* (1991)
	Advantage: Myelin sheath perimeters remain relatively constant during processing of nerve tissue (Dyck *et al.* 1980).	
	Disadvantage: Even in a healthy nerve, the shape of a fibre is not strictly circular. It may be boomerang shaped in the Schwann cell nuclear region, or crenated in the paranodal region (Karnes *et al.* 1977). In diseased nerves with myelin sheath splitting, the computer image system may measure the perimeter along the cleft of splitting which results in an incorrectly long perimeter (our experience with Quantimet 500MC system). When the axon is atrophied, the myelin sheath may be folded complexly, and the axon may lose its circularity (O'Neil and Gilliatt 1985). This results in an increase in the perimeter as the computer image system measures along the uneven edge of myelin sheath.	
(3) Based on area and perimeter	$Ds = (0.5\mathbf{P} + 2\pi\mathbf{Am}/\mathbf{P})/\pi$	Auer (1994)
	$Da = (0.5\mathbf{P} - 2\pi\mathbf{Am}/\mathbf{P})/\pi$	
	Advantage: The perimeters of the myelin sheath and area of the myelin sheath remain relatively constant during tissue preparation (Auer 1994, Dyck *et al.* 1980).	
	Disadvantage: The same as in (2).	

Abbreviations for table 2.7-1 see next page.

Abbreviations for Table 2.7-1

Bold letter: primary parameter, obtained from measuring directly

Ds: segmental fibre diameter on transverse section

Da: axonal diameter

Dm: myelin sheath thickness

Ps: segmental fibre perimeter on transverse section = perimeter of the external edge of myelin sheath

Pa: axonal perimeter = perimeter of the internal edge of myelin sheath

P: sum of the external and internal perimeters of myelin sheath = Ps + Pa

Aa: axonal area on cross section = area enclosed by myelin sheath

Am: area of myelin sheath

As: transverse area of the internodal segment

Dm*: **number of myelin lamellae** × myelin spacing factor, the latter obtained by counting the number of myelin lamellae over a given width.

All three methods rely on the assumptions that the area enclosed by the myelin sheath includes only the area of axoplasm and that the perimeter of the internal edge of myelin sheath is the perimeter of axon. In healthy nerve this assumption is acceptable because the adaxonal space, or periaxonal submyelinic space is so small, approximately 200Å (Thomas *et al.* 1997, Waxman 1985), that it can be ignored, and the shape of axon is near circular. But in axonal atrophic fibres, the adaxonal space increases and must be taken into account.

Diameters derived from measured areas, perimeters, or combined areas and perimeters have disadvantages that have not yet been overcome. Therefore, it is more accurate to use the total fibre area on cross section (As), the myelin sheath area (Am), and the axonal area (Aa) (or the area enclosed by myelin sheath (Ai)) as the parameters of fibre size because they can be measured directly.

2.8 PROJECT AIM

The aims of this project were to assess the accuracy of quantitative studies of myelinated nerve fibres obtained by fascicle and systematic sampling methods and determine the minimal sample size that would result in an accurate representation of the whole myelinated fibre population.

The total number of MF (TNMF) in a normal sural nerve varies between 3300-12300 at the level of ankle (Behse 1990, Jacobs and Love 1985), and between 3630-16330 at the level of midcalf (Schellens *et al.* 1993). Even with the help of a computer-assisted image analyzer, it is time-consuming to measure all the myelinated fibres. In the past, various sampling methods were used to overcome this problem often only measuring a few hundred myelinated fibres of myelinated fibres within a fascicular area of approximately $0.1mm^2$ (Auer 1994, Behse 1990, Jacobs and Love 1985, Vita *et al.* 1990, Schellens *et al.* 1993). However, the spatial distributions of the number and size of myelinated fibres are non-uniform within and between fascicles in peripheral nerves (Dyck *et al.* 1984, Dyck *et al.* 1986a, Dyck *et al.* 1986b, Saxod *et al.* 1985, Torch *et al.* 1989a), and pathological changes may be focal, multifocal, or diffuse (Dyck et al 1993). Therefore, morphometric results from an unsuitable sample may not be reliable.

The main aim of this study was to establish the minimal total transverse fascicular area that should be quantified in sural nerves in order to obtain data that is comparable to (and representative of) the whole myelinated fibre population.

2.9 HYPOTHESES

1. Quantitation of myelinated nerve fibres in one fascicle or part of a fascicle/s is not an accurate representation of the whole myelinated fibre population in the sural nerve.

2. Myelinated fibres in more than half of the fascicular area in every fascicle need to be counted in order to acquire results comparable to that of counting the whole myelinated fibre population in the sural nerve.

CHAPTER 3: MATERIALS AND METHODS

3.1 SELECTION OF MATERIALS

Eighteen sural nerve biopsies examined in the Neuropathology Section of the Institute of Medical and Veterinary Science (Adelaide) were randomly selected for quantitative studies on myelinated nerve fibres. Two sural nerves taken at necropsy from a subject without evidence of peripheral nerve disease served as normal controls. The clinical features of this subject and the pathological cases, including electrophysiological findings where available, are detailed in table 3.1-1.

The morphological studies on these 20 sural nerves are displayed in table 3.1-2. All the 18 pathological nerves showed different degrees of demyelination/remyelination with or without axonal degeneration.

Table 3.1-1: Summary of the clinical features of the patients whose sural nerves were used in this study

Nerve	Patient	Age	Sex	Diagnosis	Disease duration	Electrophysiology
1	(PM12)L	44	F	suicidal drowning, depression	not applicable	not done
2	" R	"	"	"	"	"
3	(18105/93)	50	F	CIDP	3yrs	↓↓ NCV
4	(PM2)	40	M	road traffic accident, heroin addiction	not known	not done
5	(06289/95)	40	F	?CIDP, ?HMSN	3yrs	↓↓ NCV
6	(08609/96)	63	F	IgM paraproteinaemic neuropathy	6 months	↓↓NCV
7	(17356/97)	67	F	IgG (κ) paraproteinaemic neuropathy	years	↓↓NCV, absent SNAP
8	(02844/96)	66	M	?CIDP	5 years	absent sural SNAPs
9	(01585/96)	43	F	oculopharyngeal dystrophy	years	not done
10	(28589/96)	31	F	CIDP	years	↓↓NCV, absent SNAPs
11	(11937/97)	64	M	critical illness neuropathy	1 month	↓NCV
12	(17459/97)	72	M	amputation due to ischaemia	not known	not done
13	(24521/97)	46	F	following legionella pneumonia	2 years	↓NCV

Table 3.1-1 (continued): Summary of the clinical features of the patients whose sural nerves were used in this study

Nerve	Patient	Age	Sex	Diagnosis	Disease duration	Electrophysiology
14	(00802/97)	61	M	motor neuropathy	20 years	denervation
15	(23670/97)	76	M	paraneoplastic (chronic lymphocytic leukaemia)	years	↓SNAP
16	(23141/97)	73	F	paraneoplastic (breast carcinoma)	4 weeks	↓NCV
17	(18621/97)	39	M	drug induced (vincristine)	months	normal NCV, ↓SNAP
18	(20797/97)	56	F	mononeuritis multiplex, vasculitis	months	not done
19	(20235/97)	54	F	aetiology unknown	years	not done
20	(17784/97)	77	F	aetiology unknown	weeks	absent sural SNAP

Abbreviations for table 3.1-1:

PM: postmortem

NCV: nerve conduction velocity

SNAP: sensory nerve action potential

not done: nerve conduction studies not performed

CIDP: chronic inflammatory demyelinating polyneuropathy

HMSN: hereditary motor and sensory neuropathy

Table 3.1-2: Pathological Features

Nerve	Plastic 1μm sections (T.S + L.S) +EM						Teased Nerve Fibres
	MF loss	ax. degen.	demyel.	remyel.	EF	inflam. cells	percentage of the total number of teased fibres
1	–	–	–	–	–	–	N/A
2	–	–	–	–	–	–	N/A
3	–	–	+	+	–	–	23%demyel./remyel. and 3% axonal degen.
4	–	+	–	+	–	–	N/A
5	++	–	+	+	++	–	44% demyel./remyel. and 5% axonal degen.
6	+++	+	+	++	+++	+++	26% demyel./remyel. and 11% axonal degen.
7	++	+	+	++	++	–	92% demyel./remyel.
8	++	–	+	++	++	–	43% demyel./remyel. and 2% axonal degen.
9	–	–	–	+	–	–	25% demyel./remyel. and 2% axonal degen.
10	+	+	+	+++	+	–	52% demyel./remyel. and 2% axonal degen.
11	+	+	+	++	+	++	60% demyel./remyel.
12	+++	+	+	+	+++	+	N/A
13	+	++	+	++	+	–	18% demyel./remyel. and 17% axonal degen.
14	++	++	+	+	++	–	15% demyel./remyel. and 73% axonal degen.
15	+	+	–	+	+	+	42% demyel./remyel. and 2% axonal degen.
16	+	+++	+	+	–	–	38% demyel./remyel. and 7% axonal degen.

Nerve	Plastic 1µm sections (T.S + L.S) +EM						Teased Nerve Fibres
	MF loss	ax. degen.	demyel.	remyel.	EF	inflam. cells	percentage of the total number of teased fibres
17	++	++	+	+	++	+++	22% demyel./remyel. and 17% axonal degen.
18	+++	+++	+	+	+++	+++	7% demyel./remyel. and 78% axonal degen.
19	+++	–	+	+	+++	–	21% demyel./remyel. and 2% axonal degen.
20	+++	++	–	++	+++	+	39% demyel./remyel. and 6% axonal degen.

* The morphological findings are reported by Dr. P.C. Blumbergs and Dr. G. Scott.

Abbreviations for table 3.1-2

-: negative

+: mild

++: moderate

+++: severe

T.S+L.S: transverse and longitudinal sections

EM: electron microscope

MF: myelinated fibre

ax. degen.: axonal degeneration

demyel.: demyelination

remyel.: remyelination

EF: endoneurial fibrosis

inflam. cells: inflammatory cells

3.2 SURAL NERVE BIOPSY

The sural nerve biopsies were performed according to a standard protocol (Cash and Blumbergs 1994). Under local anaesthesia, an incision of about 8cm was made in the furrow just behind and above the lateral malleolus. The sural nerve was exposed and approximately a 6cm length of nerve was excised and placed directly onto a sheet of dental wax. Extreme care was taken in the process of biopsy in order to avoid nerve crushing and stretching.

3.3 TISSUE PREPARATION

The sural nerve biopsies were examined according to routine methods currently used in our laboratory (Cash and Blumbergs 1994). The methods are described briefly below.

After removal from the body, the nerve is placed directly on to a sheet of dental wax for further dissection with a razor blade. One 2mm specimen orientated in the transverse plane is placed in a blob of O.C.T. (Tissue Tek) on a piece of cork with a needle in one corner. This is plunged into isopentane pre-cooled by liquid nitrogen in an upright position to be frozen. Then it is stored in liquid nitrogen for frozen section. Five-micron cross sections are cut and stained with H&E for morphological studies. Two 2mm specimens are put into 10% formal-saline for no less than 4 hours, and then embedded in paraffin. Five-micron cross sections are cut and stained with H&E, trichrome and congo red for morphological study. One 3 to 4 cm long specimen is secured at each end with cotton. A 5g stainless steel weight is attached to one end of the tissue, and it is suspended in 2.5% glutaraldehyde (in 0.05 mol/l cacodylate buffer) for 1.5 hours. Then the nerve is separated from the weight and dissected into smaller segments; 2mm in length for electron microscopy, 2mm in length oriented transversely for resin embedment and light microscopy, 4mm in length orientated

longitudinally for resin embedment and light microscopy and 15 to 20mm in length for teasing. Blocks for resin embedding and light microscopy remain in glutaraldehyde overnight and are washed in 0.05 mol/l sodium cacodylate buffer for at least half an hour with 5 changes of buffer. Then the specimens are processed as indicated in table 3.3-1. Semithin sections are cut at 1μm, with care to ensure they are precisely transverse, using a microtome.

Table 3.3-1. Resin processing schedule for nerve specimens

Step	Solution required	Time
1	1% aqueous osmium tetroxide	24 hours
2	0.05 mol/l sodium cacodylate buffer	Five changes
3	70% ethanol	30 minutes
4	95% ethanol	30 minutes
5	100% ethanol	Three changes, each of 30 minutes
6	Propylene oxide	30 minute
7	Propylene oxide: epoxy resin (1:1)	1 hour
8	Propylene oxide: epoxy resin (1:3)	1 hour
9	Epoxy resin	Two changes, each of 1 hour (under vacuum)
10	Epoxy resin	Overnight (under vacuum)
11	Fresh epoxy resin	Three changes, each of 2 hours (under vacuum)
12	Embedded in resin	
13	polymerize at 70^0C	overnight

After a further half an hour fixation in glutaraldehyde, the segment for teasing fibres is separated into fascicles. The fascicles are washed in buffer for at least half an hour with several changes of buffer. Then the specimens are processed as indicated in table 3.3-2.

Table 3.3-2. Processing schedule for teased fibre preparations

Step	Solution required	Time
1	1% aqueous osmium tetroxide	2 hours
2	0.5 mol/l sodium cacodylate buffer	several changes, minimum 30 minutes
3	45% glycerol	Overnight at 45^0C
4	66% glycerol	Overnight at 45^0C
5	100% glycerol	Overnight at 45^0C

Teased fibres were prepared by Kathy Cash.

3.4 STAINING METHODS

On micron resin cross sections were stained with 1% aqueous osmium tetroxide (step 1 of nerve processing schedule in table 3.3-1) and no additional staining of MFs was undertaken. In such preparations, the myelin sheaths were dark grey rings, while the other structures were colourless. One micron resin cross and longitudinal sections stained with toluidine blue, and 5μm paraffin cross sections stained with H&E, Trichrome, and Congo Red were used for morphological examination.

3.5 QUANTITATION

One micron resin cross sections were used for quantitation. These were prepared according to the protocol outlined in table 3.3-1, and apart from staining with 1% aqueous osmium tetroxide as part of the preparation, no other staining techniques were employed.

3.5.1 IMAGE SYSTEM

Quantimet 500MC computer-assisted image analysis system (Leica-Cambridge, UK) was used for quantitation. The Quantimet 500MC system allows customer programming of image analysis function. The software for automatic nerve fibre quantitation was written by Peter Smith and Ian Parkinson. The sequence for nerve quantitation is explained below.

3.5.2 QUANTITATING METHODS

Under low magnification, each fascicle was numbered. Using an oil lens (100x), a 3.3x tube, and a Sony CCD-camera (charge coupled device-camera), the image of the nerve was displayed onto a video display. A rectangular frame defines the measuring frame on the video image. According to the manufacturer of the image analysis system (Leica-Cambridge, UK), each measuring frame contains 202500 (405×500) pixels, and when the image of the nerve is magnified 3018 times, each pixel equals to 0.11mm along its edge. Dyck *et al.* (1984) suggested that the final magnification of about ×2000 is suitable for determining the fibre size, shape and fibre density. In a previous study we found that of this magnification (×2000) our image analysis system lost some small fibres and some fibres touched each other. However these problems were reduced at a magnification of ×3018. The intrafascicular area of each fascicle was divided into rectangular measuring frames (Figure 3.5-1A). Beginning with the upper left corner of each fascicle, fibres in the field of each measuring frame were quantitated and measured only if the lowest pixel of the fibre is within the measuring frame. Otherwise, it was measured in the adjoining field (Figure 3.5-1B). In Figure 3.5-1B, fibre x was measured in this field, and fibre y would be measured in the adjoining field. Each horizontal field was measured in sequence until more than half of the measuring frame was occupied by subperineurial space or perineurium, at which time the field was shifted one frame down and continuous fields were counted in the opposite direction until the whole fascicle had been examined. Artifacts produced in nerve biopsy and tissue preparation were excluded manually. Renaut bodies were excluded.

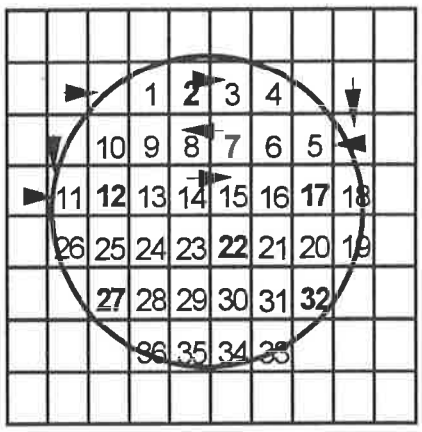

(A)

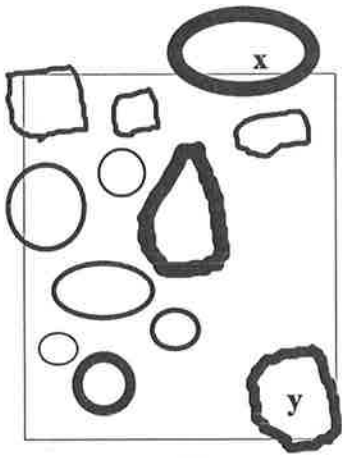

(B)

Figure 3.5-1: (A) Diagram of a fascicle that is divided into 36 rectangular measuring frames. (B) Magnification of one measuring frame. According to the set-up of the manufacturer, the area of the measuring frame is 202500 (405×500) pixels, equal to 2450μm^2.

According to the manufacturer, the microcomputer-based image analysis system (Leica-Cambridge, UK) receives a digitized image from the CCD-camera at 256 grey levels. Threshold was adjusted to capture only the dark grey myelin sheaths and generate binary images. The number of MFs within each field and the number of measuring frames within each fascicle were counted and stored on an Excel spreadsheet. For each identified MF the following measurements were made: (1) long axis (longest distance across fibre); (2) short axis (distance across the center of the fibre at right angles to the long axis); (3) area of myelin sheath (Am); (4) sum of perimeters (P) of external (Po) and internal (Pi) edge of myelin sheath. The Po was thought to be the fibre perimeter (Ps) on cross section, and the

Pi to be the axonal perimeter (Pa). The derived parameters were calculated using Visual Basic for Excel program, written by Ian Parkinson specifically for this purpose.

3.5.3 PARAMETER TRANSFORMATION

In vivo, the shape of myelinated fibres on transverse section is assumed to be nearly circular. During processing, there is shrinkage of the fascicles. The shapes of MFs are distorted, and become irregular. However, the area and perimeter of the myelin sheath remain relatively constant (Auer 1994, Dyck *et al.* 1980, Karnes *et al.* 1978). The contour of MF on cross section was converted into a myelin sheath area and perimeter-equivalent circle (Figure 3.5-2).

Figure 3.5-2: Transformation of the shape of MF on cross section

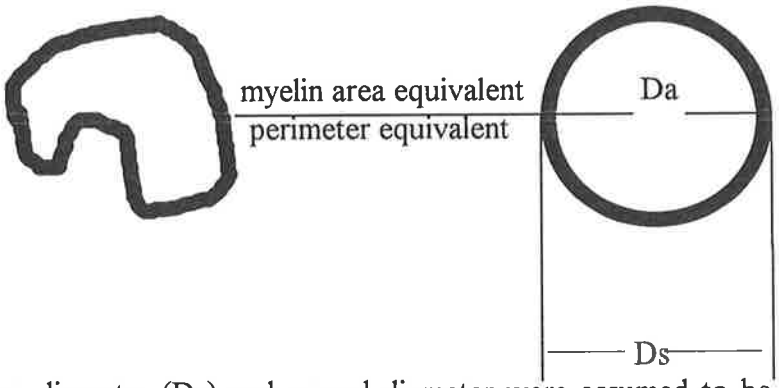

The fibre diameter (Ds) and axonal diameter were assumed to be equivalent to the outer and the inner diameter of the myelin sheath respectively, and were determined mathematically from Am and P (Auer 1994).

(1) Fascicular area of each fascicle = 2450μm^2×the number of measuring frames of each fascicle

(2) TTFA = sum of the fascicular area of every fascicle within one nerve

(3) mean MFD: calculated from the number of MFs in each measuring frame

(4) Fibre diameter and axonal diameter: $\mathbf{Ds=(0.5P+2\pi Am/P)/\pi}$

$\mathbf{Da=(0.5P-2\pi Am/P)/\pi}$

The derivation of how to get the formulae is shown below.

$$As = Aa+Am$$

$$Am = As-Aa$$

$$= \pi Ds^2/4-\pi Da^2/4$$

$$= \pi(Ds^2-Da^2)/4$$

$$= \pi(Ps^2/\pi^2-Pa^2/\pi^2)/4$$

$$= (Ps^2-Pa^2)/4\pi$$

$$= (Ps^2-(P-Ps)^2)/4\pi$$

$$= (2PPs-P^2)/4\pi$$

$$2PPs = 4\pi Am+P^2$$

$$Ps = 0.5P+2\pi Am/P$$

$$Ds = Ps/\pi = (0.5P+2\pi Am/P)/\pi$$

$$Da = Pa/\pi = (P-Ps)/\pi = (P-(0.5p+2\pi Am/P))/\pi = (0.5P-2\pi Am/P)/\pi$$

In peripheral nervous system, myelinated fibres are bigger than 1μm in diameter (Thomas *et al.* 1993). Therefore, all the objects with a diameter less than 1 μm were excluded and not quantitated.

3.6 SAMPLING METHODS

3.6.1 FASCICLE SAMPLING

Data from each fascicle forms a sample. The TNMF, TFA, MFD, Ds, and Da of each fascicle were quantitated, and the data for each fascicle compared to that of the whole myelinated nerve fibre population. In this way, fascicular representation of the whole MF population was assessed.

3.6.2 SYSTEMATIC SAMPLING OF EVERY nth MEASURING FRAME

A Visual Basic for Excel program was written for this purpose by Ian Parkinson to allow the user to extract data from every 2^{nd}, 3^{rd}, 4^{th}, ..., 10^{th} measuring frame from every fascicle to form 9 samples for each nerve. This allows investigation of whether data from 10% to 50% TTFA can reliably represent the whole population. Because the first

measuring frame was usually incomplete, we began with the 2nd field in every fascicle. For example, every 5th field sample contains the 2nd, 7th, 12th, 17th ,.....measuring frame in every fascicle (bold digits in figure 3.5-1A) within one nerve.

3.7 DISTRIBUTION OF MYELINATED FIBRE DENSITY AND FIBRE SIZE

3.7.1 DISTRIBUTION OF MYELINATED FIBRE DENSITY (MFD)

MFD is usually expressed as the number of MFs per mm^2. In these studies, MFD was also expressed as the number of MFs per measuring frame to provide a measure of its frequency distribution, which may be expressed via histograms.

3.7.2 DISTRIBUTION OF MYELINATED FIBRE DIAMETER AND AXONAL DIAMETER

By convention, the histogram representing fibre diameter distribution is generated as the graphical representation of the number of myelinated fibres per micrometer-bin. A binwidth of 1micron is used mostly, as it provides a compromise between loss of detail and limited precision of the individual bin value (Olson 1973). In this way, the histograms of both fibre diameter and axonal diameter are described with 21 parameters, 0-20μm and larger than 20μm.

3.8 STATISTICAL METHODS

The data were expressed as mean values and standard deviations (SD). Visual inspection of the histograms of the distribution of sum of the axonal and nerve fibre perimeters, myelin sheath area, fibre diameters and inner diameters of myelin sheath were not Gaussian, whereas the distribution of MFD was near Gaussian. In order to achieve uniformity, the

differences were evaluated using non-parametric tests. Differences between samples and the whole population were evaluated using Wilcoxon Rank-Sum and Komolgorov-Smirnov tests with SAS software.

The Wilcoxon Rank-Sum test compares the mean values of one sample with another. The Kolmogorov-Smirnov goodness of fit test compares the shape of cumulative frequency distributions. Samples were derived either from the whole fascicle or the systematic sampling methods and were compared with the mean fibre density, mean fibre diameter and axonal diameter, and the distributions of these measurements derived from measurement of the entire MF population of the whole nerve.

CHAPTER 4: RESULTS

4.1 GENERAL DESCRIPTION OF THE WHOLE NERVES

The number of fascicles (NF), total number of myelinated fibres (TNMF), total transverse fascicular area (TTFA), myelinated fibre density (MFD), fibre diameter (Ds), and axonal diameter (Da) of each sural nerve are displayed in table 4.1-1 (see p71).

4.1.1 FREQUENCY DISTRIBUTION OF MYELINATED FIBRE DENSITY (MFD)

The frequency distribution of MFD of all sural nerves is depicted in figure 4.1-1 (see pp72-75). In these figures, MFD is expressed as the number of myelinated fibres (MFs) per measuring frame. Each measuring frame has an area of 2450μm^2. The MF count for each measuring frame ranged from 0-28 (Figure 4.1-1). By convention, the MFD is expressed as the number of myelinated fibres/mm^2. The mean MFD, calculated from each measuring frame, was 4,934 and 5785/mm^2 in the two control nerves, and averaged 3,731/mm^2 in the 18 pathological nerves (Table 4.1-1, see p71). It can be seen that frequency distribution of MFD is near Gaussian for all sural nerves in this study.

4.1.2 FREQUENCY DISTRIBUTION OF FIBRE DIAMETER (Ds)

The frequency distributions of fibre diameter are expressed and displayed as percentage frequency histograms for each nerve in figure 4.1-2 (see pp76-79). In the 2 control nerves (nerve No.1 and 2), the frequency distribution of fibre diameter is bimodal with the first peak at 4-6μm corresponding to type-III fibres, and the second peak at 11-14μm corresponding to type-II fibres. A trough is evident at 8-9μm In the pathological group, the bimodal distribution of fibre diameter is retained in nerves No.3, 4, 5, 6, 9, 10, 11, 12, 13, 14, 15, 16, 17, 18, and 19 despite loss of larger diameter fibres in some nerves. In nerves No.7, 8 and 20, there is greater loss of larger diameter groups giving a unimodal appearance.

4.1.3 FREQUENCY DISTRIBUTION OF AXONAL DIAMETER (Da)

The frequency distribution of axonal diameter is expressed as a percentage frequency histogram, and displayed in Figure 4.1-3 (see pp80-83). In the two control nerves, the distribution of axonal diameter is bimodal with the first peak at 4-5μm, and the second peak at 7-8μm. This corresponds to the distribution of fibre diameter. The first peak of Da represents type-III fibres, and the second peak represents type-II fibres. In the pathological group, only two sural nerves have an obviously bimodal distribution of axonal diameter (No.3 and 14). The others have a unimodal or indeterminate distribution of Da.

4.2 COMPARISON OF MYELINATED FIBRE DENSITY (MFD) OBTAINED BY FASCICLE AND SYSTEMATIC SAMPLING METHODS TO THAT OF THE WHOLE MYELINATED FIBRE POPULATION

Results of the number of myelinated fibres (NMF), transverse fascicular area (TFA, mm^2) and the percentage of total transverse fascicular area (%TTFA), and myelinated fibre density (MFD) ($/mm^2$) of each sampling group, and the comparison of MFD to that of the whole myelinated fibre population of the twenty sural nerves are displayed in tables 4.2-1 to 4.2-20 (see pp84-93). Each table corresponds to one nerve, table 4.2-1 to nerve No.1, table 4.2-2 to nerve No.2, and so on.

4.2.1 FASCICLE SAMPLING

Because the frequency and the spatial distribution of myelinated fibres in the different fascicles are heterogeneous between fascicles, it is necessary to investigate i) whether the mean MFD within a fascicle is influenced by fascicular size and, ii) whether the MFD of a fascicle is comparable to the MFD of the whole nerve.

i) Comparison of Myelinated Fibre Density (MFD) Among Fascicles

The mean values and spatial distribution of MFD varied considerably between fascicles in both control and pathological nerves. To test the hypothesis that fascicle size is a function of MFD (Saxod *et al.* 1985), fascicle size (diameter and fascicular area) was plotted against mean MFD. Figure 4.2-1 (see p95) shows scatter diagrams from 6 nerves, including 2 control nerves (No.1 and 2), 2 mildly pathological nerves (No. 3 and 4) and 2 pathological nerves (No.5 and 6). The coefficients of determination (R^2) of linear regression between mean MFD of each fascicle and its fascicular area or fascicle diameter are also shown in the figure. There is no correlation between fascicle size (either diameter or area) of each fascicle and its mean MFD in the 6 nerves. We also did not find any relationship between MFD and fascicle size in the other 14 pathological nerves.

ii) Comparison of Myelinated Fibre Density of Fascicles With the Whole Myelinated Fibre Population

The percentage of fascicles in which the mean value and shape of the frequency distribution of MFD differed significantly from that of the whole nerve is shown in table 4.2-21 (see p96). The MFD of the sample differs from the whole population if either the mean MFD or MFD frequency distribution is significantly different. In only one of the 20 nerves (nerve No.5), were the MFDs of all the fascicles comparable to the whole population. In the two control nerves, there were a total of 14 fascicles, of which 8 (57.1%) had MFDs that were significantly different to the whole population. In the 18 pathological nerves, there were 168 fascicles, of which 61 had significantly different MFDs. The findings were similar in control and pathological groups (Chi-square test, P=0.1580; Fisher's exact test, P=0.1540).

In summary, comparison of MFD for each fascicle and the whole population revealed: no relationship between fascicle size and MFD for the whole population. We also compared

the MFD between each fascicle and found no correlation between fascicle size and its corresponding mean MFD in either control or pathological sural nerves (data not shown). Accordingly, it is impossible to predict which fascicle may have a MFD that can represent the whole population reliably before all the fascicles are quantitated in both control and pathological sural nerves.

4.2.2 SYSTEMATIC SAMPLING

From table 4.2-1 to 4.2-20 (pp84-93), it is evident that not all systematic samples (from every 10^{th} to every 2^{nd} field) yield a MFD similar to that of sampling the whole nerve. A sample will have a different MFD from that of the whole nerve if either the mean value or the frequency distribution of MFD is different from that of the whole population. Table 4.2-22 (see p97)shows the biggest systematic sample in which MFD differs from the whole population in mean value and/or spatial distribution with levels of significance set at $P \leq 0.05$ and $P \leq 0.2$ respectively. With significance of P value set at 0.05, only the every 8^{th} field sample of nerve No.20 (p93) has a MFD that is significantly different from the population. With significance of P value set at 0.2, the systematic sampling method in 1 control and 5 pathological nerves results in a MFD different from that of the whole nerve. The biggest sample is the every 6^{th} field in nerve No.2 (1176MFs, 0.1911mm^2TFA of 16.77% TTFA) and No.7 (1171MFs, 0.3724mm^2TFA of 17.08% TTFA). These results imply that systematic sampling every 5^{th} field or more will produce a MFD that is probably reliably representative of the whole nerve. In other words, it is necessary to count at least 20% of the TTFA in order to determine a MFD which is representative of the whole population in either control or pathological sural nerves.

4.3 COMPARISON OF FIBRE DIAMETER (Ds) AND AXONAL DIAMETER (Da) OBTAINED BY FASCICLE AND SYSTEMATIC SAMPLING METHODS TO THAT OBTAINED BY WHOLE NERVE SAMPLING

The mean values and standard deviations of Ds and Da of each sample, and the comparisons with the whole population for each nerve are displayed in table 4.3-1 to table 4.3-20 (see pp98-107), corresponding to nerves No.1 to 20. If either the mean value of Ds or Da or the spatial and frequency distributions of fibre size of a sample differ from that of the whole nerve, then this sample is not representative of the whole nerve fibre population.

4.3.1 FASCICLE SAMPLING

There is a great variation of fibre size among fascicles within the sural nerves in both control and pathological groups. Table 4.3-21 (see p108) shows the percentage of the number of fascicles in which the fibre size is significantly different from that of the whole population in each nerve. There were 8 fascicles (57.1%, 8/14) in the two control nerves and 90 (53.6%, 90/168) in the eighteen pathological nerves in which the mean diameter and distribution of fibres was significantly different to the whole population. The findings were similar in the control and pathological groups (Chi-square test, P=0.9185; Fisher's exact test, P=1.0000). Accordingly, in both control and pathological nerves, no regular pattern was found to indicate which fascicle contains fibres which reliably represent the fibre size of the whole population.

4.3.2 SYSTEMATIC SAMPLING

Table 4.3-22 (see p109) shows the largest systematic samples in which fibre diameter and/or axonal diameter are different to the whole population of each nerve. With a level of significance set at $P \leq 0.05$, there are seven nerves (1 control and 6 pathological nerves) in

which systematic samples of fibre size are significantly different to the whole nerve. For example, in nerve No.11, even systematically sampling every 3rd field, which included 1,801MFs with a 0.3945mm^2 transverse fascicular area (33.20% of TTFA), was not representative of the whole nerve (see p89 and 103). Similarly in nerve No.2 (control nerve), sampling every 2nd field, which included 3,293 MFs and 0.5660mm^2 fascicular area (49.68% of TTFA), produced a different mean fibre size and spatial distribution to the whole nerve with a level of significance set at $P \leq 0.2$ (see p84 and 98).

To test the hypothesis that data from larger samples can represent the whole population more accurately, evolution of *P*-values of fibre diameter was used as a function of the sample size (expressed as TTFA%) in figure 4.3-1 (see pp110-113). When sample size increases from about 10% up to 50%, *P*-value does not increase simultaneously. In the same way, it was also found that the precision with which axonal diameter can be estimated from a systematic sample does not increase with sample size increasing from 10% to 50% of total fascicular area.

Based on these results, it is necessary to count and measure MFs in more than half of the total fascicular area in order to obtain a reliable representation of fibre size.

Table 4.1-1: General description of 20 sural nerves

Group	Nerve No.	NF	TNMF	TTFA	mMFD	MFDSD	mDs	DsSD	mDa	DaSD
Control	1	7	4768	0.9482	4934	1676	7.81	4.17	5.79	3.17
Control	2	7	6591	1.1393	5785	1855	7.41	4.06	5.29	2.85
Average of Control		**7**	**5680**	**1.0438**	**5360**		**7.61**		**5.54**	
Pathol.	3	12	9291	1.6146	5755	1842	7.15	3.49	4.56	2.21
Pathol.	4	13	5836	1.2716	4950	1615	8.57	4.77	6.11	3.53
Pathol.	5	5	2610	0.6174	4227	1441	6.33	2.88	4.38	2.01
Pathol.	6	11	5057	2.2589	2239	1035	5.57	2.93	3.68	1.79
Pathol.	7	10	6555	2.1805	3006	1307	6.32	3.21	4.44	2.27
Pathol.	8	5	2288	0.4825	4740	1726	5.77	2.51	4.31	1.93
Pathol.	9	9	8555	1.5411	5551	1769	7.64	4.05	5.34	2.95
Pathol.	10	6	4158	0.7644	5440	1524	7.01	3.51	4.75	2.44
Pathol.	11	12	5402	1.1883	4546	1548	6.24	3.09	4.15	1.89
Pathol.	12	6	3211	1.4357	2237	954	6.88	3.31	4.94	2.35
Pathol.	13	10	6184	1.4063	4397	1412	7.55	4.01	5.34	3.10
Pathol.	14	9	4242	1.5484	2742	1040	7.80	4.37	4.80	3.28
Pathol.	15	12	6072	1.6048	3784	1358	6.51	3.60	4.66	2.63
Pathol.	16	8	3505	0.7620	4600	1673	7.17	4.15	5.30	3.20
Pathol.	17	17	8707	3.0209	2882	1052	6.88	3.53	4.41	2.47
Pathol.	18	5	3188	1.6366	1948	2456	6.67	4.59	4.33	3.59
Pathol.	19	11	2357	1.2152	1940	922	5.86	2.73	4.03	2.00
Pathol.	20	7	3109	1.4333	2169	985	6.15	3.35	4.59	2.87
Average of Pathol.		**9.33**	**5018**	**1.4435**	**3731**		**6.78**		**4.67**	

Control: control group

Pathol.: pathological group

NF: number of fascicle per sural nerve

TNMF: total number of myelinated fibres per sural nerve

TTFA: total transverse fascicular area per sural nerve (mm^2)

mMFD: mean of myelinated fibre density (number of MFs/mm^2)

MFDSD: standard deviation of myelinated fibre density

mDs: mean of fibre diameter (μm)

DsSD: 1 standard deviation of fibre diameter

mDa: mean of axonal diameter

DaSD:1 standard deviation of axonal diameter

Note: For two control and 15 pathological nerves, the mean±SD values for fibre diameter and axonal diameter are calculated from a bimodal distribution.

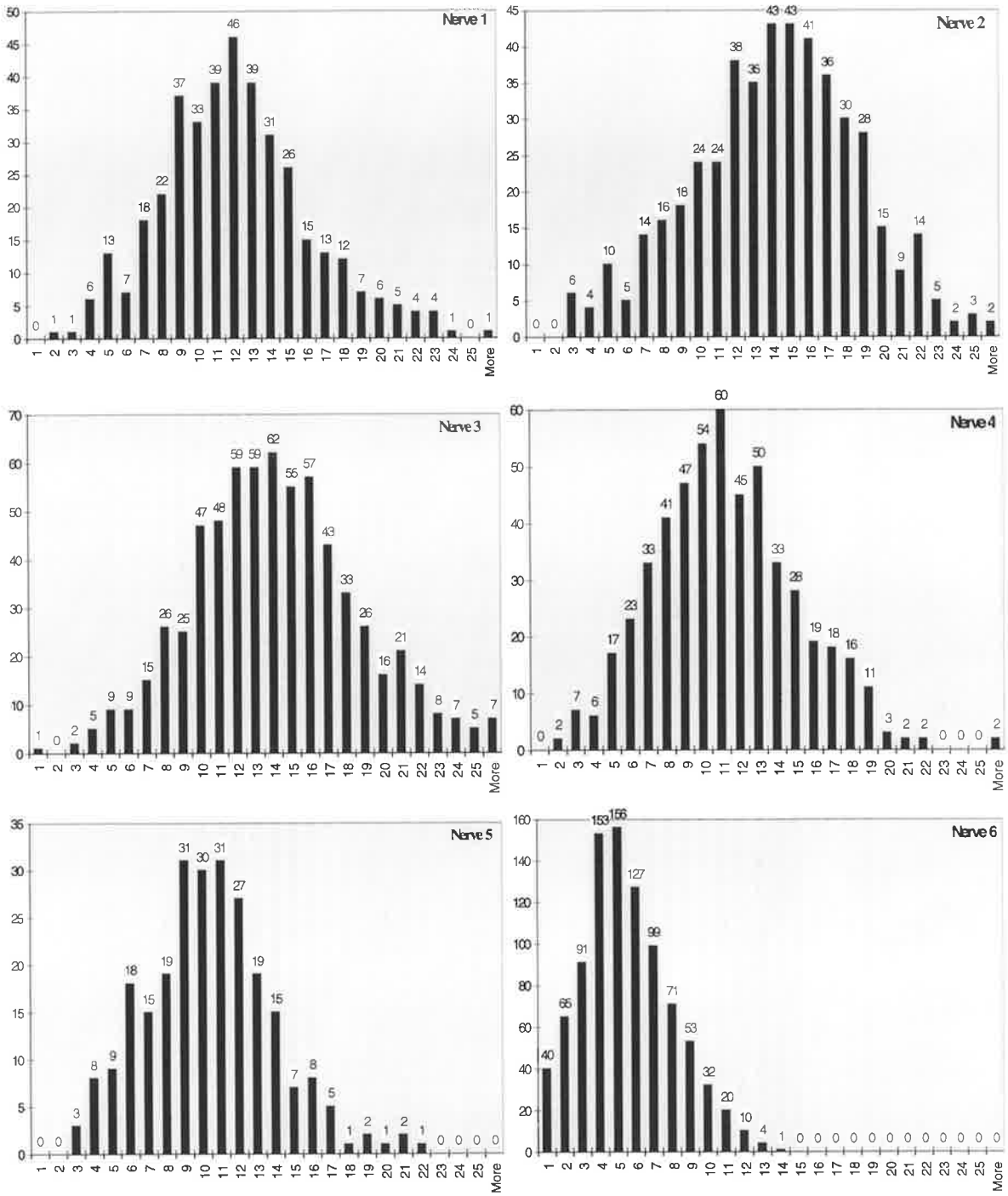

Figure 4.1-1: Distribution of myelinated fibre density in nerves No.1 to 6, expressed as number of MFs/measuring frame. The number of myelinated fibres per measuring frame is displayed on the abscissa, and the number of measuring frames is displayed on the ordinate.

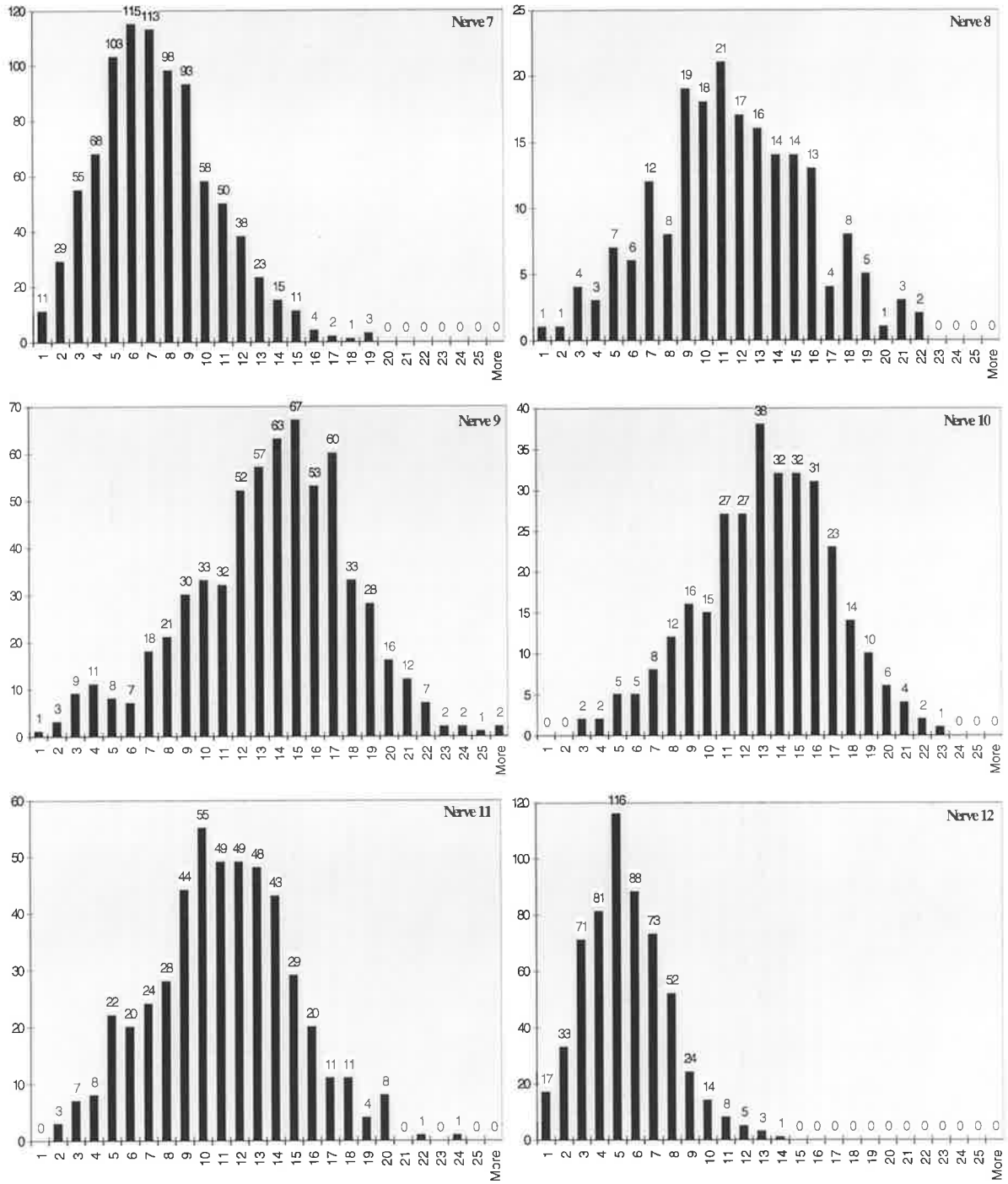

Figure 4.1-1: Distribution of myelinated fibre density in nerves No.7 to 12, expressed as number of MFs/measuring frame. The number of myelinated fibres per measuring frame is displayed on the abscissa, and the number of measuring frames is displayed on the ordinate.

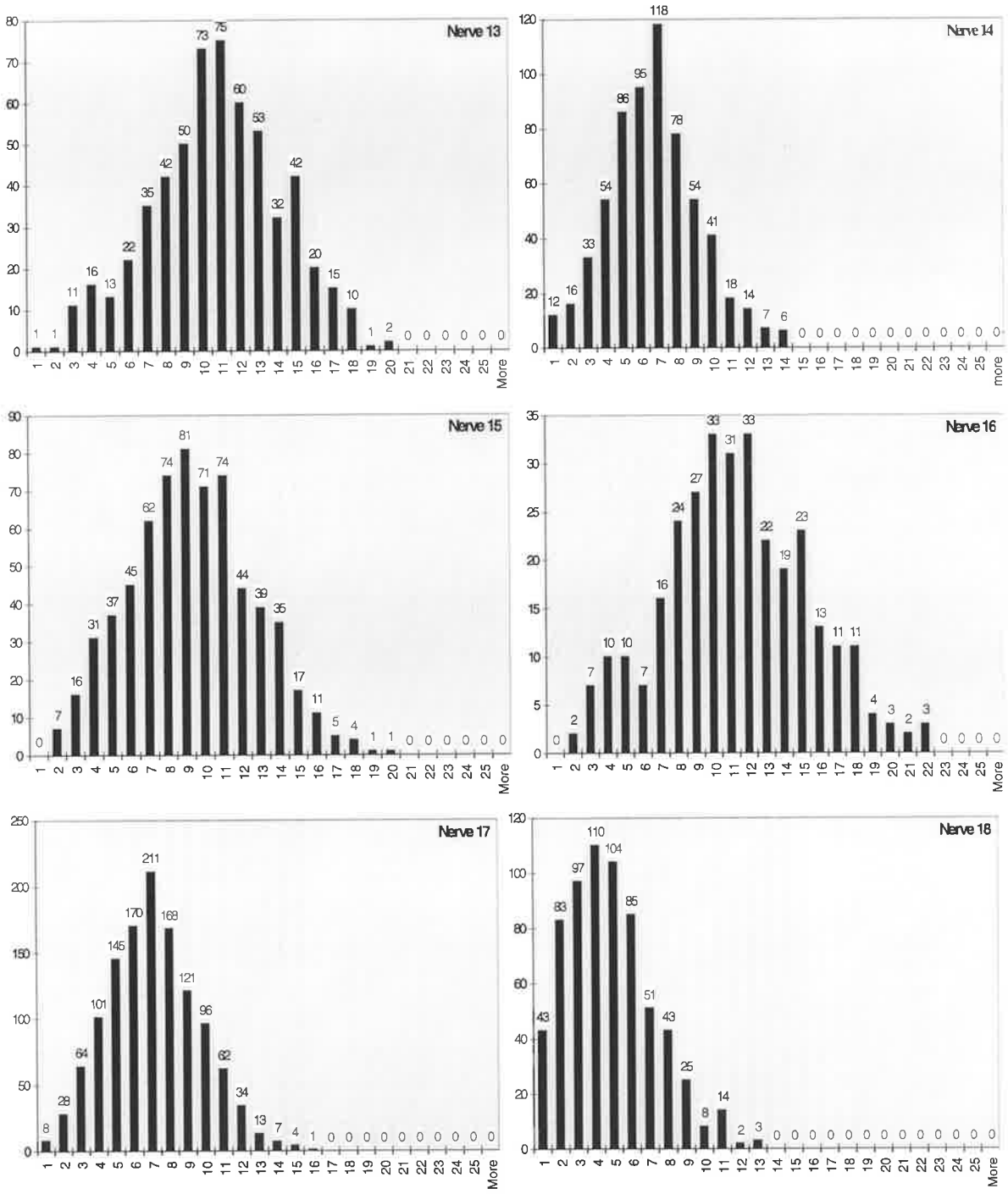

Figure 4.1-1: Distribution of myelinated fibre density in nerves No.13 to 18, expressed as number of MFs/measuring frame. The number of myelinated fibres per measuring frame is displayed on the abscissa, and the number of the measuring frames is displayed on the ordinate.

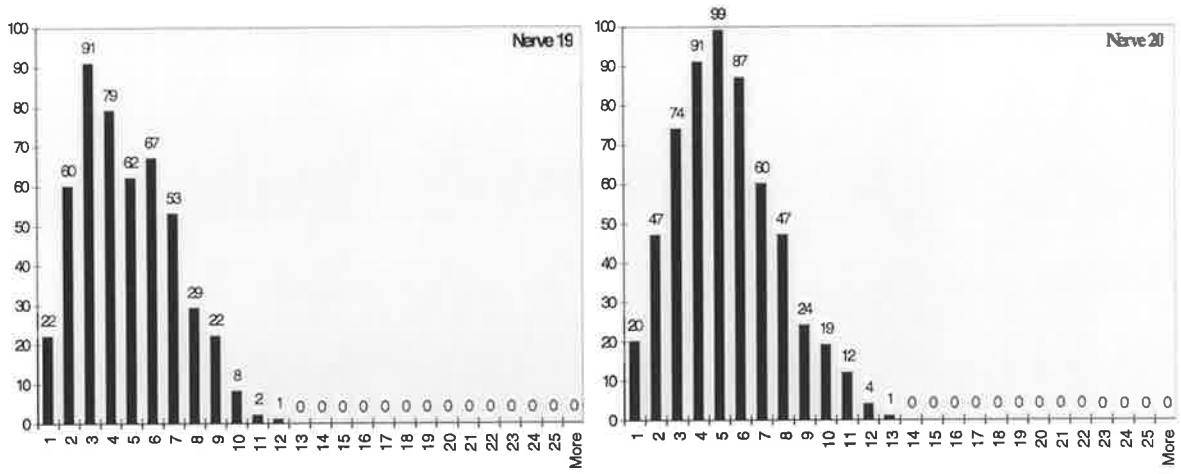

Figure 4.1-1: Distribution of myelinated fibre density nerves No.19 and 20, expressed as number of MFs/measuring frame. The number of myelinated fibres per measuring frame is displayed on the abscissa, and the number of the measuring frame is displayed on the ordinate.

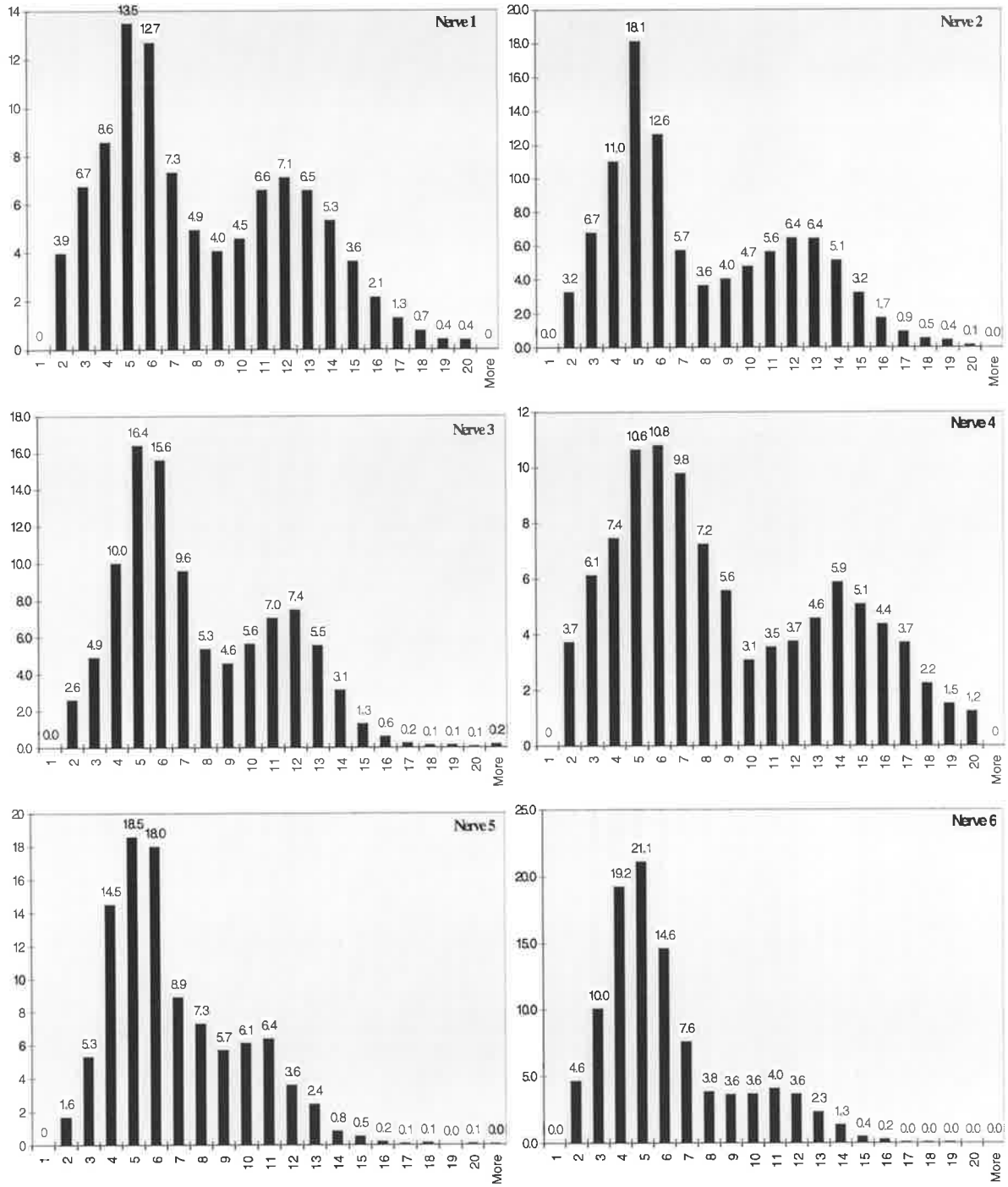

Figure 4.1-2: Histograms of fibre diameter, expressed as a percentage of the total fibre count for nerves No.1 to 6. Fibre diameter is displayed on the abscissa, and the percentage of the total myelinated fibre count is displayed on the ordinate.

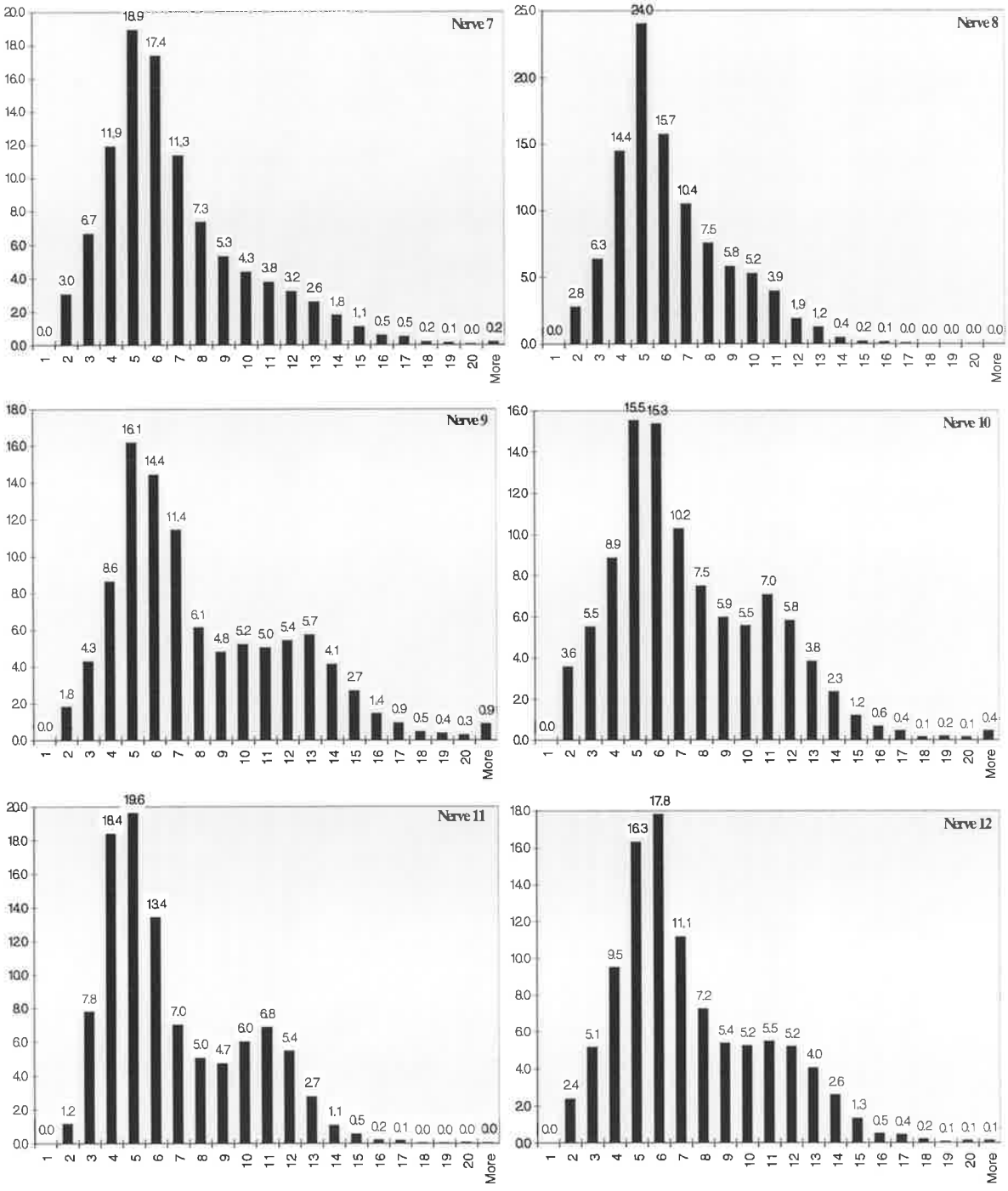

Figure 4.1-2: Histograms of fibre diameter, expressed as a percentage of the total fibre count for nerves No.7 to 12. Fibre diameter is displayed on the abscissa, and the percentage of the total myelinated fibre count is displayed on the ordinate.

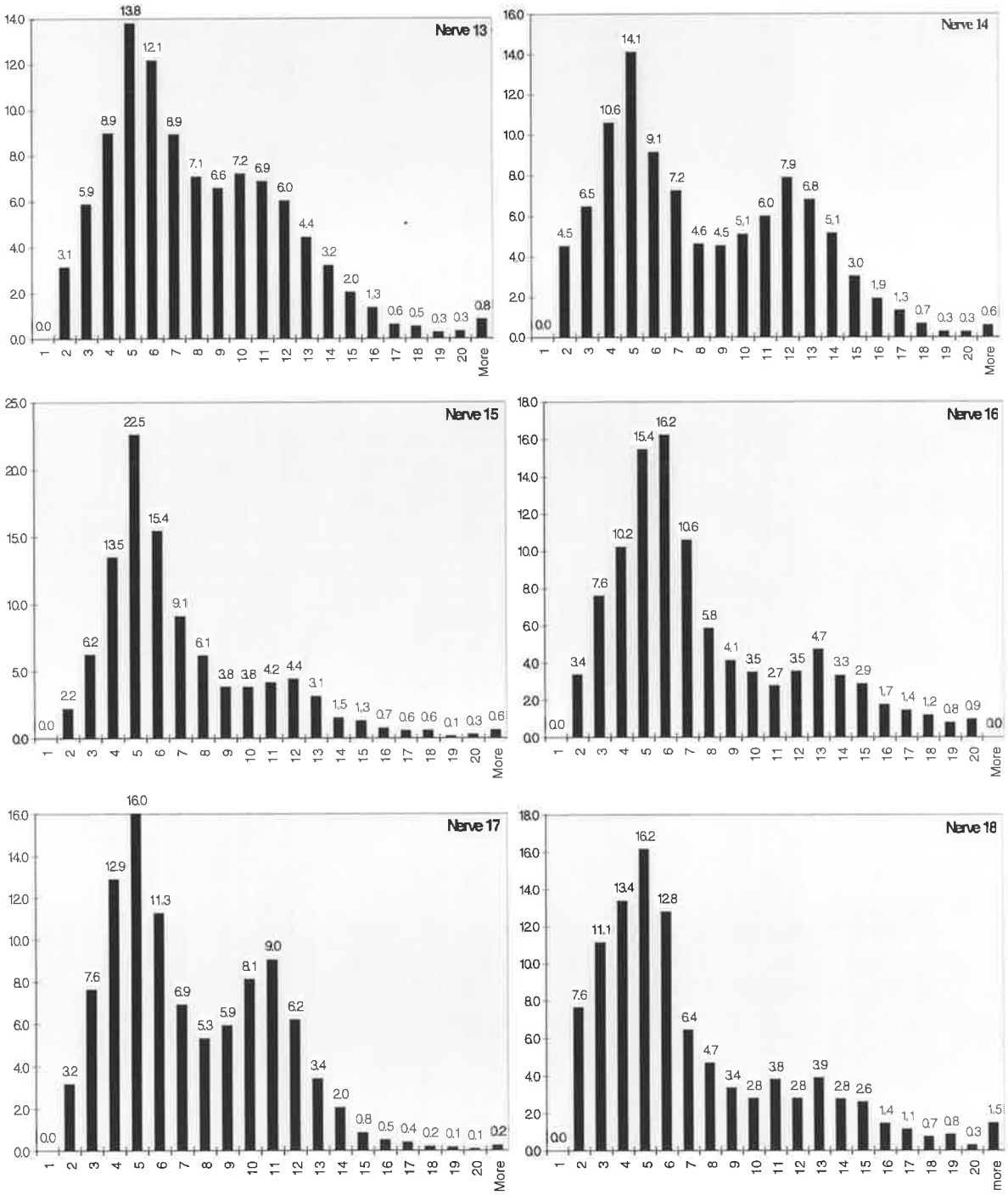

Figure 4.1-2: Histograms of fibre diameter, expressed as a percentage of the total fibre count for nerves No.13 to 18. Fibre diameter is displayed on the abscissa, and the percentage of the total myelinated fibre count is displayed on the ordinate.

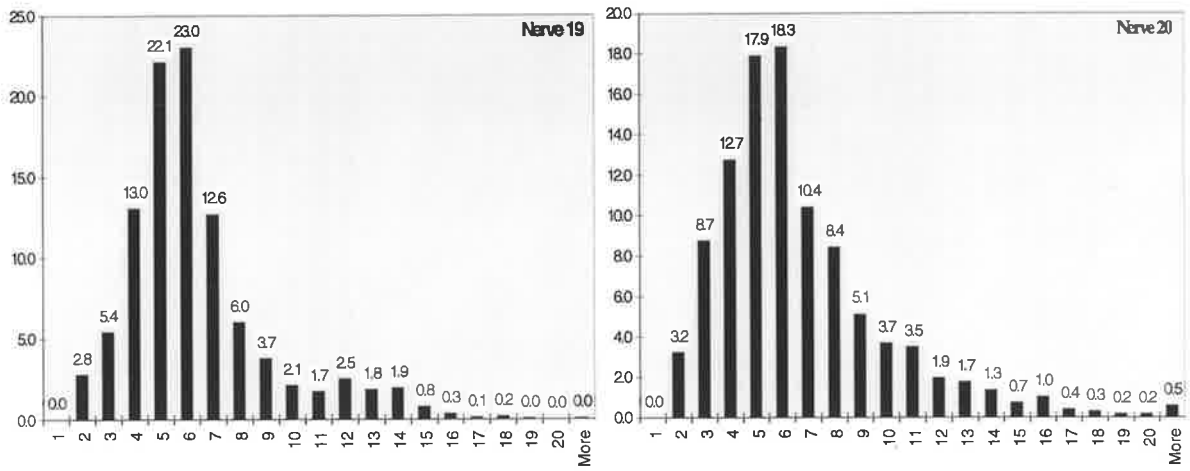

Figure 4.1-2: Histograms of fibre diameter, expressed as a percentage of the total fibre count for nerves No.19 and 20. Fibre diameter is displayed on the abscissa, and the percentage of the total myelinated fibre count is displayed on the ordinate.

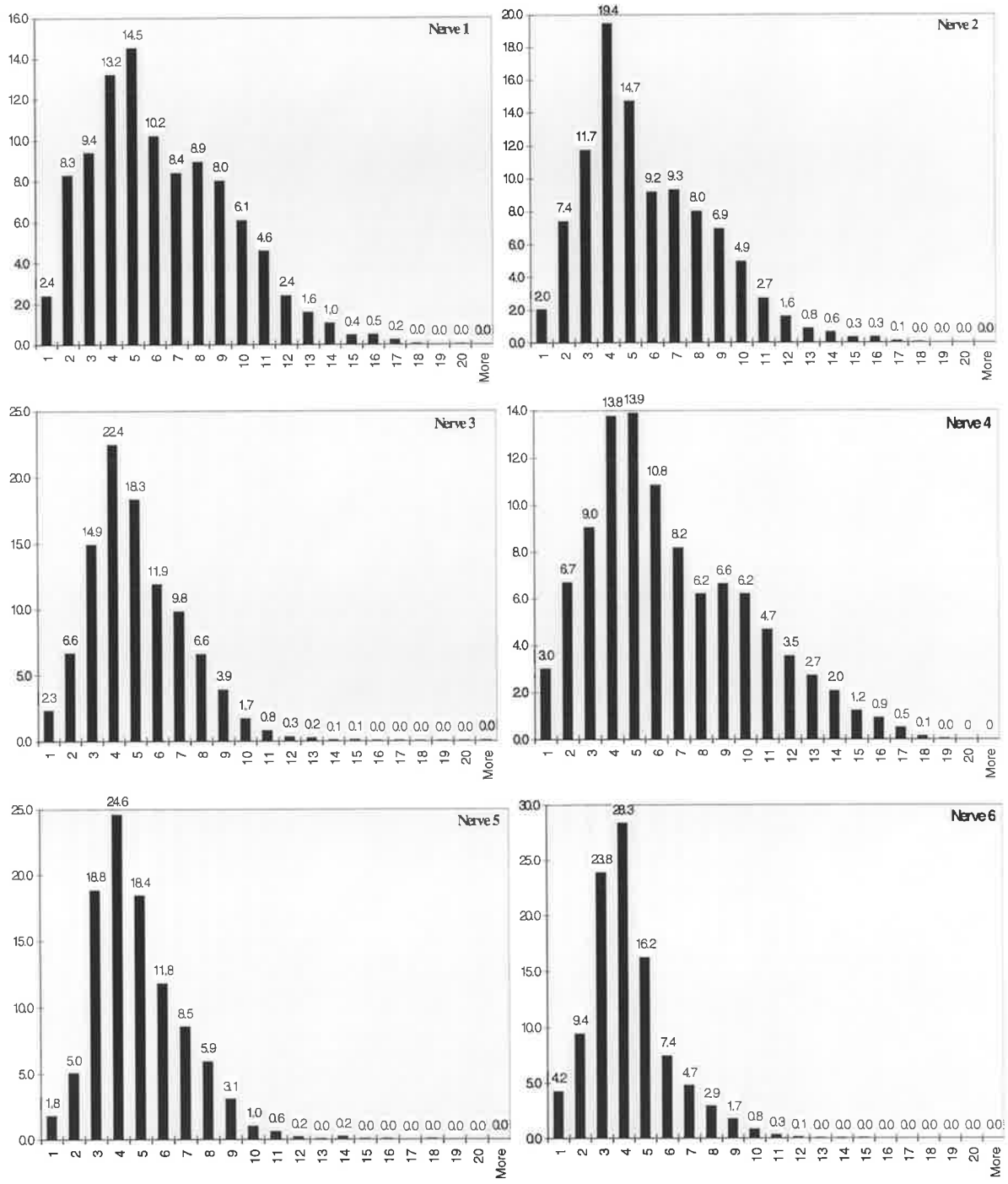

Figure 4.1-3: Histograms of axonal diameter, expressed as a percentage of the total fibre count for nerves No.1 to 6. Axonal diameter is displayed on the abscissa, and the percentage of the total myelinated fibre count is displayed on the ordinate.

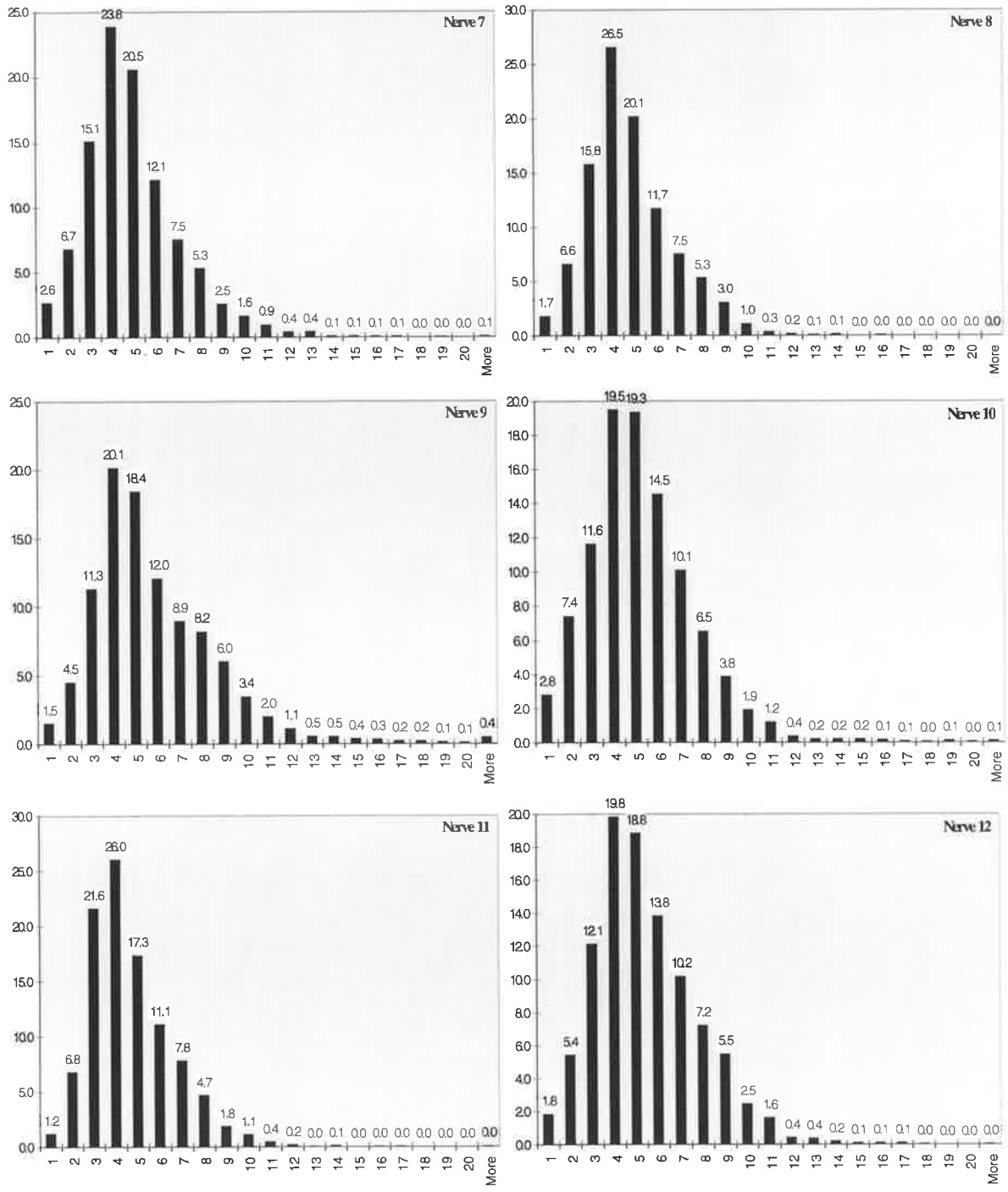

Figure 4.1-3: Histograms of axonal diameter, expressed as a percentage of the total fibre count for nerves No.7 to 12. Axonal diameter is displayed on the abscissa, and the percentage of the total myelinated fibre count is displayed on the ordinate.

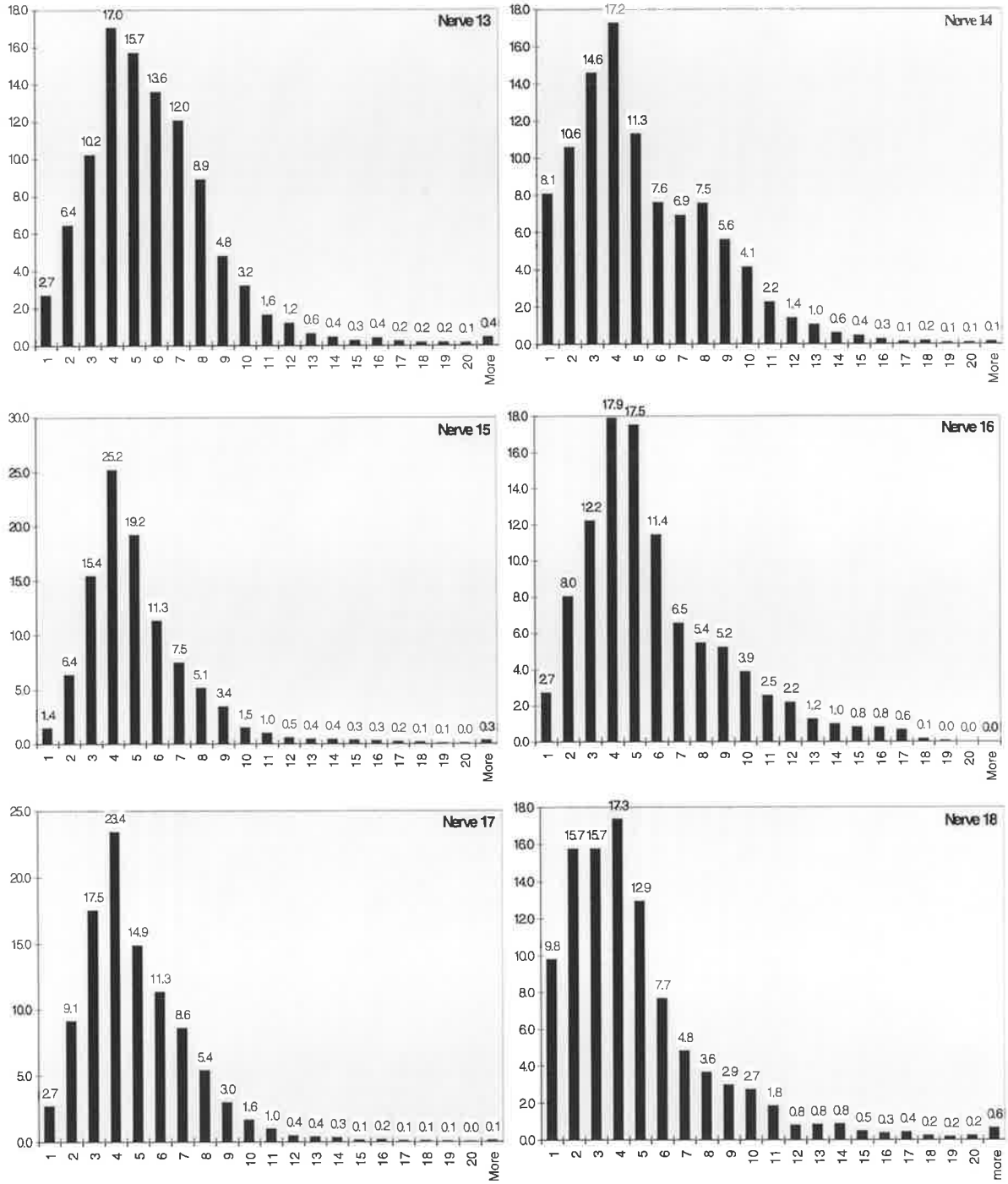

Figure 4.1-3: Histograms of axonal diameter, expressed as a percentage of the total fibre count for nerves No.13 to 18. Axonal diameter is displayed on the abscissa, and the percentage of the total myelinated fibre count is displayed on the ordinate.

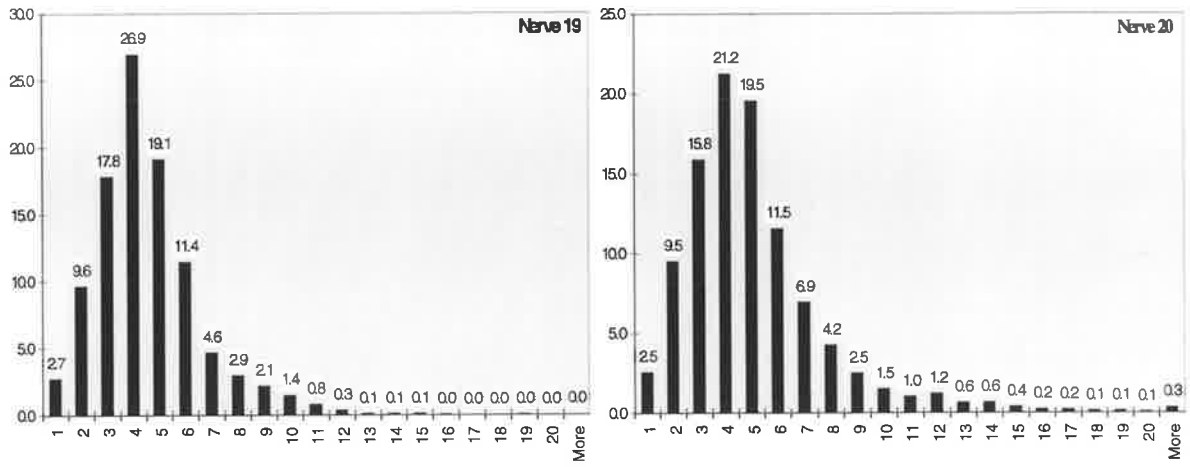

Figure 4.1-3: Histograms of axonal diameter, expressed as a percentage of the total fibre count for nerves No.19 and 20. Axonal diameter is displayed on the abscissa, and the percentage of the total myelinated fibre count is displayed on the ordinate.

Table 4.2-1

Sample Field	NMF	TFA	TTFA%	mMFD	MFDSD	Probability	
total	4678	0.9482	100.00	4934	1676	Wilcox.	K-S
1st Fasci.	1375	0.2940	31.01	4677	1392	0.1984	0.4150
2nd Fasci.*	706	0.1225	12.92	5763	2092	**0.0042**	0.0641
3rd Fasci.*	556	0.1005	10.59	5535	1972	**0.0389**	**0.0336**
4th Fasci.*	620	0.1421	14.99	4363	1068	**0.0133**	0.0697
5th Fasci.	902	0.1691	17.83	5336	1706	0.0858	0.3018
6th Fasci.*	327	0.0809	8.53	4045	1491	**0.0067**	0.1312
7th Fasci.	192	0.0392	4.13	4898	1549	0.6892	0.7719
enery 2nd	2299	0.4704	49.61	4887	1695	0.7663	1.0000
every 3rd	1606	0.3161	33.33	5081	1862	0.5296	0.9382
every 4th	1200	0.2377	25.06	5049	1715	0.5931	0.9979
every 5th	984	0.1911	20.16	5149	1948	0.4127	0.9195
every 6th	832	0.1642	17.31	5069	1869	0.7649	0.9841
every 7th	714	0.1397	14.73	5113	1921	0.7952	0.9977
every 8th	624	0.1225	12.92	5094	1761	0.6466	0.9998
every 9th	583	0.1127	11.89	5173	1949	0.5205	0.6589
every 10 th	495	0.0980	10.34	5051	1916	0.6098	0.9987

Table 4.2-2

Sample Field	NMF	TFA	TTFA%	mMFD	MFDSD	Probability	
total	6591	1.1393	100.00	5785	1855	Wilcox.	K-S
1st Fasci.*	1987	0.3112	27.31	6386	1942	**0.0007**	**0.0086**
2nd Fasci.*	905	0.1764	15.48	5130	1592	**0.0023**	**0.0184**
3rd Fasci.*	1114	0.1789	15.70	6229	1713	**0.0442**	0.1165
4th Fasci.	597	0.1029	9.03	5802	1955	0.9302	0.8842
5th Fasci.	1015	0.1813	15.91	5598	1683	0.3390	0.7188
6th Fasci.*	756	0.1470	12.90	5143	1844	**0.0188**	0.0779
7th Fasci.	217	0.0417	3.66	5210	1630	0.1402	0.0790
every 2nd	3293	0.5660	49.68	5819	1904	0.8980	1.0000
every 3rd	2227	0.3798	33.33	5864	1819	0.5462	0.9901
every 4th	1645	0.2867	25.16	5739	1912	0.5568	0.9247
every 5th	1349	0.2352	20.65	5736	1850	0.8529	0.9986
every 6th	1176	0.1911	16.77	6154	1719	*0.0949*	0.3996
every 7th	969	0.1691	14.84	5732	1930	0.7527	0.9986
every 8th	864	0.1470	12.90	5878	1856	0.8042	0.9762
every 9th	803	0.1299	11.40	6184	1631	0.1272	0.2553
every 10th	709	0.1225	10.75	5788	1894	0.9094	1.0000

Table 4.2-3

Sample Field	NMF	TFA	TTFA%	mMFD	MFDSD	Probability	
total	9291	1.6146	100.00	5755	1842	Wilcox	K-S
1st Fasci.*	1048	0.2132	13.20	4917	1345	**0.0001**	**0.0001**
2nd Fasci.*	1134	0.2401	14.87	4723	1552	**0.0001**	**0.0001**
3rd Fasci.	724	0.1348	8.35	5373	1671	0.1230	0.4991
4th Fasci.	686	0.1152	7.13	5957	1573	0.3107	0.7608
5th Fasci.*	396	0.0613	3.79	6465	1686	**0.0438**	0.1828
6th Fasci.*	854	0.1348	8.35	6338	1913	**0.0254**	0.2359
7th Fasci.	1579	0.2646	16.39	5967	1922	0.1801	0.7409
8th Fasci.*	253	0.0368	2.28	6884	1818	**0.0236**	0.0871
9th Fasci.	53	0.0098	0.61	5408	841	0.6880	0.8983
10th Fasci.*	1123	0.1593	9.86	7052	2058	**0.0001**	**0.0006**
11th Fasci.	359	0.0613	3.79	5861	1719	0.4249	0.3078
12th Fasci.	1082	0.1838	11.38	5888	1581	0.4031	0.1826
every 2nd	4553	0.7963	49.32	5792	1869	0.8290	1.0000
every 3rd	3180	0.5366	33.23	5927	1791	0.3137	0.9555
every 4th	2395	0.4067	25.19	5889	1798	0.7080	0.8127
every 5th	1866	0.3283	20.33	5684	1696	0.7636	0.9900
every 6th	1634	0.2744	16.99	5955	1821	0.4523	0.9686
every 7th	1370	0.2401	14.87	5706	1992	0.7948	0.9999
every 8th	1226	0.2083	12.90	5887	1790	0.7448	0.8658
every 9th	1090	0.1838	11.38	5773	1528	0.7706	0.9962
every 10th	890	0.1740	10.77	5663	1667	0.6232	0.9973

Table 4.2-4

Sample Field	NMF	TFA	TTFA%	m MFD	MFDSD	Probability	
total	5836	1.2716	100.00	4590	1615	Wilcox.	K-S
1st Fasci.	706	0.1421	11.18	4968	2045	0.1862	0.4622
2nd Fasci.	305	0.0711	5.59	4293	1252	0.4557	0.2791
3rd Fasci.	90	0.0196	1.54	4592	1128	0.8769	0.9977
4th Fasci.*	1041	0.2058	16.18	5058	1798	**0.0336**	0.1952
5th Fasci.	536	0.1225	9.63	4376	1416	0.5285	0.9921
6th Fasci.	421	0.0858	6.74	4910	1678	0.1671	0.1952
7th Fasci.	417	0.0858	6.74	4863	1300	0.1992	0.3803
8th Fasci.	419	0.0980	7.71	4276	1212	0.2239	0.0621
9th Fasci.	384	0.0907	7.13	4236	1226	0.1837	0.3016
10th Fasci.	677	0.1470	11.56	4605	1323	0.9007	0.9391
11th Fasci.	186	0.0466	3.66	3996	1151	0.1212	0.2834
12th Fasci.*	354	0.0907	7.13	3905	2008	**0.0190**	**0.0169**
13th Fasci.	300	0.0662	5.20	4535	1820	0.6303	0.9740
every 2nd	2884	0.6272	49.33	4598	1686	0.8647	1.0000
every 3rd	1920	0.4239	33.33	4530	1514	0.7663	1.0000
every 4th	1475	0.3210	25.24	4596	1748	0.8850	1.0000
every 5th	1245	0.2622	20.62	4749	1607	0.2831	0.9467
every 6th	1016	0.2181	17.15	4659	1422	0.6282	0.9649
every 7th	901	0.1887	14.84	4776	1710	0.3578	0.9279
every 8th	809	0.1740	13.68	4651	1768	0.7724	0.8933
every 9th	681	0.1495	11.75	4557	1621	0.8968	0.9996
every 10th	649	0.1348	10.60	4816	1589	0.2559	0.7024

Table 4.2-5

Sample Field	NMF	TFA	TTFA%	mMFD	MFDSD	Probability	
total	2610	0.6174	100.00	4227	1441	Wilcox.	K-S
1st Fasci.	760	0.1691	27.38	4496	1600	0.2596	0.8668
2nd Fasci.	505	0.1250	20.24	4042	1477	0.4078	0.7791
3th Fasci.	697	0.1740	28.17	4007	1353	0.1878	0.5620
4th Fasci.	530	0.1176	19.05	4507	1304	0.1133	0.1759
5th Fasci.	118	0.0319	5.16	3705	1020	0.2208	0.4639
every 2nd	1339	0.3038	49.20	4408	1465	0.2536	0.7756
every 3rd	877	0.2058	33.33	4261	1520	0.7940	1.0000
every 4th	666	0.1544	25.00	4315	1471	0.6253	0.9368
every 5th	523	0.1250	20.24	4186	1529	0.6715	0.9486
every 6th	462	0.1054	17.06	4385	1182	0.3036	0.6356
every 7th	394	0.0907	14.68	4346	1115	0.3426	0.3400
every 8th	342	0.0809	13.10	4230	1357	0.9380	0.7816
every 9th	311	0.0735	11.90	4231	1167	0.7168	0.9705
every 10th	290	0.0637	10.32	4553	1648	0.4673	0.9994

Table 4.2-6

Sample Field	NMF	TFA	TTFA	mMFD	MFDSD	Probability	
total	5057	2.2589	100.00	2239	1035	Wilcox.	K-S
1st Fasci.	720	0.3430	15.18	2099	924	0.2757	0.5601
2nd Fasci.	244	0.1103	4.88	2213	890	0.8907	0.8580
3rd Fasci.	340	0.1666	7.38	2041	993	0.0616	0.0841
4th Fasci.	499	0.2303	10.20	2167	1099	0.4317	0.5006
5th Fasci.	39	0.0221	0.98	1769	850	0.1960	0.7241
6th Fasci.	733	0.3210	14.21	2284	1071	0.8362	1.0000
7th Fasci.*	791	0.3063	13.56	2583	1097	**0.0005**	**0.0197**
8th Fasci.*	336	0.1152	5.10	2918	1070	**0.0001**	**0.0006**
9th Fasci.	617	0.2842	12.58	2171	914	0.7952	0.5601
10th Fasci.*	298	0.1127	4.99	2644	1074	**0.0139**	**0.0081**
11th Fasci.*	440	0.2475	10.95	1778	823	**0.0001**	**0.0076**
every 2nd	2529	1.1221	49.67	2254	1057	0.8021	1.0000
every 3rd	1693	0.7571	33.51	2236	1016	0.9490	1.0000
every 4th	1314	0.5660	25.05	2322	1033	0.2396	0.8379
every 5th	1070	0.4533	20.07	2361	1124	0.2257	0.7932
every 6th	851	0.3871	17.14	2198	1052	0.6675	0.9998
every 7th	769	0.3332	14.75	2302	1074	0.6129	0.9815
every 8th	692	0.2916	12.91	2374	1082	0.2195	0.8377
every 9th	582	0.2597	11.50	2241	1014	0.9652	0.9693
every 10th	550	0.2328	10.30	2363	1182	0.3834	0.9499

Table 4.2-7

Sample Field	NMF	TFA	TTFA%	mMFD	MFDSD	Probability	
total	6555	2.1805	100.00	3006	1307	Wilcox.	K-S
1st Fasci.*	482	0.1421	6.52	3392	1122	**0.0102**	0.1191
2nd Fasci.*	943	0.2646	12.13	3564	1347	**0.0001**	**0.0053**
3rd Fasci.	62	0.0245	1.12	2531	898	0.3337	0.6466
4th Fasci.*	941	0.3479	15.96	2705	1095	**0.0270**	0.1737
5th Fasci.*	507	0.2009	9.21	2524	923	**0.0016**	**0.0046**
6th Fasci.*	439	0.2107	9.66	2084	885	**0.0001**	**0.0001**
7th Fasci.*	1202	0.3234	14.83	3717	1276	**0.0001**	**0.0001**
8th Fasci.*	1231	0.4753	21.80	2590	1096	**0.0001**	**0.0134**
9th Fasci.*	475	0.1127	5.17	4215	1642	**0.0001**	**0.0001**
10th Fasci.*	273	0.0784	3.60	3482	1278	**0.0265**	0.1334
every 2nd	3291	1.0903	50.00	3019	1331	0.8490	1.0000
every 3rd	2233	0.7252	33.26	3079	1286	0.2935	0.6276
every 4th	1634	0.5537	25.39	2951	1399	0.4763	0.9107
every 5th	1300	0.4435	20.34	2932	1281	0.6509	0.9306
every 6th	1171	0.3724	17.08	3144	1328	*0.1743*	0.5816
every 7th	964	0.3234	14.83	2981	1315	0.8625	1.0000
every 8th	820	0.2842	13.03	2885	1353	0.4004	0.9572
every 9th	766	0.2475	11.35	3096	1218	0.3665	0.8855
every 10th	658	0.2303	10.56	2857	1148	0.5182	0.8490

Table 4.2-8

Sample Field	NMF	TFA	TTFA%	mMFD	MFDSD	Probability	
total	2288	0.4827	100.00	4740	1726	Wilcox.	K-S
1st Fasci.*	372	0.0686	14.21	5423	2356	0.0511	**0.0141**
2nd Fasci.	422	0.0833	17.26	5066	1853	0.3315	0.3704
3rd Fasci.	1039	0.2328	48.22	4464	1395	0.2155	0.1906
4th Fasci.	414	0.0882	18.27	4694	1790	0.8981	0.9575
5th Fasci.	41	0.0098	2.03	4184	391	0.4180	0.2979
every 2nd	1119	0.2401	49.75	4661	1700	0.8229	0.9996
every 3rd	781	0.1593	32.99	4904	1616	0.5579	0.9892
every 4th	585	0.1225	25.38	4776	1602	0.8017	0.9816
every 5th	486	0.0980	20.30	4959	1652	0.5579	0.9994
every 6th	419	0.0833	17.26	5030	1416	0.3370	0.8472
every 7th	342	0.0711	14.72	4814	1925	0.7907	0.9998
every 8th	338	0.0662	13.71	5110	1770	0.2115	0.2395
every 9th	306	0.0564	11.68	5430	1573	*0.0764*	0.3664
every 10th	255	0.0539	11.17	4731	1684	0.9419	1.0000

Table 4.2-9

Sample Field	NMF	TFA	TTFA%	MFD	MFDSD	Probability	
total	8555	1.5411	100.00	5551	1769	Wilcox.	K-S
1st Fasci.	1124	0.2009	13.04	5595	1817	0.8713	1.0000
2nd Fasci.*	1267	0.2034	13.20	6231	1645	**0.0004**	**0.0120**
3rd Fasci.	1430	0.2573	16.69	5559	1856	0.7430	0.9995
4th Fasci.	955	0.1715	11.13	5569	1476	0.9247	0.9575
5th Fasci.	404	0.0662	4.29	6107	2083	0.1373	0.2190
6th Fasci.	982	0.1764	11.45	5567	1632	0.7929	0.9936
7th Fasci.	1033	0.1789	11.61	5776	1838	0.3498	0.8950
8th Fasci.*	889	0.1887	12.24	4712	1663	**0.0001**	**0.0003**
9th Fasci.*	471	0.0980	6.36	4806	1472	**0.0036**	**0.0181**
every 2nd	4289	0.7644	49.60	5610	1757	0.7700	0.9980
every 3rd	2825	0.5121	33.23	5517	1771	0.7846	0.9962
every 4th	2115	0.3871	25.12	5464	1954	0.6124	0.8648
every 5th	1768	0.3161	20.51	5594	1697	0.6783	0.8097
every 6th	1435	0.2622	17.01	5474	1838	0.6111	0.9992
every 7th	1293	0.2254	14.63	5736	1830	0.4546	0.9113
every 8th	1122	0.1985	12.88	5654	1843	0.6628	0.9064
every 9th	1009	0.1764	11.45	5720	1679	0.4985	0.9641
every 10th	940	0.1642	10.65	5726	1699	0.4329	0.7442

Table 4.2-10

Sample Field	NMF	TFA	TTFA%	mMFD	MFDSD	Probability	
total	4158	0.7644	100.00	5440	1524	Wilcox.	K-S
1st Fasci.	1321	0.2401	31.41	5502	1552	0.7870	0.9954
2nd Fasci.	1321	0.2426	31.73	5446	1545	0.8531	0.9878
3rd Fasci.	943	0.1813	23.72	5201	1308	0.2264	0.5563
4th Fasci.	337	0.0539	7.05	6252	1729	**0.0282**	0.0504
5th Fasci.	127	0.0221	2.88	5760	1215	0.5684	0.9292
6th Fasci.	109	0.0245	3.21	4449	1682	0.0615	0.2133
every 2nd	2062	0.3798	49.68	5430	1510	0.8273	1.0000
every 3rd	1371	0.2548	33.33	5401	1604	0.9586	0.9992
every 4th	1053	0.1960	25.64	5372	1544	0.6253	0.9786
every 5th	860	0.1568	20.51	5485	1502	0.7152	0.9993
every 6th	701	0.1348	17.63	5202	1650	0.3388	0.6293
every 7th	625	0.1127	14.74	5546	1431	0.5595	0.9917
every 8th	569	0.1029	13.46	5530	1588	0.7139	0.9939
every 9th	474	0.0882	11.54	5374	1649	0.8558	0.9995
every 10th	438	0.0809	10.58	5417	1514	0.9332	0.9999

Table 4.2-11

Sample Field	NMF	TFA	TTFA%	mMFD	MFDSD	Probability	
total	5402	1.1883	100.00	4546	1548	Wilcox.	K-S
1st Fasci.	179	0.0417	3.51	4298	1652	0.4092	0.4515
2nd Fasci.*	730	0.1348	11.34	5417	1637	**0.0001**	**0.0001**
3rd Fasci.	421	0.1005	8.45	4191	1477	0.1174	0.3888
4th Fasci.	248	0.0613	5.15	4049	1580	0.1330	0.6069
5th Fasci.	444	0.0980	8.25	4531	1527	0.9844	0.9914
6th Fasci.	464	0.1005	8.45	4619	1441	0.6707	0.8685
7th Fasci.	599	0.1397	11.75	4289	1498	0.1969	0.2415
8th Fasci.*	186	0.0490	4.12	3796	1085	**0.0173**	0.1239
9th Fasci.	707	0.1495	12.58	4731	1635	0.3824	0.8063
10th Fasci.	365	0.0760	6.39	4805	1436	0.2814	0.7873
11th Fasci.	699	0.1544	12.99	4529	1357	0.8250	0.9848
12th Fasci.	360	0.0833	7.01	4322	1642	0.4210	0.7315
every 2nd	2649	0.5831	49.07	4543	1572	0.8467	1.0000
every 3rd	1801	0.3945	33.20	4566	1562	0.8613	0.9989
every 4th	1361	0.2965	24.95	4591	1613	0.9054	0.9673
every 5th	1054	0.2401	20.21	4290	1403	0.4468	0.9323
every 6th	938	0.2034	17.11	4613	1570	0.7493	0.9997
every 7th	867	0.1764	14.85	4915	1282	*0.0554*	0.2624
every 8th	744	0.1519	12.78	4898	1736	0.2481	0.9617
every 9th	655	0.1421	11.96	4609	1716	0.9706	0.8867
every 10th	530	0.1250	10.52	4242	1440	0.2200	0.8358

Table 4.2-12

Sample Field	NMF	TFA	TTFA%	mMFD	MFDSD	Probability	
total	3211	1.4357	100.00	2237	954	Wilcox.	K-S
1st Fasci.*	217	0.0858	5.97	2531	999	**0.0456**	0.1431
2nd Fasci.	903	0.3871	26.96	2333	966	0.3621	0.9975
3rd Fasci.	976	0.4631	32.25	2108	963	0.1036	0.4655
4th Fasci.	586	0.2622	18.26	2235	855	0.9528	0.8882
5th Fasci.	349	0.1715	11.95	2035	946	0.1224	0.3089
6th Fasci.*	180	0.0662	4.61	2721	913	**0.0102**	0.0581
every 2nd	1556	0.7130	49.66	2182	944	0.4026	0.9736
every 3rd	1070	0.4802	33.45	2228	990	0.8361	1.0000
every 4th	792	0.3626	25.26	2184	897	0.5399	0.9694
every 5th	666	0.2916	20.31	2284	1013	0.7695	0.9946
every 6th	537	0.2450	17.06	2192	1047	0.5126	0.8334
every 7th	461	0.2083	14.51	2214	832	0.8782	0.9610
every 8th	417	0.1862	12.97	2240	915	0.9195	0.9966
every 9th	359	0.1617	11.26	2220	961	0.8671	0.9986
every 10th	351	0.1470	10.24	2388	1078	0.3927	0.8364

Table 4.2-13

Sample Field	NMF	TFA	TTFA%	mMFD	MFDSD	Probability	
total	6184	1.4063	100.00	4397	1412	Wilcox.	K-S
1st Fasci.*	1263	0.2524	17.94	5005	1334	**0.0001**	**0.0004**
2nd Fasci.	730	0.1740	12.37	4197	1331	0.2830	0.9495
3rd Fasci.	777	0.1764	12.54	4405	1440	0.9571	0.9957
4th Fasci.*	527	0.1348	9.58	3911	1346	**0.0220**	0.1800
5th Fasci.*	743	0.1519	10.80	4891	1501	**0.0133**	0.2418
6th Fasci.*	570	0.1201	8.54	4748	1515	**0.0486**	0.2359
7th Fasci.*	442	0.1176	8.36	3759	1078	**0.0017**	**0.0255**
8th Fasci.	90	0.0245	1.74	3673	1138	0.0831	0.1693
9th Fasci.*	353	0.0931	6.62	3792	1280	**0.0087**	0.0538
10th Fasci.	689	0.1617	11.50	4261	1253	0.3122	0.5132
every 2nd	3057	0.6983	49.65	4378	1342	0.9528	0.9944
every 3rd	2041	0.4680	33.28	4362	1493	0.9629	0.9272
every 4th	1539	0.3577	25.44	4302	1394	0.6065	0.9914
every 5th	1270	0.2867	20.38	4430	1225	0.9996	0.9734
every 6th	1029	0.2377	16.90	4330	1407	0.7407	0.8203
every 7th	915	0.2083	14.81	4394	1191	0.9570	0.9520
every 8th	809	0.1813	12.89	4462	1360	0.5991	0.9538
every 9th	710	0.1642	11.67	4325	1504	0.8119	1.0000
every 10th	657	0.1495	10.63	4396	1346	0.9968	0.9918

Table 4.2-14

Sample Field	NMF	TFA	TTFA%	mMFD	MFDSD	Probability	
total	4245	1.5484	100.00	2742	1040	Wilcox.	K-S
1st Fasci.*	523	0.2083	13.45	2507	991	**0.0381**	0.4696
2nd Fasci.	655	0.2426	15.66	2700	968	0.7269	0.9747
3rd Fasci.*	83	0.0417	2.69	1993	815	**0.0027**	**0.0027**
4th Fasci	327	0.1250	8.07	2617	942	0.4438	0.9186
5th Fasci.	470	0.1715	11.08	2741	904	0.9840	0.9972
6th Fasci.	445	0.1544	9.97	2883	950	0.2694	0.9551
7th Fasci.*	978	0.3038	19.62	3219	1102	**0.0001**	**0.0004**
8th Fasci.*	229	0.0980	6.33	2337	891	**0.0144**	0.2386
9th Fasci.	535	0.2034	13.13	2631	1148	0.3947	0.9777
every 2nd	2108	0.7669	49.53	2749	1031	0.8795	0.9439
every 3rd	1404	0.5145	33.23	2729	1041	0.9629	1.0000
every 4th	1060	0.3896	25.16	2721	992	0.6044	0.9828
every 5th	904	0.3136	20.25	2883	1009	0.2093	0.3790
every 6th	737	0.2646	17.09	2785	1026	0.8053	0.9744
every 7th	598	0.2254	14.56	2653	1056	0.6166	0.9836
every 8th	543	0.2009	12.97	2703	961	0.6530	0.9356
every 9th	475	0.1789	11.55	2656	1007	0.3161	0.5512
every 10th	441	0.1617	10.44	2727	1130	0.5174	0.3307

Table 4.2-15

Sample Field	NMF	TFA	TTFA%	mMFD	MFDSD	Probability	
total	6072	1.6048	100.00	3784	1358	Wilcox.	K-S
1st Fasci.*	753	0.1789	11.15	4210	1402	**0.0202**	0.2417
2nd Fasci.*	685	0.2009	12.52	3410	1366	**0.0114**	0.0528
3rd Fasci.	708	0.1911	11.91	3705	1305	0.7836	0.9740
4th Fasci.	179	0.0466	2.90	3845	1461	0.9254	0.9981
5th Fasci.	287	0.0809	5.04	3550	1111	0.4001	0.5641
6th Fasci.	653	0.1764	10.99	3702	1554	0.4039	0.7402
7th Fasci.	99	0.0245	1.53	4041	1704	0.7372	0.9479
8th Fasci.	520	0.1446	9.01	3597	1094	0.3809	0.6005
9th Fasci.	220	0.0539	3.36	4082	1464	0.2159	0.4075
10th Fasci.	572	0.1593	9.92	3592	1396	0.3964	0.5946
11th Fasci.*	1052	0.2548	15.88	4129	1323	**0.0146**	0.0708
12th Fasci.	344	0.0931	5.80	3695	1048	0.7036	0.9116
every 2nd	3072	0.7938	49.47	3870	1339	0.4019	0.9980
every 3rd	2005	0.5341	33.28	3754	1418	0.9096	0.9862
every 4th	1570	0.4067	25.34	3860	1360	0.5360	0.9929
every 5th	1255	0.3308	20.61	3794	1359	0.9463	1.0000
every 6th	1068	0.2720	16.95	3927	1521	0.3697	0.7290
every 7th	910	0.2377	14.81	3829	1503	0.9968	0.9961
every 8th	795	0.2058	12.82	3863	1636	0.9537	0.9828
every 9th	722	0.1838	11.45	3929	1697	0.5812	0.9094
every10th	678	0.1691	10.53	4011	1734	0.5685	0.8696

Table 4.2-16

Sample Field	NMF	TFA	TTFA%	mMFD	MFDSD	Probability	
total	3505	0.7620	100.00	4600	1673	Wilcox.	K-S
1st Fasci.*	627	0.1225	16.08	5118	1755	**0.0453**	0.1433
2nd Fasci.	969	0.2254	29.58	4299	1521	0.1364	0.3325
3rd Fasci.*	603	0.1054	13.83	5724	1698	**0.0001**	**0.0028**
4th Fasci.	89	0.0221	2.89	4036	1107	0.2307	0.2626
5th Fasci.	156	0.0343	4.50	4548	1448	0.9860	0.9975
6th Fasci.	377	0.0882	11.58	4274	1329	0.3432	0.3119
7th Fasci.	461	0.1078	14.15	4276	1556	0.3538	0.7826
8th Fasci.*	223	0.0564	7.40	3957	1967	**0.0344**	0.0739
every 2nd	1725	0.3773	49.52	4572	1614	0.8923	0.9905
every 3rd	1170	0.2573	33.76	4548	1760	0.9452	0.9865
every 4th	915	0.1936	25.40	4727	1705	0.5442	0.8378
every 5th	709	0.1568	20.58	4522	1636	0.7683	1.0000
every 6th	615	0.1348	17.68	4564	1732	0.9078	0.9999
every 7th	501	0.1127	14.79	4445	1626	0.5265	0.9798
every 8th	495	0.1029	13.50	4810	1544	0.3363	0.3630
every 9th	444	0.0907	11.90	4898	1443	0.3075	0.5711
every 10th	371	0.0858	11.25	4327	1521	0.4614	0.9954

Table 4.2-17

Sample Field	NMF	TFA	TTFA%	mMFD	MFDSD	Probability	
total	8707	3.0209	100.00	2882	1052	Wilcox.	K-S
1st Fasci.	598	0.2205	7.30	2712	991	0.1329	0.4175
2nd Fasci.	766	0.2793	9.25	2743	865	0.2401	0.3677
3rd Fasci.*	196	0.0539	1.78	3636	796	**0.0004**	**0.0193**
4th Fasci.	74	0.0270	0.89	2746	818	0.7441	0.8883
5th Fasci.	257	0.0907	3.00	2838	1201	0.9139	0.9723
6th Fasci.*	913	0.3430	11.35	2662	870	**0.0234**	**0.0263**
7th Fasci.	595	0.2230	7.38	2669	1060	0.0541	0.2124
8th Fasci.*	446	0.1764	5.84	2528	846	**0.0027**	**0.0162**
9th Fasci.	195	0.0662	2.19	2948	956	0.7515	1.0000
10th Fasci.	1084	0.3724	12.33	2911	1075	0.7232	0.9963
11th Fasci.*	989	0.2769	9.16	3572	1070	**0.0001**	**0.0001**
12th Fasci.	710	0.2303	7.62	3083	1163	0.1075	0.6472
13th Fasci.*	1012	0.3822	12.65	2647	1005	**0.0091**	0.0740
14th Fasci.	279	0.0882	2.92	3163	1088	0.0811	0.2623
15th Fasci.	416	0.1372	4.54	3032	1100	0.1866	0.2704
16th Fasci.*	121	0.0319	1.05	3799	1358	**0.0148**	0.2417
17th Fasci.	56	0.0221	0.73	2540	700	0.3568	0.5129
every 2nd	4338	1.5019	49.72	2888	1044	0.9581	1.0000
every 3rd	2890	1.0070	33.33	2870	986	0.9082	1.0000
every 4th	2213	0.7595	25.14	2914	1061	0.6610	0.7747
every 5th	1736	0.6125	20.28	2834	1052	0.4525	0.9318
every 6th	1456	0.5121	16.95	2843	974	0.5870	0.9659
every 7th	1304	0.4435	14.68	2941	1055	0.4863	0.9807
every 8th	1143	0.3920	12.98	2916	1017	0.5951	0.7446
every 9th	1030	0.3479	11.52	2960	923	0.3581	0.4125
every10th	924	0.3185	10.54	2901	1057	0.9213	0.9994

Table 4.2-18

Sample Field	NMF	TFA	TTFA%	mMFD	MFDSD	Probability	
total	3188	1.6366	100.00	1948	2456	Wilcox.	K-S
1st Fasci.	1042	0.5072	30.99	2055	2550	0.1834	0.7449
2nd Fasci.*	527	0.3038	18.56	1735	2876	**0.0234**	0.0868
3rd Fasci.*	644	0.2842	17.37	2266	2544	**0.0011**	**0.0062**
4th Fasci.*	698	0.4312	26.35	1619	2080	**0.0001**	**0.0040**
5th Fasci.*	277	0.1103	6.74	2512	2170	**0.0002**	**0.0086**
every 2nd	1603	0.8159	49.85	1965	2526	0.8331	1.0000
every 3rd	1046	0.5464	33.39	1915	2625	0.6058	0.8161
every 4th	806	0.4092	25.00	1970	2724	0.9974	1.0000
every 5th	677	0.3283	20.06	2062	2531	0.2813	0.9806
every 6th	522	0.2793	17.07	1869	2564	0.3752	0.5867
every 7th	489	0.2377	14.52	2058	2567	0.3175	0.8604
every 8th	404	0.2083	12.73	1940	2370	0.9186	1.0000
every 9th	358	0.1838	11.23	1948	2852	0.8795	0.9889
every 10th	331	0.1691	10.33	1958	2108	0.9153	0.9977

Table 4.2-19

Sample Field	NMF	TFA	TTFA%	mMFD	MFDSD	Probability	
total	2357	1.2152	100.00	1940	922	Wilcox.	K-S
1st Fasci.	325	0.1779	14.64	1817	871	0.3130	0.6414
2nd Fasci.	251	0.1250	10.28	2009	934	0.4727	0.3636
3rd Fasci.	89	0.0417	3.43	2137	784	0.3173	0.7135
4th Fasci.	279	0.1519	12.50	1837	861	0.4108	0.7303
5th Fasci.	201	0.1152	9.48	1746	828	0.1853	0.3643
6th Fasci.	55	0.0294	2.42	1871	861	0.8103	1.0000
7th Fasci.	294	0.1568	12.90	1875	922	0.5789	1.0000
8th Fasci.*	106	0.0441	3.63	2404	959	**0.0435**	0.4123
9th Fasci.	194	0.0858	7.06	2262	1001	0.0606	0.2637
10th Fasci.	242	0.1299	10.69	1864	995	0.4931	0.9844
11th Fasci.	321	0.1568	12.90	2047	974	0.4363	0.8546
every 2nd	1154	0.6003	49.40	1923	924	0.7061	0.9995
every 3rd	795	0.4067	33.47	1955	962	0.9949	0.9823
every 4th	611	0.3063	25.20	1995	985	0.7238	0.9997
every 5th	488	0.2524	20.77	1934	961	0.9585	0.9989
every 6th	405	0.2083	17.14	1945	956	0.8599	0.9496
every 7th	367	0.1813	14.92	2024	994	0.5901	0.9535
every 8th	336	0.1593	13.10	2110	900	*0.1163*	0.4001
every 9th	264	0.1397	11.49	1890	871	0.6058	0.6406
every10th	276	0.1348	11.09	2048	976	0.5348	0.9976

Table 4.2-20

Sample Field	NMF	TFA	TTFA%	mMFD	MFDSD	Probability	
total	3109	1.4333	100.00	2169	985	Wilcox.	K-S
1st Fasci.	839	0.3920	27.35	2140	931	0.6254	0.7709
2nd Fasci.*	659	0.2646	18.46	2490	1050	**0.0031**	**0.0066**
3rd Fasci.*	632	0.3553	24.79	1779	906	**0.0001**	**0.0155**
4th Fasci.	100	0.0539	3.76	1855	814	0.1347	0.5872
5th Fasci.*	273	0.1103	7.69	2476	974	**0.0418**	0.4152
6th Fasci.	217	0.9800	68.38	2214	933	0.7130	0.9908
7th Fasci.*	389	0.1593	11.11	2443	935	**0.0289**	0.0802
every 2nd	1587	0.7130	49.74	2226	996	0.6007	0.9973
every 3rd	1051	0.4753	33.16	2211	1013	0.6279	1.0000
every 4th	816	0.3577	24.96	2281	1031	0.3233	0.9886
every 5th	616	0.2891	20.17	2131	997	0.6679	0.9813
every 6th	537	0.2426	16.92	2214	1005	0.7004	1.0000
every 7th	437	0.2107	14.70	2074	903	0.6223	0.8822
*every 8th**	447	0.1813	12.65	2466	1052	***0.0245***	*0.1930*
every 9th	331	0.1642	11.45	2016	971	0.2767	0.8248
every 10th	329	0.1495	10.43	2201	1031	0.9980	0.9999

Abbreviations for Table 4.2-1 to 4.2-20 see next page

Abbreviations for Table 4.2-1 to 4.2-20

* The MFD of this sample significantly differed from that of the whole nerve in mean value and/or spatial distribution at the level of significance set at $P \leq 0.05$.

Bold data: The P values are less than 0.05.

Italic: The biggest systematic sample of which the MFD is different from that of the whole nerve in mean value and/or in spatial distribution with cut-off of P value set at 0.2.

every nth: every nth field sample

nth Fasci.: nth fascicle sample

NMF: number of myelinated fibres

TFA: transverse fascicular area

TTFA%: TFA/TTFA%

mMFD: mean of MFD

MFDSD: standard deviation of MFD

Wilcox.: Wilcoxon Rank-Sum test evaluates the mean values.

K-S: Kolmogorov-Smirnov test evaluates the shapes of frequency distributions.

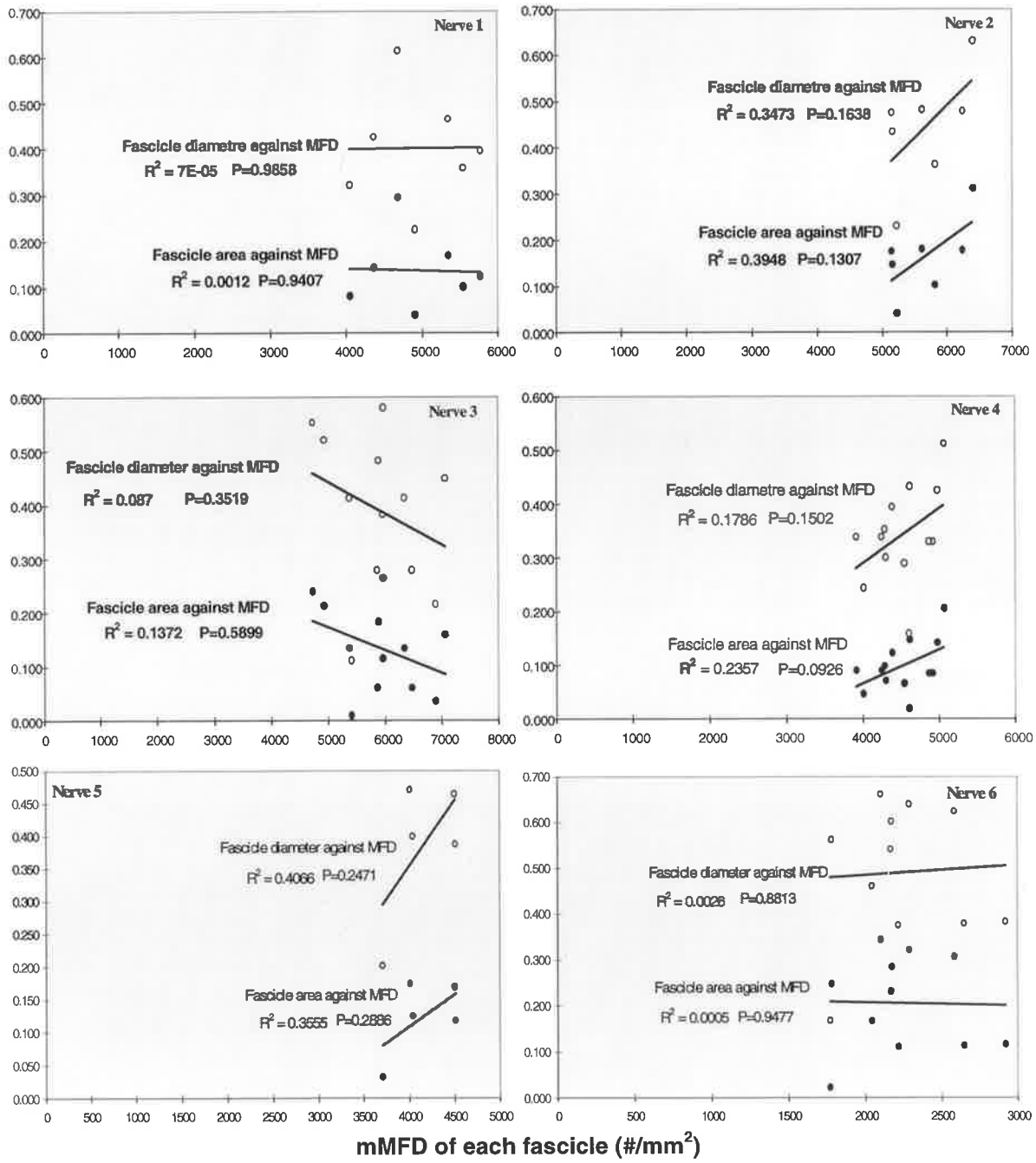

Figure 4.2-1: Fascicle diameter (open circle) and fascicle area (filled circle, mm^2) are plotted against the mean MFD in 6 nerves (No.1 to 6). There is no relationship between fascicle size and mean MFD for either control (No.1 and 2) or pathological nerves (No.3-6). The mean MFD is displayed on the abscissa, and the fascicle diameter (mm) and area (mm^2) are displayed on the ordinate.

Table 4.2-21: Comparison of myelinated fibre density of fascicles with the whole myelinated nerve fibre population. Values are percentage of the number of fascicles in which the MFD was significantly different from that of the whole nerve. Mean values were compared using Wilcoxon Rank-Sum test. The Shapes of the frequency distributions were compared using Kolmogorov-Smirnov goodness of fit test. Differences were considered significant when $P \leq 0.05$.

		Percentage of the number of fascicles		
Group	Nerve No.	mean MFD	MFD fd	total
Control	1	57.1	14.3	57.1 (4/7)
Control	2	57.1	28.6	57.1 (4/7)
Pathol.	3	50	30	50 (6/12)
Pathol.	4	15.4	7.7	15.4 (2/13)
Pathol.	5	0	0	0 (0/5)
Pathol.	6	36.4	36.4	36.4 (4/11)
Pathol.	7	90	60	90 (9/10)
Pathol.	8	0	20	20 (1/5)
Pathol.	9	33.3	33.3	33.3 (3/9)
Pathol.	10	16.7	16.7	16.7 (1/6)
Pathol.	11	16.7	8.3	16.7 (2/12)
Pathol.	12	33.3	0	33.3 (2/6)
Pathol.	13	60	20	60 (6/10)
Pathol.	14	44.4	22.2	44.4 (4/9)
Pathol.	15	25	0	25 (3/12)
Pathol.	16	37.5	12.5	37.5 (3/8)
Pathol.	17	35.3	23.5	35.3 (6/17)
Pathol.	18	80	60	80 (4/5)
Pathol.	19	9.1	0	9.1 (1/11)
Pathol.	20	57.1	28.6	57.1 (4/7)

Control: control group

Pathol.: pathological group

fd: frequency distribution

( ): ratio of number of fascicles different from the total number fascicles constituting the whole nerve

Table 4.2-22: The largest systematic sample in which the MFD differed from that of the whole nerve in mean value and/or frequency distribution summarized from table 4.2-1–20

Level of significance		P≤0.05				P≤0.2			
		Sample	Sample Size			Sample	Sample Size		
Group	Nerve No.		TFA	%TTFA	NMF		TFA	%TTFA	NMF
Control	1	-	-	-	-	-	-	-	-
Control	2	-	-	-	-	every 6th	0.1911	16.77	1176
Pathol.	3	-	-	-	-	-	-	-	-
Pathol.	4	-	-	-	-	-	-	-	-
Pathol.	5	-	-	-	-	-	-	-	-
Pathol.	6	-	-	-	-	-	-	-	-
Pathol.	7	-	-	-	-	every 6th	0.3724	17.08	1171
Pathol.	8	-	-	-	-	every 9th	0.0564	11.68	306
Pathol.	9	-	-	-	-	-	-	-	-
Pathol.	10	-	-	-	-	-	-	-	-
Pathol.	11	-	-	-	-	every 7th	0.1764	14.85	867
Pathol.	12	-	-	-	-	-	-	-	-
Pathol.	13	-	-	-	-	-	-	-	-
Pathol.	14	-	-	-	-	-	-	-	-
Pathol.	15	-	-	-	-	-	-	-	-
Pathol.	16	-	-	-	-	-	-	-	-
Pathol.	17	-	-	-	-	-	-	-	-
Pathol.	18	-	-	-	-	-	-	-	-
Pathol.	19	-	-	-	-	every 8th	0.1593	13.10	336
Pathol.	20	every 8th	0.1813	12.65	447	every 8th	0.1813	12.65	447

Control: control group

Pathol.: pathological group

TFA: transverse fascicular area (mm^2)

%TTFA: TFA/TTFA×100%

NMF: the number of MFs in this sample

every nth: every nth field sample

-: The MFDs derived from the different systematic sample sizes were not significantly different from the MFD for the whole myelinated fibre population at the set P values.

Table 4.3-1

Sample Field	mDs	DsSD	Probability		mDa	DaSD	Probability	
total	7.81	4.17	Wilcox.	K-S	5.79	3.17	Wilcox.	K-S
1st Fasci.	7.91	4.14	0.5121	0.0811	5.77	3.09	0.7981	0.4793
2nd Fasci.*	7.40	3.70	0.0514	**0.0017**	5.38	2.69	**0.0243**	**0.0004**
3rd Fasci.	7.61	4.07	0.2451	0.4327	5.66	3.05	0.4206	0.8557
4th Fasci.*	8.68	4.43	**0.0001**	**0.0002**	6.33	3.29	**0.0001**	**0.0034**
5th Fasci.*	7.68	4.64	0.0776	**0.0042**	5.91	3.71	0.4779	**0.0023**
6th Fasci.	7.69	3.92	0.9625	0.5008	5.88	3.12	0.4971	0.4741
7th Fasci.*	7.25	3.14	0.4997	**0.0025**	5.29	2.24	0.2402	**0.0022**
enery 2nd	7.96	4.23	*0.1828*	0.6733	5.90	3.22	*0.1790*	0.5338
every 3rd	7.73	4.09	0.5798	0.7715	5.69	3.09	0.4140	0.8427
every 4th	7.95	4.21	0.3072	0.5809	5.88	3.21	0.3892	0.3506
every 5th	7.62	4.23	0.1150	0.1026	5.65	3.24	0.1045	0.1757
every 6th	7.78	4.23	0.8000	0.9096	5.75	3.23	0.6773	0.8592
every 7th	7.75	4.08	0.8241	0.8707	5.75	3.11	0.9879	0.8641
every 8th	7.80	4.15	0.9257	0.7791	5.78	3.18	0.9933	0.9826
every 9th	7.67	4.07	0.5134	0.6881	5.68	3.08	0.5309	0.8410
every 10th	7.69	4.38	0.3753	0.1385	5.75	3.42	0.3780	0.2102

Table 4.3-2

Sample Field	mDs	DsSD	Probability		mDa	DaSD	Probability	
total	7.41	4.06	Wilcox.	K-S	5.29	2.85	Wilcox.	K-S
1st Fasci.*	7.05	3.74	**0.0008**	**0.0003**	4.92	2.43	**0.0002**	**0.0001**
2nd Fasci.*	7.77	4.63	0.3382	**0.0017**	5.72	3.50	0.0552	**0.0001**
3rd Fasci.	7.38	3.96	0.7731	0.6971	5.25	2.73	0.9513	0.9252
4th Fasci.	7.56	4.05	0.3651	0.2064	5.52	2.96	0.0782	0.0602
5th Fasci.*	7.87	4.29	**0.0009**	**0.0120**	5.57	3.05	**0.0169**	**0.0109**
6th Fasci.	7.41	3.99	0.4394	0.0743	5.33	2.78	0.5124	0.8214
7th Fasci.*	6.94	3.51	0.6027	**0.0270**	4.93	2.46	0.2065	0.0605
every 2nd	7.27	4.03	*0.0818*	0.2288	5.19	2.83	*0.0812*	*0.1384*
every 3rd	7.39	4.09	0.7421	0.8203	5.27	2.88	0.6109	0.9137
every 4th	7.29	4.05	0.2271	0.5933	5.20	2.83	0.2028	0.4298
every 5th	7.41	4.09	0.9650	0.9821	5.30	2.88	0.9844	0.9951
every 6th*	7.12	4.03	**0.0146**	**0.0270**	5.10	2.84	**0.0165**	0.0649
every 7th*	7.67	4.08	0.0576	0.1215	5.47	2.86	**0.0375**	0.2216
every 8th*	7.29	4.19	0.2098	0.0457	5.17	2.93	0.1193	**0.0452**
every 9th	7.55	4.12	0.4638	0.8408	5.36	2.91	0.5273	0.7640
every 10th*	6.89	3.94	**0.0017**	**0.0001**	4.96	2.73	**0.0033**	**0.0002**

Table 4.3-5

Sample Field	mDs	DsSD	Probability		mDa	DaSD	Probability	
total	6.33	2.88	Wilcox.	K-S	4.38	2.01	Wilcox.	K-S
1st Fasci.*	5.98	2.65	**0.0126**	0.1369	4.26	1.87	0.4171	0.4968
2nd Fasci.	6.58	3.11	0.1884	0.3303	4.47	2.11	0.3502	0.3656
3rd Fasci.	6.45	3.06	0.7540	0.4942	4.41	2.16	0.5416	0.2052
4th Fasci.	6.26	2.68	0.9305	0.9579	4.31	1.85	0.8433	0.9917
5th Fasci.*	7.09	2.91	**0.0020**	**0.0155**	4.82	2.09	**0.0211**	0.0849
every 2nd	6.23	2.79	0.2767	0.7525	4.27	1.93	0.3389	0.9335
every 3rd	6.15	2.80	*0.1393*	0.4982	4.29	2.00	0.2258	0.4554
every 4th	6.25	2.85	0.5291	0.6514	4.35	1.98	0.8162	0.9703
every 5th	6.17	2.89	0.1870	0.4442	4.28	1.97	0.2667	0.5222
every 6th	6.17	2.80	0.4402	0.8010	4.30	2.01	0.5783	0.6348
every 7th	6.10	2.93	0.0802	0.0863	4.26	2.10	0.1501	0.1950
every 8th	6.25	2.67	0.8911	0.9621	4.35	1.78	0.7854	0.8680
every 9th	6.04	2.68	0.1665	0.1733	4.20	1.88	0.1847	0.2813
every 10th	6.08	2.89	0.1151	0.2356	4.19	1.97	0.0982	0.1022

Table 4.3-6

Sample Field	mDs	DsSD	Prabability		mDa	DaSD	Probability	
total	5.57	2.93	Wilcox.	K-S	3.68	1.79	Wilcox.	K-S
1st Fasci.*	5.71	2.93	0.1064	0.2290	3.81	1.72	**0.0062**	**0.0100**
2nd Fasci.	5.59	2.96	0.9826	0.9962	3.67	1.75	0.8743	0.9811
3rd Fasci.	5.73	2.97	0.2725	0.5980	3.62	1.77	0.4258	0.2186
4th Fasci.	5.57	2.83	0.7261	0.8440	3.70	1.74	0.7211	0.8338
5th Fasci.	6.39	3.07	0.0659	0.0568	4.26	2.24	0.0891	0.1260
6th Fasci.*	5.34	2.92	**0.0051**	**0.0035**	3.48	1.73	**0.0006**	**0.0003**
7th Fasci.	5.66	3.08	0.8465	0.6672	3.69	1.85	0.8116	0.9092
8th Fasci.*	5.89	3.32	0.3043	0.1182	3.98	2.05	**0.0367**	0.0655
9th Fasci.	5.52	2.73	0.5609	0.4467	3.69	1.66	0.4718	0.3324
10th Fasci.	5.43	2.86	0.3888	0.5805	3.76	1.86	0.8865	0.5247
11th Fasci.*	5.27	2.66	0.1604	0.1203	3.46	1.76	0.0735	**0.0321**
every 2nd	5.55	2.94	0.6362	0.9998	3.68	1.80	0.9465	1.0000
every 3rd	5.51	2.90	0.4537	0.9301	3.63	1.76	0.2862	0.6874
every 4th	5.44	2.93	*0.0581*	*0.1814*	3.58	1.76	*0.0560*	0.2066
every 5th	5.59	2.88	0.5283	0.4558	3.69	1.73	0.6505	0.4556
every 6th	5.52	2.84	0.9765	0.9310	3.65	1.71	0.9603	0.9532
every 7th	5.63	3.02	0.9124	0.0935	3.74	1.90	0.5129	0.0805
every 8th	5.44	2.93	0.1386	0.2733	3.59	1.75	0.1558	0.1829
every 9th*	5.29	2.77	**0.0486**	0.0678	3.54	1.68	0.0564	0.0687
every 10th	5.54	2.78	0.5363	0.4311	3.68	1.71	0.5135	0.6610

Table 4.3-7

Sample Field	mDs	DsSD	Probability		mDa	DaSD	Probability	
total	6.32	3.21	Wilcox.	K-S	4.44	2.27	Wilcox.	K-S
1st Fasci.*	5.98	2.77	0.3003	**0.0194**	4.39	2.10	0.6996	0.3098
2nd Fasci.*	6.60	3.42	**0.0006**	**0.0001**	4.81	2.70	**0.0001**	**0.0001**
3rd Fasci.	6.12	2.40	0.9153	0.2006	4.27	1.30	0.9030	0.2692
4th Fasci.*	6.42	2.98	**0.0466**	**0.0362**	4.61	2.03	**0.0008**	**0.0059**
5th Fasci.*	6.85	3.55	**0.0031**	**0.0010**	4.78	2.54	**0.0017**	**0.0010**
6th Fasci.*	5.42	2.79	**0.0001**	**0.0001**	3.82	2.12	**0.0001**	**0.0001**
7th Fasci.*	6.53	3.61	0.5614	**0.0001**	4.43	2.36	0.1069	**0.0030**
8th Fasci.	6.42	3.29	0.6115	0.2556	4.37	2.21	0.2979	0.4703
9th Fasci.*	5.67	2.21	**0.0158**	**0.0001**	4.01	1.59	**0.0021**	**0.0001**
10th Fasci.*	5.78	2.69	**0.0184**	**0.0193**	4.11	1.98	**0.0155**	**0.0095**
every 2nd	6.27	3.14	0.5280	0.7700	4.41	2.20	0.5394	0.9141
every 3rd	6.37	3.16	0.4947	0.8027	4.45	2.16	0.7785	0.9108
every 4th	6.30	3.13	0.9649	0.9176	4.44	2.19	0.8534	0.5032
every 5th	6.34	3.47	0.6522	0.8821	4.43	2.55	0.3298	0.6123
every 6th	6.26	3.03	0.8917	0.2916	4.39	2.09	0.6386	0.2204
every 7th	6.21	3.33	0.3871	0.4293	4.32	2.47	*0.1932*	0.3506
every 8th	6.37	3.26	0.7001	0.9830	4.47	2.30	0.8566	0.9626
every 9th	6.53	3.36	0.2404	0.5117	4.56	2.34	0.4106	0.5904
every 10th	6.25	3.28	0.3549	0.6634	4.37	2.34	0.1874	0.2534

Table 4.3-8

Sample Field	mDs	DsSD	Probability		mDa	DaSD	Probability	
total	5.77	2.51	Wilcox.	K-S	4.31	1.93	Wilcox.	K-S
1st Fasci.	5.68	2.36	0.9735	0.3881	4.30	1.82	0.6079	0.3609
2nd Fasci.*	6.23	2.83	**0.0041**	**0.0265**	4.66	2.17	**0.0021**	**0.0002**
3rd Fasci.	5.74	2.49	0.6245	0.7111	4.30	1.93	0.8365	0.9986
4th Fasci.*	5.42	2.29	**0.0126**	0.0539	3.92	1.69	**0.0003**	**0.0026**
5th Fasci.	6.16	2.24	0.1485	0.3220	4.64	1.79	0.1784	0.1461
every 2nd	5.87	2.53	0.2600	0.7155	4.37	1.91	0.2728	0.7453
every 3rd	5.72	2.57	0.3214	0.3182	4.28	2.02	0.3925	0.5854
every 4th	5.95	2.52	*0.0959*	0.3606	4.43	1.89	*0.1549*	0.2601
every 5th	5.71	2.48	0.6065	0.8248	4.29	1.89	0.9497	0.8458
every 6th	5.84	2.60	0.8170	0.9681	4.36	2.01	0.8223	0.9962
every 7th	5.73	2.57	0.4669	0.3073	4.25	1.97	0.4365	0.4424
every 8th	5.89	2.46	0.3606	0.8239	4.39	1.83	0.3513	0.6139
every 9th*	5.46	2.47	**0.0141**	**0.0067**	4.09	1.90	**0.0391**	**0.0472**
every 10th	5.87	2.54	0.5889	0.9422	4.37	1.92	0.6246	0.9154

Table 4.3-9

Sample Field	mDs	DsSD	Probability		mDa	DaSD	Probability	
total	7.64	4.05	Wilcox.	K-S	5.34	2.95	Wilcox.	K-S
1st Fasci.*	7.12	3.63	**0.0002**	**0.0005**	4.97	2.41	**0.0032**	**0.0051**
2nd Fasci.*	7.64	4.40	0.1180	**0.0054**	5.37	3.25	0.2169	0.0732
3rd Fasci.*	7.92	4.22	0.1020	**0.0137**	5.61	3.03	**0.0007**	**0.0026**
4th Fasci.*	8.14	4.30	**0.0013**	**0.0011**	5.74	3.17	**0.0001**	**0.0003**
5th Fasci.*	6.80	2.98	**0.0095**	**0.0001**	4.74	1.92	**0.0044**	**0.0001**
6th Fasci.	7.78	4.44	0.7533	0.6861	5.46	3.54	0.8645	0.3844
7th Fasci.*	7.32	3.93	**0.0281**	0.2134	5.19	3.02	**0.0453**	0.0958
8th Fasci.*	7.87	3.92	**0.0169**	**0.0234**	5.24	2.84	0.5717	0.3095
9th Fasci.*	7.76	3.16	**0.0130**	**0.0001**	5.27	2.31	0.1334	**0.0108**
every 2nd	7.60	4.08	0.3712	0.7662	5.32	3.01	0.5774	0.9378
every 3rd	7.70	4.02	0.5024	0.8336	5.39	2.95	0.3138	0.4977
every 4th	7.64	4.14	0.6734	0.8121	5.35	3.09	0.7789	0.9820
every 5th	7.69	4.22	0.8851	0.8655	5.39	3.18	0.9422	0.9673
every 6th	7.72	4.13	0.6510	0.6667	5.43	3.09	0.3057	0.3188
every 7th	7.68	4.15	0.8658	0.8988	5.38	3.14	0.9422	0.8435
every 8th	7.72	4.19	0.7029	0.9730	5.40	3.12	0.8925	0.9805
every 9th	7.86	4.15	*0.1064*	0.3398	5.50	3.09	*0.0837*	0.2900
every 10th	7.56	4.26	0.1791	0.1087	5.33	3.21	0.3156	0.1446

Table 4.3-10

Sample Field	mDs	DsSD	Probability		mDa	DaSD	Probability	
total	7.01	3.51	Wilcox.	K-S	4.75	2.44	Wilcox.	K-S
1st Fasci.	7.18	3.62	0.2303	0.8247	4.82	2.50	0.5659	0.9049
2nd Fasci.*	6.80	3.59	**0.0245**	**0.0015**	4.58	2.56	**0.0174**	**0.0049**
3rd Fasci.*	7.28	3.45	**0.0135**	**0.0285**	5.00	2.33	**0.0009**	**0.0157**
4th Fasci.	7.10	3.33	0.3084	0.0599	4.85	2.33	0.3144	0.4304
5th Fasci.*	5.85	2.48	**0.0006**	**0.0001**	4.11	1.63	**0.0037**	**0.0004**
6th Fasci.*	6.32	2.91	0.0536	0.0802	4.15	1.75	**0.0246**	0.0656
every 2nd	6.97	3.56	0.4902	0.7191	4.72	2.45	0.6118	0.9409
every 3rd	7.09	3.64	0.6568	0.9872	4.81	2.58	0.7680	0.9999
every 4th	7.04	3.61	0.9412	0.9777	4.75	2.45	0.9390	0.8487
every 5th	6.94	3.50	0.5745	0.5294	4.72	2.43	0.6769	0.8802
every 6th	7.04	3.72	0.7818	0.9322	4.75	2.60	0.6730	0.8881
every 7th	7.06	3.58	0.6811	0.5117	4.82	2.59	0.5266	0.7145
every 8th	7.02	3.65	0.6694	0.2954	4.76	2.44	0.8838	0.4534
every 9th	7.35	3.82	*0.0769*	*0.1116*	5.03	2.82	*0.0692*	*0.1051*
every 10th	7.13	3.67	0.6765	0.8218	4.83	2.54	0.6699	0.8519

Table 4.3-11

Sample Field	mDs	DsSD	Probability		mDa	DaSD	Probability	
total	6.24	3.09	Wilcox.	K-S	4.15	1.89	Wilcox.	K-S
1st Fasci.*	5.61	2.51	**0.0292**	**0.0176**	3.92	1.50	0.3016	0.0510
2nd Fasci.	6.05	2.91	0.2401	0.1709	4.07	1.65	0.8880	0.1456
3rd Fasci.*	6.79	3.46	**0.0116**	**0.0001**	4.53	2.32	**0.0043**	**0.0001**
4th Fasci.	6.58	3.23	0.1635	0.1567	4.31	2.07	0.3833	0.2509
5th Fasci.*	6.55	3.20	0.0860	**0.0241**	4.11	1.84	0.7309	0.7715
6th Fasci.*	6.14	3.11	0.3412	0.7214	4.00	1.96	**0.0356**	**0.0427**
7th Fasci.	6.38	3.17	0.5705	0.1427	4.19	1.90	0.6216	0.5059
8th Fasci.	6.16	3.11	0.6526	0.6671	4.13	1.99	0.6235	0.8602
9th Fasci.	6.14	2.96	0.4476	0.0669	4.27	1.82	0.1749	0.1910
10th Fasci.*	6.44	3.32	**0.0001**	**0.0001**	4.28	2.00	**0.0001**	**0.0001**
11th Fasci.	5.35	2.21	0.4016	0.7539	3.66	1.51	0.7670	0.8225
12th Fasci.*	6.26	3.03	0.7321	0.2515	4.17	1.87	0.1026	**0.0115**
every 2nd	6.28	3.10	0.6015	0.9999	4.19	1.93	0.4730	0.9096
*every 3rd**	6.40	3.06	***0.0190***	***0.0134***	4.23	1.86	***0.0254***	***0.0240***
every 4th	6.17	3.10	0.3354	0.6873	4.13	1.91	0.3954	0.6434
every 5th	6.29	3.10	0.5884	0.8911	4.16	1.87	0.7740	0.9734
every 6th*	6.40	3.06	0.0669	0.2269	4.26	1.87	**0.0359**	**0.0494**
every 7th	6.17	2.98	0.7893	0.9845	4.07	1.82	0.4817	0.6613
every 8th	6.07	2.98	0.2060	0.2282	4.06	1.83	0.1971	0.2992
every 9th	6.41	3.12	0.1799	0.1711	4.29	1.90	0.0637	0.0607
every 10th	6.13	3.09	0.3332	0.7850	4.12	1.96	0.4591	0.7408

Table 4.3-12

Sample Field	mDs	DsSD	Probability		mDa	DaSD	Probability	
total	6.88	3.31	Wilcox.	K-S	4.94	2.35	Wilcox.	K-S
1st Fasci.*	6.72	3.50	0.5218	0.2610	4.67	2.70	0.0593	**0.0113**
2nd Fasci.	6.94	3.21	0.3539	0.7829	4.88	2.16	0.9682	0.9543
3rd Fasci.	6.73	3.32	0.1577	0.5473	4.93	2.42	0.4807	0.5706
4th Fasci.	7.07	3.34	0.2986	0.1445	5.06	2.27	0.1701	0.5075
5th Fasci.	6.72	3.11	0.7934	0.4252	4.93	2.24	0.7503	0.3140
6th Fasci.	7.23	3.83	0.6423	0.5896	5.28	2.89	0.4625	0.1633
every 2nd	6.82	3.27	0.6888	0.9068	4.91	2.32	0.8255	0.9645
every 3rd	6.79	3.30	0.5075	0.7632	4.87	2.30	0.4119	0.8459
every 4th	6.58	3.05	*0.0783*	*0.1708*	4.78	2.16	0.2469	0.2777
every 5th	7.00	3.48	0.5801	0.9738	5.03	2.47	0.6011	0.9657
every 6th	6.70	3.26	0.2800	0.5129	4.80	2.28	0.2491	0.5465
every 7th*	7.23	3.48	**0.0341**	0.1368	5.21	2.54	**0.0366**	0.1127
every 8th	6.57	3.00	0.1839	0.2287	4.76	2.13	0.2845	0.4295
every 9th	6.62	3.45	0.0955	0.1420	4.80	2.50	0.1632	0.4196
every 10th	6.98	3.49	0.7261	0.9473	5.02	2.50	0.7848	0.9549

Table 4.3-13

Sample Field	mDs	DsSD	Probability		mDa	DaSD	Probability	
total	7.55	4.01	Wilcox.	K-S	5.34	3.10	Wilcox.	K-S
1st Fasci.*	7.44	3.65	0.8443	0.4518	5.14	2.52	0.4953	**0.0201**
2nd Fasci.*	7.36	3.91	0.1930	0.3134	5.10	2.92	**0.0307**	0.1517
3rd Fasci.*	8.02	5.68	0.3309	**0.0001**	6.22	5.13	0.2816	**0.0001**
4th Fasci.	7.58	3.47	0.2610	0.2549	5.15	2.38	0.7900	0.4018
5th Fasci.	7.32	3.66	0.3640	0.3649	5.24	2.62	0.7848	0.6471
6th Fasci.*	8.10	4.42	**0.0061**	**0.0012**	5.87	3.59	**0.0005**	**0.0012**
7th Fasci.	7.26	3.43	0.5768	0.1605	5.05	2.33	0.4852	0.4105
8th Fasci.*	6.40	2.93	**0.0128**	0.0501	4.55	1.93	**0.0300**	**0.0470**
9th Fasci.*	8.00	3.75	**0.0074**	0.0675	5.49	2.54	**0.0202**	**0.0268**
10th Fasci.*	7.31	3.30	0.6824	0.1134	4.97	2.14	0.1415	**0.0404**
every 2nd	7.59	4.06	0.6555	0.9965	5.37	3.16	0.5813	0.9493
every 3rd	7.59	4.02	0.7076	0.9172	5.34	3.06	0.8275	0.9913
every 4th	7.72	4.10	*0.1001*	*0.0524*	5.45	3.21	*0.0737*	*0.0681*
every 5th	7.63	4.02	0.4791	0.5794	5.38	3.09	0.5096	0.5553
every 6th	7.51	3.99	0.7426	0.9827	5.28	3.06	0.5474	0.9837
every 7th*	7.89	4.29	0.0710	**0.0141**	5.57	3.40	0.1372	0.1201
every 8th*	7.95	4.38	**0.0166**	0.0726	5.62	3.48	**0.0199**	**0.0355**
every 9th	7.59	3.98	0.7575	0.9357	5.31	2.93	0.8022	0.9784
every 10th	7.56	3.95	0.7667	0.8472	5.34	3.00	0.5680	0.5366

Table 4.3-14

Sample Field	mDs	DsSD	Probability		mDa	DaSD	Probability	
total	7.80	4.37	Wilcox.	K-S	4.80	3.28	Wilcox.	K-S
1st Fasci.	7.95	4.46	0.4711	0.4401	4.97	3.49	0.3175	0.5165
2nd Fasci.*	7.49	4.52	**0.0428**	**0.0030**	4.68	3.53	0.0748	0.0725
3rd Fasci.*	7.06	4.02	0.2124	0.1126	3.99	3.02	**0.0207**	0.0709
4th Fasci	7.71	4.16	0.8981	0.9962	4.51	3.14	0.0983	0.1263
5th Fasci.	7.97	4.38	0.4900	0.2300	4.78	3.25	0.8629	0.8269
6th Fasci.	7.86	3.84	0.3357	0.2015	4.51	2.70	0.4417	0.2612
7th Fasci.*	8.48	4.37	**0.0001**	**0.0001**	5.29	3.23	**0.0001**	**0.0001**
8th Fasci.*	6.61	3.68	**0.0001**	**0.0005**	4.03	2.82	**0.0002**	**0.0002**
9th Fasci.*	7.23	4.45	**0.0025**	0.9693	4.81	3.45	0.6271	0.8452
every 2nd	7.89	4.34	0.4028	0.9065	4.85	3.30	0.5276	0.9757
every 3rd	7.96	4.50	0.3404	0.6078	4.99	3.47	*0.1251*	0.3562
every 4th	7.86	4.28	0.5864	0.9392	4.81	3.24	0.8836	0.9012
every 5th	7.68	4.26	0.5762	0.7827	4.73	3.16	0.7621	0.5410
every 6th	8.11	4.54	0.1142	0.3355	5.05	3.54	0.0689	0.0872
every 7th	7.79	4.32	0.8911	0.8457	4.77	3.22	0.8698	0.9778
every 8th	7.93	4.30	0.3609	0.6491	4.91	3.27	0.3790	0.5463
every 9th	8.16	4.64	0.1371	0.2358	5.12	3.60	0.0733	0.0889
every 10th	7.93	4.33	0.5096	0.6023	4.88	3.26	0.5007	0.5613

Table 4.3-15

Sample Field	mDs	DsSD	Probability		mDa	DaSD	Probability	
total	6.51	3.60	Wilcox.	K-S	4.66	2.63	Wilcox.	K-S
1st Fasci.*	6.17	2.97	0.2089	0.2071	4.20	1.85	**0.0003**	**0.0005**
2nd Fasci.*	6.03	3.20	**0.0005**	**0.0028**	4.18	2.14	**0.0001**	**0.0006**
3rd Fasci.*	6.71	4.12	0.9354	0.1205	4.99	3.21	0.1820	**0.0185**
4th Fasci.*	6.48	3.01	0.1846	**0.0230**	4.38	2.05	0.2888	0.1976
5th Fasci.*	7.58	4.92	**0.0053**	**0.0159**	5.69	3.98	**0.0001**	**0.0012**
6th Fasci.*	7.09	4.71	0.2705	**0.0051**	5.34	3.79	**0.0052**	**0.0009**
7th Fasci.	6.84	3.76	0.5031	0.8492	4.88	2.76	0.6353	0.5920
8th Fasci.	6.31	3.16	0.7203	0.2836	4.46	2.18	0.7948	0.5661
9th Fasci.	6.41	3.02	0.6780	0.6787	4.40	1.79	0.8326	0.4269
10th Fasci.*	6.67	3.64	0.1943	0.3727	4.87	2.61	**0.0202**	**0.0225**
11th Fasci.*	6.16	2.92	0.1779	0.0771	4.41	1.88	0.5244	**0.0211**
12th Fasci.*	6.82	3.30	**0.0189**	0.0624	4.76	2.14	0.0530	0.0544
every 2nd	6.46	3.58	0.5653	0.9850	4.63	2.61	0.4608	0.8997
every 3rd	6.51	3.59	0.9317	0.9636	4.65	2.60	0.7397	0.9368
every 4th	6.45	3.57	0.5282	0.9138	4.61	2.59	0.4317	0.9292
every 5th	6.63	3.69	0.2124	0.4745	4.77	2.74	0.2167	0.7481
every 6th	6.51	3.58	0.9231	0.9592	4.67	2.62	0.9547	0.9407
every 7th	6.53	3.61	0.7378	0.9318	4.67	2.66	0.8647	0.9827
every 8th	6.51	3.61	0.9793	0.9553	4.64	2.61	0.7139	0.9760
every 9th	6.60	3.78	0.7855	0.9855	4.74	2.84	0.9501	0.9531
every10th	6.40	3.46	0.7125	0.6194	4.60	2.51	0.6228	0.8208

Table 4.3-16

Sample Field	mDs	DsSD	Probability		mDa	DaSD	Probability	
total	7.17	4.15	Wilcox.	K-S	5.30	3.20	Wilcox.	K-S
1st Fasci.	7.06	4.19	0.2934	0.5067	5.22	3.19	0.5433	0.8126
2nd Fasci.	7.39	4.16	0.0897	0.2546	5.46	3.17	0.0753	0.2540
3rd Fasci.	6.93	3.91	0.2989	0.4932	5.11	2.96	0.2865	0.3408
4th Fasci.*	6.18	4.43	**0.0017**	**0.0018**	4.75	3.74	**0.0085**	**0.0122**
5th Fasci.	6.86	4.07	0.3888	0.3546	5.06	3.17	0.3414	0.6758
6th Fasci.	7.35	4.40	0.7401	0.5079	5.46	3.52	0.6785	0.5997
7th Fasci.	7.17	4.09	0.9341	0.7978	5.29	3.15	0.9820	0.7159
8th Fasci.*	7.51	4.12	0.0608	**0.0061**	5.41	3.26	0.4915	0.2965
every 2nd	7.21	4.14	0.7009	0.9987	5.31	3.17	0.7247	0.9998
every 3rd	7.23	4.14	0.5890	0.7600	5.34	3.17	0.5921	0.6043
every 4th	7.15	4.17	0.7348	0.9187	5.26	3.19	0.7597	0.9901
every 5th	7.39	4.19	*0.1542*	0.3893	5.51	3.23	*0.0635*	0.2091
every 6th	7.31	4.18	0.3941	0.8643	5.42	3.22	0.3670	0.8274
every 7th	7.55	4.43	0.1390	0.2645	5.60	3.44	0.1061	0.2513
every 8th	7.19	4.21	0.8747	0.7870	5.28	3.25	0.7775	0.7857
every 9th	7.10	3.90	0.7528	0.3973	5.26	2.98	0.6977	0.6797
every 10th*	7.55	4.30	0.1325	0.3635	5.64	3.29	**0.0373**	0.1371

Table 4.3-17

Sample Field	mDs	DsSD	Probability		mDa	DaSD	Probability	
total	6.88	3.53	Wilcox.	K-S	4.41	2.47	Wilcox.	K-S
1st Fasci.*	7.18	3.72	0.0848	**0.0419**	4.75	2.68	**0.0036**	**0.0010**
2nd Fasci.*	7.27	3.42	**0.0004**	**0.0003**	4.62	2.30	**0.0006**	**0.0038**
3rd Fasci.*	6.28	3.01	**0.0470**	0.0689	4.01	1.90	0.0630	0.0659
4th Fasci.*	5.42	2.65	**0.0005**	**0.0114**	3.46	1.62	**0.0008**	**0.0105**
5th Fasci.	6.69	3.22	0.7039	0.3487	4.27	2.19	0.9233	0.4787
6th Fasci.*	6.83	3.31	0.7857	0.0947	4.30	2.16	0.7267	**0.0437**
7th Fasci.*	7.39	3.94	**0.0082**	**0.0050**	4.93	3.05	**0.0007**	**0.0001**
8th Fasci.*	7.58	3.75	**0.0001**	**0.0008**	4.70	2.64	**0.0158**	**0.0292**
9th Fasci.	7.03	3.24	0.3395	0.2425	4.14	1.98	0.4945	0.4981
10th Fasci.*	6.74	3.45	0.2353	0.3251	4.17	2.28	**0.0082**	**0.0155**
11th Fasci.	6.67	3.43	0.0887	0.1528	4.22	2.23	0.2021	0.2772
12th Fasci.*	6.66	3.38	0.0842	**0.0199**	4.18	2.23	**0.0141**	**0.0045**
13th Fasci.*	7.76	3.96	**0.0001**	**0.0001**	5.31	3.12	**0.0001**	**0.0001**
14th Fasci.*	5.55	3.14	**0.0001**	**0.0001**	3.53	2.26	**0.0001**	**0.0001**
15th Fasci.*	5.86	2.81	**0.0001**	**0.0001**	3.70	1.71	**0.0001**	**0.0001**
16th Fasci.*	4.94	2.45	**0.0001**	**0.0001**	3.04	1.57	**0.0001**	**0.0001**
17th Fasci.*	4.37	2.43	**0.0001**	**0.0001**	2.72	1.59	**0.0001**	**0.0001**
every 2nd	6.93	3.56	0.4919	0.8990	4.45	2.50	0.3743	0.8636
every 3rd	6.89	3.50	0.8282	0.9603	4.40	2.41	0.8215	0.9871
every 4th	6.89	3.55	0.9837	0.9996	4.41	2.50	0.9839	0.9987
every 5th	6.94	3.65	0.7244	0.8929	4.45	2.62	0.7222	0.7015
every 6th	6.86	3.57	0.7045	0.8527	4.42	2.51	0.9983	0.9412
every 7th	6.88	3.48	0.8798	0.9771	4.38	2.37	0.8522	0.9365
every 8th	6.98	3.60	0.4729	0.5461	4.46	2.56	0.5898	0.5416
every 9th	6.96	3.48	0.4148	0.7620	4.43	2.38	0.4950	0.6739
every10th	7.06	3.74	0.2839	0.2638	4.53	2.71	0.4034	0.3691

Table 4.3-18

Sample Field	mDs	DsSD	Probability		mDa	DaSD	Probability	
total	6.67	4.59	Wilcox.	K-S	4.33	3.59	Wilcox.	K-S
1st Fasci.	6.81	4.75	0.6346	0.4231	4.54	3.86	0.4660	0.5109
2nd Fasci.	6.88	4.92	0.9350	0.3477	4.32	3.91	0.1622	0.0754
3rd Fasci.*	6.83	4.36	0.0713	**0.0438**	4.46	3.07	**0.0036**	**0.0019**
4th Fasci.*	6.38	4.60	0.0707	0.2078	4.09	3.69	**0.0353**	0.1538
5th Fasci.	6.10	3.70	0.3226	0.1642	3.87	2.57	0.4862	0.2565
every 2nd	6.63	4.61	0.6044	0.9830	4.34	3.60	0.9415	0.9972
every 3rd	6.82	4.70	0.3400	0.4415	4.42	3.70	0.4406	0.4827
every 4th	6.61	4.52	0.9068	0.9418	4.32	3.57	0.9523	0.9998
every 5th	6.63	4.51	0.9020	0.9977	4.30	3.48	0.8081	0.9527
every 6th	6.73	4.73	0.9475	0.9850	4.35	3.67	0.8314	0.7036
every 7th	6.33	4.24	*0.1821*	*0.1708*	4.07	3.19	*0.1645*	*0.1828*
every 8th	6.62	4.67	0.8078	0.8974	4.32	3.76	0.9258	0.9295
every 9th	6.43	4.29	0.6376	0.8367	4.06	3.26	0.4610	0.5868
every 10th	6.74	4.67	0.6806	0.8983	4.41	3.74	0.4785	0.7891

Table 4.3-19

Sample Field	mDs	DsSD	Probability		mDa	DaSD	Probability	
total	5.86	2.73	Wilcox.	K-S	4.03	2.00	Wilcox.	K-S
1st Fasci.*	6.32	3.11	**0.0250**	**0.0097**	4.55	2.34	**0.0001**	**0.0026**
2nd Fasci.*	5.50	2.75	**0.0213**	0.0948	3.85	1.98	0.2612	0.4656
3rd Fasci.*	5.01	1.96	**0.0082**	**0.0473**	3.69	1.61	0.2266	0.2155
4th Fasci.	5.78	2.84	0.5893	0.6564	4.21	2.08	0.0797	0.0553
5th Fasci.	5.97	2.77	0.9794	0.2917	3.95	1.94	0.5160	0.7460
6th Fasci.	5.89	3.22	0.5432	0.7125	3.79	2.24	0.1234	0.2034
7th Fasci.	5.95	2.88	0.9811	0.8674	4.03	2.12	0.7284	0.9623
8th Fasci.	5.99	2.57	0.2999	0.4046	4.03	1.80	0.7787	0.7494
9th Fasci.	5.76	2.16	0.4062	0.3564	4.05	1.56	0.2152	0.0971
10th Fasci.	6.19	2.95	0.1395	0.6776	3.93	2.00	0.2493	0.2935
11th Fasci.*	5.57	2.19	0.4925	0.0823	3.70	1.70	**0.0109**	0.0558
every 2nd	5.96	2.81	0.4634	0.9696	4.09	2.04	0.5470	0.9763
every 3rd	5.88	2.96	0.5757	0.9124	4.01	2.12	0.4183	0.5358
every 4th	5.95	2.84	0.6270	0.9699	4.09	2.08	0.6093	0.6921
every 5th	5.72	2.70	0.2859	0.7768	3.97	1.97	0.5733	0.9455
every 6th	5.92	2.97	0.6006	0.6778	4.02	2.07	0.4934	0.2814
every 7th	6.06	2.79	*0.1410*	0.2844	4.14	2.05	0.2493	0.2326
every 8th	6.00	2.97	0.6681	0.8441	4.11	2.19	0.7593	0.6882
every 9th	5.78	2.92	0.3270	0.2539	3.87	2.11	0.0808	0.0874
every10th	5.82	2.81	0.6433	0.8571	4.00	2.02	0.7131	0.3327

Table 4.3-20

Sample Field	mDs	DsSD	Probability		mDa	DaSD	Probability	
total	6.15	3.35	Wilcox.	K-S	4.59	2.87	Wilcox.	K-S
1st Fasci.	6.28	3.36	0.2380	0.5002	4.66	2.85	0.4347	0.7255
2nd Fasci.*	5.74	2.89	**0.0137**	**0.0068**	4.33	2.44	0.1031	0.1099
3rd Fasci.	6.45	3.95	0.6847	0.2297	4.95	3.50	0.1998	0.0824
4th Fasci.	6.08	3.47	0.6694	0.5508	4.54	2.96	0.9136	0.9450
5th Fasci.	5.88	2.57	0.7356	0.4123	4.09	1.98	0.1330	0.2080
6th Fasci.*	6.55	3.37	**0.0164**	0.1404	4.53	2.75	0.7299	0.7010
7th Fasci.	6.05	3.39	0.3881	0.4203	4.65	2.93	0.7402	0.3652
every 2nd	6.10	3.32	0.6020	0.9655	4.55	2.84	0.7564	0.9997
every 3rd	5.97	3.16	0.2168	0.7720	4.41	2.64	*0.1932*	0.6581
every 4th	6.14	3.22	0.6444	0.9529	4.55	2.73	0.8353	0.9773
every 5th	6.21	3.33	0.4732	0.6556	4.68	2.88	0.2886	0.3133
every 6th	6.02	3.18	0.5443	0.6886	4.44	2.64	0.5261	0.9619
every 7th	6.02	3.18	0.6727	0.5732	4.45	2.64	0.4733	0.5590
every 8th	5.96	3.08	0.5060	0.6487	4.38	2.58	0.2820	0.6188
every 9th	6.06	3.29	0.7243	0.9762	4.47	2.74	0.4707	0.8543
every 10th	6.26	3.41	0.5030	0.8406	4.72	2.92	0.2598	0.6732

Abbreviations for Table 4.3-1 to 4.3-20 see next page

Abbreviations for Table 4.3-1 to 4.3-20

every nth: every nth field sample

nth Fasci.: nth fascicle sample

mDs: mean of myelinated fibre diameter

DsSD: standard deviation of Ds

mDa: mean of axonal diameter

DaSD: standard deviation of Da

Wilcox.: Wilcoxon Rank-Sum test evaluates the mean values

K-S: Kolmogorov-Smirnov goodness of fit test evaluates the shapes of frequency distributions.

Table 4.3-21: Comparison of myelinated fibre size (Ds and Da) in fascicles with the whole nerve fibre population. Values are percentage of the number of fascicles in which the fibre size was significantly different from that of the whole nerve. Mean values were compared using Wilcoxon Rank-Sum test. The Shapes of the frequency distributions were compared using Kolmogorov-Smirnov goodness of fit test.

Level of significance set at P≤0.0500		Percentage of the Number of Fascicles						
	Parameter	Fibre Diameter			Axonal Diameter			Total of
Group	Nerve No.	mean	spatial dis.	total of Ds	mean	spatial dis.	total of Da	Ds & Da
Control	1	14.3	57.1	57.1	28.6	57.1	57.1	57.1 (4/7)
Control	2	28.6	57.1	57.1	28.6	42.9	42.9	57.1 (4/7)
Pathol.	3	25	33.3	33.3	25	25	25	41.7 (5/12)
Pathol.	4	15.4	38.5	38.5	7.7	23.1	23.1	38.5 (5/13)
Pathol.	5	40	20	40	20	0	20	40 (2/5)
Pathol.	6	9.1	9.1	9.1	27.3	27.3	36.4	36.4 (4/11)
Pathol.	7	60	80	80	60	70	70	80 (8/10)
Pathol.	8	40	20	40	40	40	40	40 (2/5)
Pathol.	9	66.7	77.8	88.9	55.6	55.6	66.7	88.9 (8/9)
Pathol.	10	50	50	50	66.7	50	66.7	66.7 (4/6)
Pathol.	11	25	33.3	33.3	25	33.3	33.3	50 (6/12)
Pathol.	12	0	0	0	0	16.7	16.7	16.7 (1/6)
Pathol.	13	30	20	40	40	60	70	70 (7/10)
Pathol.	14	44.4	33.3	44.4	33.3	22.2	33.3	55.6 (5/9)
Pathol.	15	25	33.3	41.7	41.7	58.3	58.3	75 (9/12)
Pathol.	16	12.5	25	25	12.5	12.5	12.5	25 (2/8)
Pathol.	17	58.8	64.7	70.6	70.6	76.5	76.5	82.4 (14/17)
Pathol.	18	0	20	20	40	20	40	40 (2/5)
Pathol.	19	27.3	18.2	27.3	18.2	9.1	18.2	36.4 (4/11)
Pathol.	20	28.6	14.3	28.6	0	0	0	28.6 (2/7)

Abbreviations for table 4.3-21

Control: control nerve

Pathol: pathological nerve

spatial dis.: spatial distribution

total of Ds and Da: A sample is thought to have a significantly different fibre size compared to the whole population if its Ds or Da is different from the whole population.

Table 4.3-22: The largest systematic sample in which the fibre size is different from that of the whole nerve

Level of significance		P≤0.0500				P≤0.2000			
		Sample	Sample Size			Sample	Sample Size		
Group	Nerve No.		TFA	%TTFA	NMF		TFA	%TTFA	NMF
Control	1	-	-	-	-	every 2nd	0.4704	49.61	2299
Control	2	every 6th	0.1911	16.77	1176	every 2nd	0.5660	49.68	3293
Pathol.	3	-	-	-	-	every 3rd	0.5366	33.23	3180
Pathol.	4	-	-	-	-	every 3rd	0.4239	33.33	1920
Pathol.	5	-	-	-	-	every 3rd	0.2058	33.33	877
Pathol.	6	every 9th	0.2597	11.50	582	every 4th	0.5660	25.05	1314
Pathol.	7	-	-	-	-	every 7th	0.3234	14.83	964
Pathol.	8	every 9th	0.0564	11.68	306	every 4th	0.1225	25.38	585
Pathol.	9	-	-	-	-	every 9th	0.1764	11.45	1009
Pathol.	10	-	-	-	-	every 9th	0.0882	11.54	474
Pathol.	11	every 3rd	0.3945	33.20	1801	every 3rd	0.3945	33.20	1801
Pathol.	12	every 4th	0.3626	25.26	792	every 7th	0.2083	14.51	461
Pathol.	13	every 4th	0.3577	25.44	1539	every 7th	0.2083	14.81	915
Pathol.	14	-	-	-	-	every 3rd	0.5145	33.23	1404
Pathol.	15	-	-	-	-	-	-	-	-
Pathol.	16	every 10th	0.0858	11.25	371	every 5th	0.1568	20.58	709
Pathol.	17	-	-	-	-	-	-	-	-
Pathol.	18	-	-	-	-	every 7th	0.2377	14.52	489
Pathol.	19	-	-	-	-	every 7th	0.1813	14.92	367
Pathol.	20	-	-	-	-	every 3rd	0.4753	33.16	1051

Key words for table 4.3-22

Control: control group

Pathol.: pathological group

TFA: transverse fascicular area (mm^2)

%TTFA: TFA/TTFA×100%

NMF: the number of MFs in this sample

every nth: every nth field sample

-: There is no systematic sample (from every 10^{th} to every 2^{nd} field sample) of which the fibre size is significantly different from that of the whole population in this nerve at that level of P value.

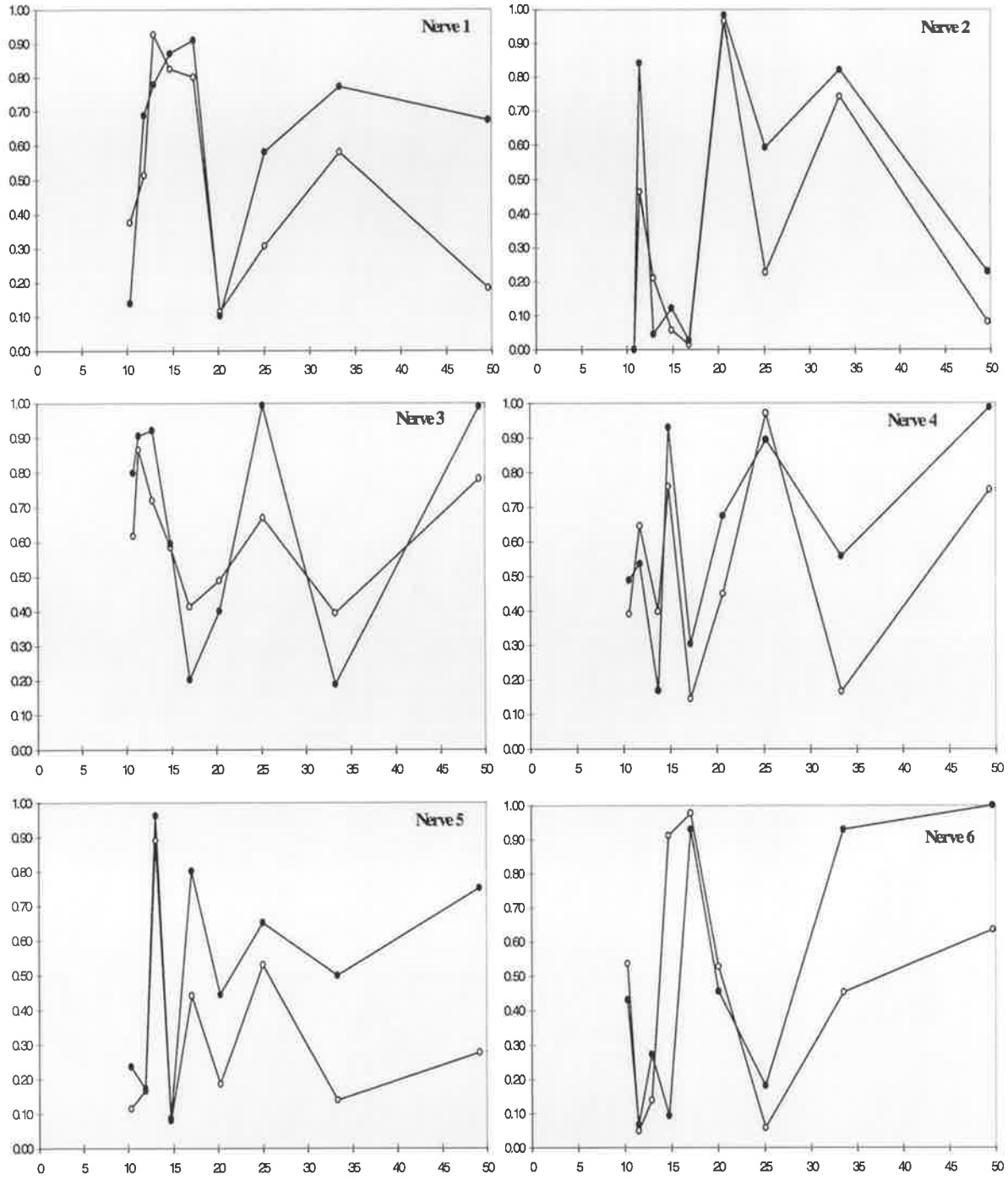

Figure 4.3-1: *P*-value of Ds plotted against systematic sample size (nerve No.1 and 6). Wilcoxon Rank-Sum test (open circle) and Kolmogorov-Smirnov goodness of fit test (filled circle) are used to examine mean value, and frequency and spatial distribution respectively. P values are displayed on the ordinate.

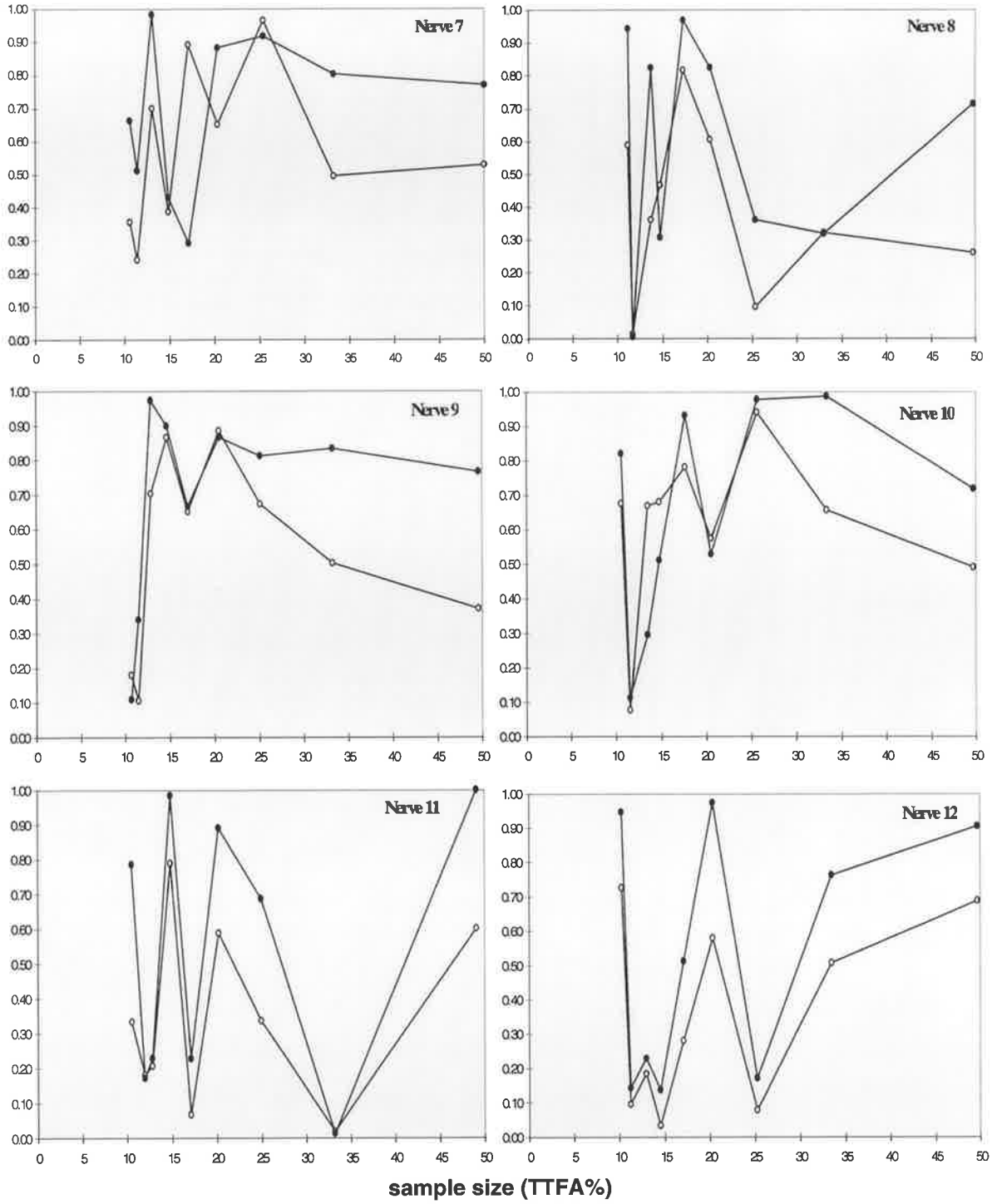

Figure 4.3-1: *P*-value of Ds plotted against systematic sample size (nerve No.7 to 12). Wilcoxon Rank-Sum test (open circle) and Kolmogorov-Smirnov goodness of fit test (filled circle) are used to examine mean value, and frequency and spatial distribution respectively. P values are displayed on the ordinate.

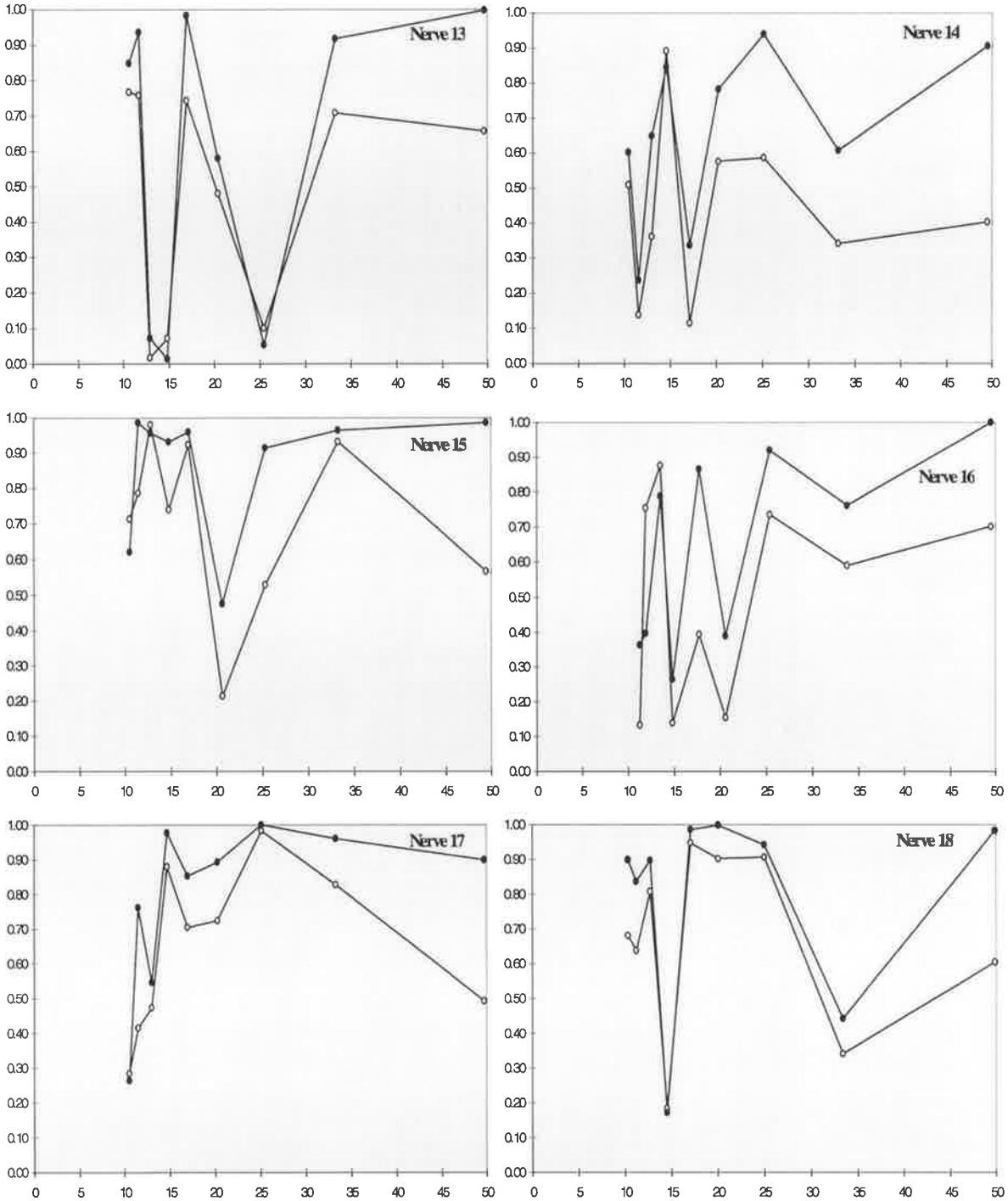

Figure 4.3-1: *P*-value of Ds plotted against systematic sample size (nerve No.13 to 18). Wilcoxon Rank-Sum test (open circle) and Kolmogorov-Smirnov goodness of fit test (filled circle) are used to examine mean value, and frequency and spatial distribution respectively. P values are displayed on the ordinate.

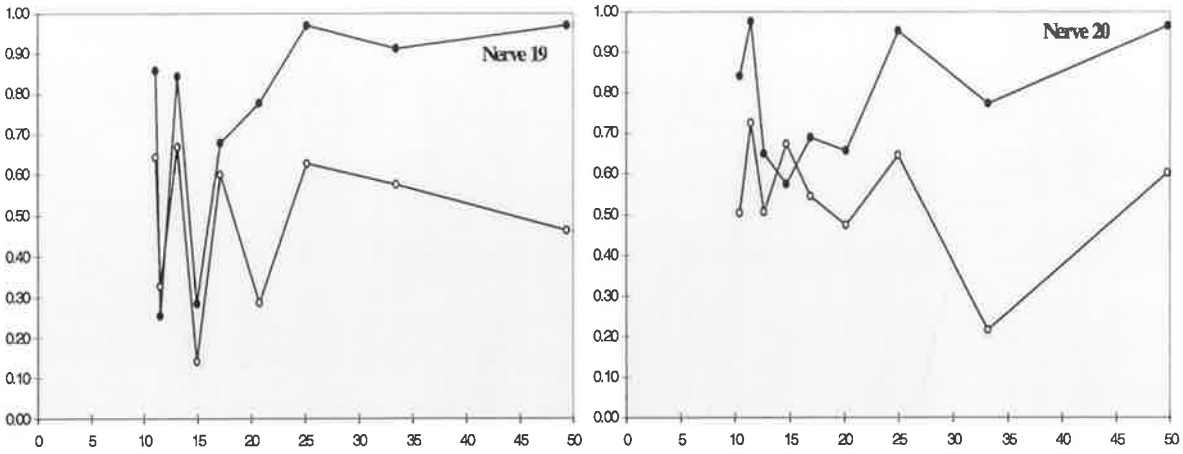

Figure 4.3-1: *P*-value of Ds plotted against systematic sample size (nerve No.19 and 20). Wilcoxon Rank-Sum test (open circle) and Kolmogorov-Smirnov goodness of fit test (filled circle) are used to examine mean value, and frequency and spatial distribution respectively. P values are displayed on the ordinate.

CHAPTER 5: DISCUSSION

The sural nerve is the most common peripheral nerve studied in humans. Most of the morphometric data about sural nerve has been obtained using various sampling methods. However, there is no clear consensus in the literature as to which sampling method is most accurate.

The three commonest sampling methods used in previous quantitative studies are: i) fascicle sampling, ii) random sampling of the fascicular area in the whole nerve and iii) systematic sampling of the fascicular area of every fascicle in the whole nerve (Dyck *et al.* 1984, Dyck *et al.* 1986a, Dyck *et al.* 1986b, Mayhew *et al.* 1981, Saxod *et al.* 1985, Tang and Ebbesson 1972, Thomas *et al.* 1993, Torch *et al.* 1989a). Fascicle sampling is performed on tissue obtained by fascicular biopsy. Some researchers prefer fascicular biopsy to whole nerve biopsy in order to minimize resultant sensory deficits (Dyck and Lofgren 1966, Dyck *et al.* 1993, Thomas 1970) and avoid the risk of 'trophic' ulceration (Llewelyn *et al.* 1991). Systematic sampling is recommended when the whole nerve is available because it can provide information about the spatial distribution of nerve fibres (Dyck *et al.* 1984, Dyck *et al.* 1986a, Dyck *et al.* 1986b) and it is more accurate than random sampling (Mayhew *et al.* 1981). Sample size may be based on either the number of myelinated fibres or the transverse fascicular area. In most previous studies, hundreds to one or two thousand MFs or the fibres in about $0.1mm^2$ fascicular area were measured (Behse 1990, Dyck *et al.* 1986a, Dyck *et al.* 1986b, Gabreëls-Festen *et al.* 1992, Gabreëls-Festen *et al.* 1995, Jacobs and Love 1985, Llewelyn *et al.* 1991, Schellens *et al.* 1993). However there is no consensus as to how many myelinated fibres need to be measured in order to produce a statistically valid representation of the whole myelinated fibre population in a sural nerve. In morphometric studies of myelinated fibres in sural nerves, Ferriere *et al.* (1985) and Schröder *et al.* (1978) found that the thickness of the myelin sheath was linearly related to the axonal diameter for all the myelinated fibres. But Friede and Beuche (1985) found that

type-III and type-II fibres had different relationships between the thickness of myelin sheath and axonal diameter, and that the separation of the two populations was more distinct if more MFs were measured. This suggests that a small sample size may introduce bias, and that accurate estimation of the myelinated fibres in sural nerve needs a suitable sample size.

The characteristics of individual myelinated fibres vary greatly, and there is a non-uniform distribution of myelinated fibres in peripheral nerves (Dyck *et al.* 1984, Dyck *et al.* 1986a, Dyck et al 1986b, Saxod *et al.* 1985, Torch *et al.* 1989a). In pathological nerves, loss of myelinated fibres may be focal, multifocal or diffuse, and the changes of spatial pattern of MFs may be an indicator of the underlying pathological mechanism (Dyck *et al.* 1984, Dyck *et al.* 1986a, Dyck *et al.* 1986b, Dyck *et al.* 1993). Therefore when assessing the accuracy of sampling methods, the spatial distributions of myelinated fibre density and fibre size should be compared as well as the mean values.

5.1 FASCICLE SAMPLING METHOD

5.1.1 TRANSVERSE FASCICULAR AREA, MYELINATED FIBRE DENSITY AND MYELINATED FIBRE DENSITY FREQUENCY DISTRIBUTION

The fascicle size varies widely in peripheral nerves (Behse 1990, Jacobs and Love 1985, O'Sullivan and Swallow, 1968, Saxod *et al.* 1985, Swallow 1966, Torch *et al.* 1989a, Walsh 1971), and the number of MFs within each fascicle varies according to its fascicular area (Swallow 1966, O'Sullivan and Swallow 1968, Saxod *et al.* 1985). In control human sural nerves, the size of individual fascicles varies from less than 100μm in diameter to 0.46mm^2 in transverse area (Jacobs and Love 1985, O'Sullivan and Swallow 1968, Walsh 1971). The small number of myelinated fibres in small fascicles less then 100μm can be ignored in quantitative studies (O'Sullivan and Swallow *et al.* 1968, Swallow 1966), and

were excluded from quantitation in this study. There were a total of 14 fascicles in the two control sural nerves in this study. The fascicular area of individual fascicles varied from 0.0392mm^2 to 0.2940mm^2, similar to that of O'Sullivan and Swallow (1968) and Walsh (1971), but greater than that of Jacobs and Love (1985). The difference may be due to different methods of tissue preparation and counting. Dyck *et al.* (1981b) proved that hypersosmolar fixatives caused severe shrinkage of fascicular area. In this study, the nerve tissues were fixed in isosmotic fixatives, dehydrated in graded concentrations of ethanol and propylene oxide, and embedded in resin. We did not compare the fascicular area in plastic and cryostat sections. In accord with previous studies, the estimated shrinkage of fascicular area in our series was about 10% (Behse 1990, Dyck *et al.* 1981b). In our study, the transverse fascicular area of each fascicle was obtained by additions of the areas of all the measuring frames in the fascicle. Previous studies have obtained TFA by drawing the contour of the fascicle under lower magnification, and cutting out and weighing the resultant tracing (Behse 1990), or tracing the outer edges of the endoneurium with a cursor, and calculating the fascicular area with a digitizer (Dyck *et al.* 1986a). Uniform measurements of fibre diameter, axonal diameter and fascicular area at the same final magnification would allow an easier comparison of data obtained in different laboratories.

The mean myelinated fibre density (MFD) varies considerably among fascicles in peripheral nerves. In one control anterior tibial nerve, Swallow (1966) found that mean MFD varied from 5900 to 9088/mm^2 in 5 fascicles. In control sural nerves, Behse (1990) found the myelinated fibre density of fascicles deviated from the mean fibre density of the nerve by between –21% to +37%. In the two control nerves in this study, the mean MFD of each fascicle varied from 4045 to 5763/mm^2 in nerve No.1, and from 5130 to 6386/mm^2 in nerve No.2. The deviation of MFD of each fascicle from the mean MFD of the whole nerve ranged from –18% to +17% in nerve No.1 and from –11% to 10% in nerve No.2.

In studies of superficial peroneal nerves, Saxod *et al.* (1985) concluded that the myelinated fibre density is related to fascicle diameter. We did not find any correlation between the mean MFD of each fascicle and the fascicle size (fascicular area or fascicle diameter) in either the control or pathological sural nerves (Figure 4.2-1). Our reinterpretation of the data presented by Saxod *et al.* (1985) shows that the number of constituent myelinated fibres was positively linearly related to the fascicular area of each fascicle within control superficial peroneal nerves contrary to the conclusion made by the authors. Similar results were obtained in the control sural nerves in this study. Accordingly, it is impossible to predict which fascicle may have a myelinated fibre density comparable to that of the whole nerve before quantifying all the fascicles.

The comparisons of frequency distribution of myelinated fibres between the whole population and fascicle samples or between fascicle samples revealed that the frequency distributions were different between fascicles in control sural nerve, and there was no relationship between fascicle size and its MF frequency distribution to that of the whole nerve.

The mean fibre density and its frequency distribution varied considerably among fascicles in our control sural nerves, and the variation was not related to the fascicle size. Therefore, it is impossible to ascertain which fascicle is a statistically valid sample to represent the myelinated fibre density and the fibre density spatial distribution of the whole population in control sural nerves.

In neurological disorders and neuropathies, the pathological changes affecting fascicles may be patchy. For example, in diabetic distal polyneuropathy, the pathological changes may be

more severe in some fascicles, while others are relatively exempt from damage (Dyck *et al.* 1986a, 1986b). The mechanism of patchy damage is unclear in most peripheral nerve diseases. For this reason it is necessary to study all the fascicles when investigating the morphological and morphometric changes in peripheral nerves. In our material the biggest variance of fascicular mean MFD was found in nerve No.7, with the highest mean MFD of 4215/mm^2 in the 9th fascicle and the lowest of 2084/mm^2 in the 6th fascicle (see p87). The highest mean MFD was 202% of the lowest. We were unable to establish any criteria by which a single fascicle, representative of the mean MFD and the MFD frequency distribution of the whole nerve, could be selected in either the control or pathological nerves. Thomas *et al.* (1993) showed that there was less variation in fibre densities than the number of fibres in fascicular biopsies and concluded that the mean MFD was the measurement of choice. However we found that MFD varied considerably in agreement with previous studies (Swallow 1966, Saxod *et al.* 1985). Thus the myelinated fibre density derived from one fascicle or part of a fascicle/s is not an accurate representation of the whole MF population.

5.1.2 MYELINATED FIBRE SIZE (FIBRE AND AXONAL DIAMETER)

The spatial pattern of MFs in the fascicles of peripheral nerve is heterogeneous not only in fibre number but also in fibre size (Dyck *et al.* 1984, Dyck *et al.* 1986a, Dyck *et al.* 1986b, Torch *et al.* 1989a). In previous studies only the fibre diameter was assessed when investigating the mean value of fibre size and size spatial distribution (Dyck *et al.* 1984, Dyck *et al.* 1986a, Dyck *et al.* 1986b, Mayhew *et al.* 1981, Torch *et al.* 1989a). Although the thickness of the myelin sheath in normal peripheral nerves may be positively related to the total fibre size or axonal size on cross section (Behse 1990, Dyck et al 1971a, Dyck *et al.* 1971c, Friede 1972, Friede and Samorajski 1967, Ferriere *et al.* 1985, Jacobs and Love 1985, King 1994, Schröder *et al.* 1978, Thomas *et al.* 1993), that does not mean that fibres,

which have the same fibre diameter or axonal diameter on cross section, always have the same thickness of myelin sheath even in normal peripheral nerves. As part of the present study, MFs were divided into 20 subgroups based on axonal diameter (Da): $Da \leq 1\mu m$, $1 < Da \leq 2\mu m$ and so on. Analysis of the histograms of the thickness of myelin sheath showed that every subgroup had a spectrum of the thickness of myelin sheath and a spectrum of g-ratio in both control and pathological nerves. In pathological nerves, an atrophic axon with a thick myelin sheath may have the same total fibre diameter as a remyelinating fibre which has a relatively normal axon and disproportionately thin myelin. A comprehensive representation of fibre size should include accurate representations of both fibre diameter and axonal diameter in mean values and spatial distributions.

Fibre size and its spatial distribution also varied considerately among fascicles within the nerve both in the control and pathological groups, and these variations did not relate to fascicle size and the mean MFD of individual fascicles. 57.1% of the fascicles in 2 control nerves, and 53.6% (16.7% to 88.9%) of the fascicles in 18 pathological nerves had significantly different fibre size (fibre diameter and/or axonal diameter) mean values and/or size spatial distribution to the whole MF populations. Both the fibre size and its spatial distribution varied considerably, and no regular pattern was found to predict this variation. Quantifying the features of individual MFs in only one or a few fascicles (Dyck *et al.* 1971a, Dyck *et al.*1986a, Dyck *et al.* 1986b, Engelstad *et al.* 1997, Llewelyn *et al.* 1991, Thomas *et al.* 1971, Thomas *et al.* 1987, Webster *et al.* 1967) may produce biased results.

Thus it is impossible to determine which fascicle to measure to obtain an accurate representation of mean fibre size and spatial distribution of the whole MF population. Quantification of all the constituent fascicles is necessary in morphometric studies of sural nerve to ensure accurate results. Pollock *et al.* (1983) studied a series of patients who had

undergone fascicular or whole sural nerve biopsies, and found that the resultant neurological deficits were similar in the two groups after 5 years. Accordingly, it is probably better to perform whole sural nerve biopsies because quantitative studies will be more accurate and the procedure is surgically simpler than fascicular biopsy.

5.2 SYSTEMATIC SAMPLING METHODS

Systematic sampling methods include systematic sampling of the fascicles (Dyck *et al.* 1986b) and systematic sampling of the fascicular area in every fascicle of the nerve (Dyck *et al.* 1984, Dyck *et al.* 1986a, Saxod *et al.* 1985, Tang and Ebbesson 1972, Torch *et al.* 1989a).[1] In this study we assessed the accuracy of systematic sampling of the fascicular area in every fascicle of the nerve.

An important advantage of this systematic sampling method is that it can be used to recognize the spatial distribution of myelinated fibres (Dyck *et al.* 1984, Dyck *et al.* 1986a, Dyck *et al.* 1986b, Torch *et al.* 1989a). Loss of fibres is one of the most common pathological phenomena in peripheral neuropathies. The loss of MFs may be focal, multifocal, or diffuse (Dyck *et al.* 1993). By comparing the density and size of myelinated fibres using measuring frames, focal, multifocal and diffuse changes of myelinated fibre density and fibre size can be recognized (Dyck *et al.* 1993). The spatial pattern of nerve fibre abnormality may be useful in diagnostic evaluation (Dyck *et al.* 1984). For example ischaemic neuropathies due to focal pathological change of small arteries usually show patchy loss of myelinated fibres that varies from fascicle to fascicle (Dyck *et al.* 1984). Dyck and co-workers (Dyck *et al.* 1986b, Sugimura and Dyck 1982) found patchy multifocal fibre loss in diabetic neuropathies. Since capillary basement membranes are thickened (Aagenaes and Moe 1961, Siperstein *et al.* 1966, Siperstein *et al.* 1968), with

capillary thrombosis (Timperley *et al.* 1976, Williams *et al.* 1980) and in the absence of any direct affect of hyperglycemia on nerve (Service *et al.* 1985), they proposed that diabetic neuropathies were caused by ischaemia due to the microvascular pathological abnormality (Dyck *et al.* 1986a, 1986b).

In order to determine the spatial distribution of MFs, it is necessary to select a suitable size measuring frame. If the measuring frame is too large, multiple fields of a fascicle cannot be surveyed and variability of density within fascicles cannot be estimated. If too small, the measuring frame would contain few or no fibres. Dyck *et al.* (1984, 1986a, 1986b) estimated the spatial distribution of MFs at a final magnification of approximately ×2000 in human and animal peripheral nerves. In human superficial peroneal nerves, a final magnification of ×1130 was used to estimate fibre density spatial distribution (Saxod *et al.* 1985), and a magnification of ×2100 was employed to determine the fibre size distribution (Torch *et al.* 1989a). Initially we used a magnification of ×2371 to determine fibre size and frequency distribution. But some scattered small thin myelinated fibres were missed by the image analysis system probably because the myelin sheath was too thin and the colour too pale. On the other hand, some myelinated fibres, especially clusters of regenerating fibres with closely touching fibres were misinterpreted by the image analysis system as distorted larger fibre(s). When the final magnification was changed to ×3018 (×100 objective), these problems were minimized. At the final magnification of ×3018, the area of each measuring frame is 2450μm^2. Within each measuring frame the number of MFs ranged from 2 to 26 in the two control sural nerves, and from 0 to 28 in the eighteen pathological nerves. For morphometric studies of diseased sural nerves, the final magnification of ×3000 may be more suitable than that of ×2000 in determining the number, shape, size, and spatial distribution of myelinated fibres.

Although systematic sampling methods have been used in previous studies of peripheral nerve (Dyck *et al.* 1984, Dyck *et al.* 1986a, Dyck *et al.* 1986b, Ebbesson 1963, Ebbesson 1968, Mayhew *et al.* 1981, Saxod *et al.* 1985, Tang and Ebbesson 1972, Torch *et al.* 1989a), little information is available about their accuracy relative to measurements of MFs in the whole nerve, especially in human sural nerve. Mayhew *et al.* (1981) showed that systematic sampling of the fascicular area was more accurate than random sampling in quantitating rat tibial nerves. Tang and Ebbesson (1972) found that the MFs in about 50% of the total fascicular area needed to be counted in both systematic and random sampling methods to obtain accurate data representative of the total number of MFs in cranial nerves. Saxod *et al.* (1985) pointed out that MFD can only be reliably established by counting all the fibres within a fascicle or a nerve in human superficial peroneal nerves. In rats, Dyck *et al.* (1984) used the systematic sampling method to quantitate MFs in every 3rd field in sciatic, peroneal and tibial nerves in a study of spatial distribution of MFs. In quantitative studies of human diabetic neuropathies (with and without vasculitis), Dyck *et al.* (1986b) sampled every 12th field in large fascicles. Torch *et al.* (1989) found that measurements performed on up to 10% of the total myelinated fibres in control human superficial peroneal nerve were not an accurate representation of the whole MF population.

To the best of our knowledge, no previous study has assessed the accuracy of fibre density and fibre size obtained by systematic sampling to that obtained by whole nerve sampling in human sural nerves.

5.2.1 MYELINATED FIBRE DENSITY (MFD)

The variation of MFD in systematic samples was not as great as that in fascicle samples. However, there were still some samples in which the MFD differed from that of the whole

population in both control and pathological nerves. At the level of significance set at $P \leq 0.05$, the MFD differed significantly from that of the whole nerve in only every 8^{th} field sample of one pathological nerve. If P is set at 0.2, 1 control (50%, 1/2) and 5 (27.8%, 5/18) pathological nerves had systematic samples in which MFD differed from that of the whole nerve. Even sampling every 6^{th} field in a control and a pathological nerve (No.2 and 7, see p111) still cannot obtain the MFD that reliably represents the whole myelinated fibre population. In the control nerves, the variation of MFD between systematic samples suggested that the spatial distribution of myelinated fibres was non-uniform within fascicles, confirming the findings of other researchers (Dyck *et al.* 1984, Dyck *et al.* 1986a, Dyck *et al.* 1986b, Saxod *et al.* 1985, Torch *et al.* 1989a). In the pathological nerves, the variation of MFD in systematic samples may reflect the intrinsic pattern of non-uniform distribution in normal nerve or may be secondary to the pathologic process. Patchy loss of MFs and reduction of fibre density were obvious by visual inspection in some pathological nerves. Severe loss of MFs decreases both fibre density and variation of fibre density within fascicles. Less severe focal pathological change probably produces an increased variability of MFD (Dyck *et al.* 1986a). In nerve No.3, showing only mild pathological changes, the variation of MFD within fascicles ranged from 0 to 28/measuring frame, bigger than that in the two control nerves. Increased focal fibre density may also occur as in clusters of regenerating nerve fibres.

In normal rat sural nerve it has been reported that large fibres approach a random distribution, while small fibres tend to be clustered (Dyck *et al.* 1984). However visual inspection of our human materials, showed that the distribution of large and small fibres was heterogeneous within fascicles in both control and pathological sural nerves. The pattern of spatial distribution of MFs within peripheral nerves has been divided into two groups: weakly and strongly heterogeneous (Saxod *et al.* 1985). In our study we did not

deliberately select the nerves in which MF spatial distribution was strongly heterogeneous, but we did exclude nerves with a mean myelinated fibre density so low that one measuring frame contained an average less than 2 myelinated fibres. In previous studies, myelinated fibre density in whole sural nerve was usually derived from about 10% of the total transverse fascicular area (TTFA) or about $0.1mm^2$ of fascicular area (Gabreëls-Festen *et al.* 1992, Gabreëls-Festen *et al.* 1995, Jacobs and Love 1985, Schellens *et al.* 1993, Tohgi *et al.* 1977b). Although the fibre densities of most systematic samples in this study were not significantly different from that of the whole nerve ($P \leq 0.05$), we found that the myelinated fibre density of the systematic sample derived from up to 17% of TTFA or $0.3724mm^2$ fascicular area (see p97) differed from that of the whole population at the level of significance set at 0.2. This result is consistent with the findings of Saxod *et al.* (1985) and Tang and Ebbesson (1972).

Behse (1990) suggests that the number of fibres per nerve is a more reliable parameter than the fibre density if different methods of tissue preparation and staining are used because the shrinkage of the endoneurial area and of the fibre size may be different. However in nerve No.20, sampling every 7^{th} field produced a fascicular area of $0.2107mm^2$ (14.7% of TTFA) and 437 myelinated fibres, while sampling every 8^{th} field resulted in a fascicular area of $0.1813mm^2$ (12.7% of TTFA) and 447 myelinated fibres (see p93). The larger fascicular area sample contained less fibres than the sample of smaller fascicular area because of the great variation of myelinated fibre spatial distribution. Therefore, myelinated fibre density derived from systematic sampling the fascicular area in every fascicle of the sural nerve is relatively comparable to that of sampling the whole nerve, but is still not completely representative of the whole MF population.

5.2.2 MYELINATED FIBRE SIZE (FIBRE AND AXONAL DIAMETER)

Torch *et al.* (1989) proved that measurements performed on up to 10% of the total myelinated fibres in superficial peroneal nerves were not representative of the fibre diameter of the whole population. We studied sample sizes varying from 10% to 50% of the total fascicular area, roughly corresponding to 10% to 50% of the total number of myelinated fibres. Our results show that even sampling 50% of the total fascicular area in control sural nerve still cannot produce fibre or axonal diameters that are representative of values obtained by whole nerve sampling. This applies to both the mean values and the frequency distributions of fibre and axonal diameters. This is because the spatial size distribution of MFs within fascicles is non-uniform in control sural nerve. In pathological nerves, selective loss of myelinated fibres and clusters of regenerating fibres produce an uneven spatial distribution of fibre size.

It is commonly accepted that the accuracy of the representation of samples increases with increasing sample size, but this was not the case in our study. Similar findings were reported by Torch *et al.* (1989). This finding is attributed to the heterogeneous spatial distribution of fibre size within fascicles. We found that even sampling every 2nd field the P value was less than 0.2 in control sural nerves. This indicates that the MFs in more than half of the fascicular area in every fascicle needs to be counted in order to get results representative of the whole myelinated fibre population in the sural nerve.

5.3 COMPARISON OF DATA RELATING TO FASCICLE NUMBERS, TOTAL TRANSVERSE FASCICULAR AREA, TOTAL NUMBER OF MYELINATED FIBRES, MYELINATED FIBRE DENSITY AND FIBRE SIZE WITH THAT REPORTED IN THE LITERATURE

The number of fascicles, total transverse fascicular area, total number of myelinated fibres and myelinated fibre density in the two control sural nerves and the pathological sural nerves in this series are similar to those reported in previous studies (Behse *et al.* 1990, Jacobs and Love 1985, O'Sullivan and Swallow 1968). Comparison of fibre and axonal diameter in our study with that reported in the literature revealed a slightly greater fibre size in this series with consequent shift in the histograms of frequency distributions of fibre and axonal diameter to the right by approximately 2-3μm. Two reasons may account for these differences. First, the nerve tissues in our study were fixed in isosmolar fixatives and embedded in resin reducing the shrinkage factor (Dyck *et al.* 1980). Second, the myelinated fibre diameter and axonal diameter were derived from the myelin sheath area combined with the perimeters of the myelin sheath, not from the axonal area and the total area of fibre on cross section. During tissue preparation, shrinkage is unavoidable, but the myelin sheath area and the perimeter remain relatively constant (Auer *et al.* 1994, Dyck *et al.* 1980).

5.4 CONTROLS

For each of the twenty sural nerves, the results obtained by sampling were compared to those obtained by study of the whole nerve. Accordingly, the effects of aging, the type of pathological process and variation between nerves were not relevant to this study (Behse 1990, Jacobs and Love 1985, Schellens *et al.* 1993, Saxod *et al.* 1985, Tohgi *et al.* 1977b, Thomas *et al.* 1993, Thomas *et al.* 1997). Moreover, since the specimen fixation and embedding methods were identical in all cases, their influence on nervous structures (Behse 1990, Dyck *et al.* 1981b) also did not affect the results.

Conclusions

1. The mean values, frequency distribution and spatial distribution of myelinated fibre density, fibre diameter and axonal diameter are heterogeneous between fascicles in both control and pathological sural nerves.
2. There is no relationship between the myelinated fibre density of each fascicle and the fascicle diameter or area in the sural nerve.
3. Morphometric results from one or part of a fascicle cannot accurately represent the whole myelinated fibre population in the sural nerve.
4. Systematic sampling of the myelinated fibres in half of the fascicular area of every fascicle in the sural nerve is not accurately representative of the whole myelinated fibre population.
5. In morphometric studies of the sural nerve, the accuracy of representation of samples does not increase with increasing sample size from 10% to 50% of the total transverse fascicular area.

Bibliography

Aagenaes O, Moe H. Light and electron-microscopy study of skin capillaries of diabetics. Diabetes 1961; 10: 253-259.

Aguayo AJ, Charron L, Bray GM. Potential of Schwann cells from unmyelinated nerves to produce myelin: A quantitative ultrastructural and autoradiographic study. J Neurocytol 1976; 5: 565-573.

Aguayo AJ Nair CPV, Bray GM. Peripheral nerve abnormalities in the Riley-Day syndrome. Arch Neurol 1971; 24: 106-116.

Albelda SM, Buck CA. Integrins and other cell adhesion molecules. FASEB J 1990; 4: 2868-2880.

Arbuthnott ER, Boyd IA, Kalu KU. Ultrastructural dimensions of myelinated peripheral nerve fibres in the cat and their relation to conduction velocity. J Physiol 1980; 308: 125-157.

Archer AG, Watkins PGJ, Thomas PK, Sharma AK, Payan J. The natural history of acute painful neuropathy in diabetes mellitus. J Neurol Neurosurg Psychiat 1983; 46: 491-499.

Atsumi T, Miyatake T. Morphometry of the degenerative process in the hypoglossal nerve in amyotrophic lateral sclerosis. Acta Neuropathol (Berl) 1987; 73: 25-31.

Auer RN. Automated nerve fibre size and myelin sheath measurement using microcomputer-based digital image analysis: theory, method and results. J Neurosci Meth 1994; 51: 229-238.

Bardosi A, Friede, RL, Ropte S, Goebel HH. A morphometric study on sural nerves in metachromatic leucodystrophy. Brain 1987; 110: 683-694.

Behse F. Morphometric studies on the human sural nerve. Acta Neurol Scand 1990; 82(suppl 132): 4-38.

Behse F, Buchthal F. Normal sensory conduction in the nerves of the leg of man. J Neurol Neurosurg Psychiat 1971; 34: 404-414.

Behse F, Buchthal F, Carlsen F, Knappeis GG. Hereditary neuropathy with liability to pressure palsies: electrophysiological and histopathological aspects. Brain 1972; 95: 777-794.

Behse F, Buchthal F, Carlsen F. nerve biopsy and conduction studies in diabetic neuropathy. J Neurol Neurosurg Psychiat 1977; 40: 1072-1082.

Beuche W, Friede RL. A new approach toward analyzing peripheral nerve fiber populations. II. Foreshortening of regenerated intenodes corresponds to reduced sheath thickness. J Neuropathol Exp Neurol 1985; 44: 78-84.

Blight AR, Decrescito, V. Morphometric analysis of experimental spinal cord injury in the cat: the relation of injury intensity of survival of myelinated axons. Neuroscience 1986; 19: 321-341.

Bohlega SA, Stigsby B, Haider A, McLeon D. Guillain-Barre syndrome with severe demyelination mimicking axonopathy. Muscle Nerve 1997; 20: 514-516.

Bots GThAM, Maat-Schieman M. Patholology of nerves. In: Vinken PJ, Bruyn GW, Klawans HL, editors. Handbook of Clinical Neurology. New York: Elsevier Science Publishers BV, 1987; 51: 63-84.

Boyd IA, Davey MR. Composition of peripheral nerves. Edinburgh; Livingstone, 1968.

Boyd IA, Kalu KU. The relation between axon size and number of lamellae in the myelin sheath for afferent fibres in groups I, II and III in the cat. J Physiol 1973; 232: 31-33.

Bradley WG, Good P, Rasool CG, Adelman LS. Morphometric and biochemical studies of peripheral nerves in amyotrophic lateral sclerosis. Ann Neurol 1983; 14: 267-277.

Brady RO, Quarles RH. Developmental and pathophysiological aspects of the myelin-associated glycoprotein. Cell Mol Neurobiol 1988; 8: 139-148.

Brown MJ, Martin JR, Asbury AK. Painful diabetic neuropathy. Arch Neurol 1976; 33: 164-171.

Buchthal F, Carlsen F, Behse F. Schmidt-Lanterman clefts: A morphometric study in human sural nerve. Amer J Anat 1987; 180: 156-160.

Bunge MB, Williams AK, Wood PM. Neuron-Schwann cell interaction in basal lamina formation. Dev Biol 1982; 92: 449-460.

Bunge MB, Williams AK, Wood PM, Unitto J, Jeffrey JJ. Comparison of nerve cell and nerve cell plus cultures, with particular emphasis on basal lamina and collagen formation. J cell Biol 1980; 84: 184-202.

Burgoon MP, Grumet M, Mauro V, Edelman GM, Cunninggham BA. Structure of the chicken neuron-glia cell adhesion molecule, Ng-CAM: origin of the polypeptides and relation to the Ig superfamily. J Cell Biol 1991; 112: 1017-1029.

Carpenter S. An ultrastructural study of an acute fatal cases of the Guillain-Barré syndrome. J Neurol Sci 1972; 15: 125-140.

Cash K, Blumbergs PC. Neuromuscular tissue. In: Laboratory histopathology: a complete reference, Churchill Livingstone, 1994; 2: 7.3-1 - 7.3-25.

Cavallari V, Maiorana MC, Scimone S. Computer-assisted morphometry of the peripheral nervous system, a diagnostic tool. Path Res Pract 1989; 185: 803-806.

Cavanagh JB. Peripheral nerve changes in ortho-cresyl phosphate poisoning in the cat. J Path Bact 1964; 87: 365-383.

Celio MR. The Schmidt-Lanterman incisures of the myelin sheath of Mauthner axons: places of longitudinal growth of myelin? Brain Res 1976; 108: 221

Chaia NL, Hess PR, Hosoi M, Rhoades RW. Morphological characteristics of low-threshold primary afferents in the trigeminal subnuclei interpolaris and caudalis (the medullary dorsal horn) of the Golden hamster. J Comp Neurol 1987; 264: 527-546.

Clemence A, Mirsky R, Jessen KR. Non-myelinforming Schwann cells proliferate rapidly during Wallerian degeneration in the rat sciatic nerve. J Neurocytol 1989; 18: 185-192.

Dewaegh SM, Lee VMY, Brady ST. Local modulation of neurofilament phosphorylation, axonal caliber, and slow axonal transport by myelinating Schwann cells. Cell 1992; 68: 451-463.

Ding Y, Brunden KR. The cytoplasmic domain of myelin glycoprotein P_0 interacts with negatively charged phospholipid bilayers. J Biol Chem 1994; 269: 10764-10770.

Dunn RF, O'Leary DP, Kumley WE. Quantitative analysis of micrographs by computer graphics. J Neurosci Methods 1975; 4: 267-276.

D'Urso D, Brophy PJ, Staugaitis SM. Protein zero of peripheral nerve myelin: biosynthesis, membrane insertion and evidence for homotypic interaction. Neuron 1990; 4: 449-460.

Dyck PJ. Experimental hypertrophic neuropathy: Pathogenesis of onion-bulb formations produced by repeated tourniquet applications. Arch Neurol 1969; 21: 73-95.

Dyck PJ, Lambert EH. Numbers and diameters of nerve fibres and compound action potential of sural nerve: controls and hereditary neuromuscular disorders. Trans Amer Neurol Ass 1966; 191: 214-217.

Dyck PJ, Lambert EH. Dissociated sensation in amyloidosis. Compound action potential, quantitative histologic and teased-fiber, and electron microscopic studies of sural nerve biopsies. Arch Neurol 1969; 20: 490

Dyck PJ, Lofgren EP. Method of fascicular biopsy of human peripheral nerve for electrophysiologic and histologic study. Mayo Clin Proc 1966; 41: 778-784.

Dyck PJ, Gutrecht JA, Karnes WE, Dale AJD. Histologic and teased-fiber measurements of sural nerve in disorders of lower motor and primary sensory neurons. Proc Mayo Clin 1968; 43: 81-123.

Dyck PJ, Lofgren EP. Nerve biopsy: choice of nerve, method, symptoms and usefulness. Med Clin N Amer 1968; 52: 885-893.

Dyck PJ, Ellefson RD, Lais AC, Smith RC, Taylor WF, Van Dyke RA. Histologic and lipid studies of sural nerves in inherited hypertrophic neuropathy: preliminary report of a lipid abnormality in nerve and liver in Dejerine-Sottas disease. Mayo Clin Proc 1970; 45: 286-327.

Dyck PJ, Johnson WJ, Lambert EH, O'Brien PC. Segmental demyelination secondary to axonal degeneration in uremic neuropathy. Mayo Clin Proc 1971a; 46: 400-431.

Dyck PJ, Lambert EH, Nichols PC. Quantitative measurement of sensation related to compound action potential and number and sizes of myelinated and unmyelinated fibers of sural nerves in health, Friedreich's ataxia, hereditary sensory neuropathy, and tabes dorsalis. In: Cobb WA, editor. Handbook of Electroencephalography and Clinical Neurophysiology. Amsterdam, Elsevier, 1971b; 9: 83-118.

Dyck PJ, Lambert EH, Saunders K, O'Brien PC. Severe hypomyelination and marked abnormality of conduction in Dejerine-Sottas hypertrophic neuropathy: Myelin thickness and compound action potential of sural nerve in vitro. Mayo Clin Proc 1971c; 46: 432-436.

Dyck PJ, Low PA, Sparks MF, Hexum LA, Karnes JL. Effect of serum hyperosmolality on morphometry of healthy human sural nerve. J Neuropathol Exp Neurol 1980; 39: 285-295.

Dyck PJ, Lais AC, Karnes JL, Sparks M, Hunder H, Low PA, Windebank AJ. Permanent axotomy, a model of axonal atrophy and secondary segmental demyelination and remyelination. Ann Neurol 1981a; 9: 575-583.

Dyck PJ, Lambert EH, Windebank AJ, Lais AA, Sparks MF, Karnes J, Sherman WR, Hallcher LM, Low PA, Service FJ. Acute hyperosomalar hyperglycemia causes axonal shrinkage and reduced nerve conduction velocity. Exp Neurol 1981b; 71: 507-514.

Dyck PL, Karnes J, Sparks M, Low PA. The morphometric composition of myelinated fobres by nerve, level and species related to nerve microenvironment and ischaemia. Clin Neurophysiol [suppl.] 1982; 36: 39-55.

Dyck PJ, Karnes J, O'Brien P, Nukada H, Lais A, Low P. Spatial pattern of nerve fiber abnormality indicative of pathologic mechanisms. Am J Pathol 1984; 117: 225-238.

Dyck PJ, Lais A, Karnes J, Sparks M, Dyck PJB. Peripheral axotomy induces neurofilament decrease, atrophy, demyelination and degeneration of root and fasciculus gracilis fibers. Brain Res 1985; 340: 19-36.

Dyck PJ, Karnes JL, O'Brien P, Okazaki H, Lais A, Engelstad J. The spatial distribution of fiber loss in diabetic polyneuropathy suggests ischemia. Ann Neurol 1986a; 19: 440-449.

Dyck PJ, Lais A, Karmes JL, O'Brien P, Rizza R. Fiber loss is primary and multifocal in sural nerves in diabetic polyneuropathy. Ann Neurol 1986b; 19: 425-439.

Dyck PJ. Detection, characterization and staging of polyneuropathy: assessed in diabetics. Muscle Nerve 1988; 11: 21-32.

Dyck PJ, Kratz KM, Lehman KA, Kames JL The Rochester Diabetic Neuropathy Study: design, criteria for types of neuropathy, selection bias and reproducibility of neuropathic tests. Neurology 1991; 41: 799-807.

Dyck PJ, Giannini C, Lais A. Pathologic alterations of nerves. In: Dyck PJ, Thomas PK, Lambert EH, Bunge RP, editors. Peripheral Neuropathy, 3rd edition. Philadelphia: WB Saunders, 1993: 514-595.

Dyck PJ, Dyck PJB, Grant IA, Robert DF. Ten steps in characterizing and diagnosing patients with peripheral neuropathy. Neurology 1996; 47: 10-17.

Ebbesson SOE. A quantitative study of human superior cervical sympathetic ganglia. Anta Rec 1963; 146: 353-356.

Ebbesson SOE. Quantitative studies of superior cervical sympathetic ganglia in a variety of primates, including man. I. The ratio of preganglionic to ganglionic neurons. J Morph 1968; 124: 117-131.

Einheber S, Milner TA, Giancotti F, Salzer JL. Axonal regulation of Schwann cell integrin expression suggests a role for $\alpha 6\beta 4$ in myelination. J Cell Biol 1993; 123: 1223-1236.

Engelstad JK, Davies JL, Giannina C, O'Brien PC, Dyck PJ. No evidence for axonal atrophy in human diabetic polyneuropathy. J Neuropathol Exp Neurol 1997; 56: 255-262.

Espir MLE, Harding DTC. Apparatus for measuring and counting myelinated merve fibres. J Neuro Neurosurg Psychiat 1961; 24: 287-290.

Esiri MM. Oppenheimer's Diagnostic Neuropathology: A practical manual. 2nd edition. Blackwell Science, 1995: 377-388.

Ewart DP, Kuzon JWM, Fish JS, Mckee NH. Nerve fibre morphometry: a comparison of techniques. J Neurosci Methods 1989; 29: 143-150.

Ferriere G, Denef JF, Rodriguez J, Guzzetta F. Morphometric studies of normal sural nerves in children. Muscle Nerve 1985; 8: 697-704.

Frasher JP. On methods of measuring neve fibres. J Anat 1980; 130: 139-151.

Friede RL. Control of myelin formation by axon caliber (with a model of the control mechanism). J Comp Neur 1972; 144: 232-252.

Friede RL, Beuche W. Combined scatter diagrams of sheath thickness and fibre in human sural nerves: changes with age and neuropathy. J Neurol Neurosurg Psychiat 1985a; 48: 749-756.

Friede RL, Beuche W. A new approach toward analyzing peripheral nerve fiber population I. Variance in sheath thickness corresponds to different geometric proportions of the internodes. J Neuropathol Exp Neurol 1985b; 44: 60-72.

Friede RL, Bischhausen R. How are sheath dimentions affected by axonal caliber and internodal length? Brain Res, 1982; 235: 335-350.

Friede RL, Meier T, Diem M. How is the exact length of an internode determined? J Neurol Sci 1981; 50: 217-228.

Friede RL, Samorajski T. Relation between the number of myelin lamellae and axon circumference of fibers of vagus and sciatic nerves of mice. J Comp Neur 1967; 130: 223-232.

Friede RL, Samorajski T. The clefts of Schmidt-Lanterman: a quantitative electron microscopic study of their structure in developing and adult sciatic nerves of the rat. Anat Rec 1969; 165: 89-101.

Gabreëls-Festen AAWM, Joosten EMG, Gabreëls FJM, Jannekens, Janssen-van Kempen TW. Early morphological features in dominantly inherited demyelinating motor and sensory neuropathy (HMSN type I). J Neurol Sci 1992; 107: 145-154.

Gabreëls-Festen AAWM, Bolhuis PA, Hoogendijk JE, Valentijn LJ, Eshuis EJ, Gabreëls, FJ. Charcot-Marie-Tooth disease type 1A: morphological phenotype of the 17p duplication versus PMP22 point mutations. Acta Neuropathol (Berl) 1995; 90: 645-649.

Gamble HJ, Eames RA. An electron microscope study of the connective tissues of human peripheral nerve. J Anat 1964; 98: 655-663.

Garven HSD, Gairns FW, Smith G. The nerve fibre populations of the nerves of the leg in chronic occlusive arterial disease in man. Scot Med J 1962; 7: 250-265.

Ghabriel MN, Allt G. The role of Schmidt-Lanterman incisures in Wallerian degeneration. I. A quantitative teased fibre study. Acta Neuropathol (Berl) 1979; 48: 83-93.

Ghabriel MN, Allt G. Schmidt-Lanterman incisures. I. A quantitatve teased fibre study of remyelinating peripheral nerve fibres. Acta Neuropathol (Berl) 1980; 52: 85-95.

Ghabriel MN, Allt G. Incisures of Schmidt-Lanterman. Progr Neurobiol 1981; 17: 25-58.

Goebel HH, Schmidt PF, Bohl J, Tettenborn B, Krämer G, Gutmann L. Polyneuropathy due to acute arsenic intoxication: biopsy studies. J Neuropathol Exp Neurol 1990; 49: 137-149.

Grage FH, Armstrong DM, Williams LR, Varon S. Morphological reponse of axotomized septal neurons to nerve growth factor. J Comp Neurol 1988; 269: 147-155.

Griffiths IR, Duncan ID. Age changes in the dorsal and ventral lumbar nerve roots of dogs. Acta Neuropathol (Berl) 1975; 32: 75-85.

Griffin JW, Stocks EA, Fahnestock K, Praagh AV, Trapp BD. Schwann cell proliferation following lysolecithin-induced demyelination. J Neurocytol 1990; 19: 367-384.

Griffin JW, Kidd G, Trapp BD. Interactions between axons and Schwann cells. In: Dyck PJ, Thomas PK, Lambert EH, Bunge RP, eds. Peripheral Neuropathy, 3rd edn. Philadelphia: W. B. Saunders, 1993; pp: 317-330.

Grutrecht JA, Dyck PJ. Quantitative teased fiber and histologic studies of human sural nerve during postnatal development. J Comp Neurol 1970; 138: 117-130.

Hahn AF, Chang Y, Webster HF. Development of myelinated nerve fibres in the sixth cranial nerve of the rat: quantitative electron microscope study. J Comp Neurol 1987; 269: 147-155.

Hall SM, Williams PL. Studies on the incisures of Schimidt and Lantermann. J Cell Sci 1970; 6: 767-792.

Hall SM, Williams PL. The distribution of electron-dense tracers in peripheral nerve fibres. J Cell Sci 1971; 8: 541-555.

Hamida MB, Letaief F, Hentati F, Hamida CB. Morphometric study of the sensory nerve in classical (or Charcot disease) and juvenile amyotrophic lateral sclerosis. J Neurol Sci 1987; 78: 313-329.

Hasan SU, Sarnat HB, Auer RN. Vagal nerve maturation in the fetal lamb: An ultrastructural and morphometric study. The Anatomical Record 1993; 237: 527-537.

Heumann R, Lindholm D, Bandtlow C, Meyer M, Radeke MJ, Misko TP, Shooter E, Thoenen H. Differential regulation of mRNA encoding nerve growth factor and its receptor in rat sciatic nerve during development, degeneration, and regeneration: Role of macrophage. Proc Natl Acad Sci U.S.A. 1987; 84: 8735-8739.

Hiscoe HB. Distribution of nodes and incisures in normal and regenerated nerve fibres. Anat Rec 1947; 99: 447- 476.

Hopkins A. The effect of acrylamide on the peripheral nervous system of the baboon. J Neurol Neurosurg Psychiatry 1970; 33: 805-816.

Hoffman PN, Griffin JW. The control of axonal caliber. In: Dyck PJ, Thomas PK, Lambert EH, Bunge RP, editors. Peripheral Neuropathy, 3rd edition. Philadelphia: WB Saunders, 1993: 389-402.

Hynes RO. Integrins: Versatility, modulation, and signaling in cell adhesion. Cell 1992; 69: 11-25.

Jacobs JM, Love S. Qualitative and quantitative morphology of human sural nerve at different ages. Brain 1985; 108: 897-924.

Jakobsen J. Axonal dwindling in early experimental diabetes. I. A study of cross-sectioned nerves. Diabetologia 1976; 12: 539-546.

Johnson EMJ, Taniuchi M, DiStefano PS. Expression and possible function of nerve growth factor receptors on Schwann cells. Trends Neurosci 1988; 11: 299-304.

Karnes J, Robb R, O'Brien PC, Lambert EH, Dyck PJ. Computerized image recognition for morphometry of nerve attribute of shape of sampled transverse sections of myelinated fibres which best estimates their average diameter. J Neurol Sci 1977; 34: 43-51.

King RHM. Diseases of peripheral nerves In: Adams JH, Graham DJ, editors. An Introduction to Neuropathology, 2nd edition. Singapore: Geoff Nuttall, 1994.

Kocen RS, Thomas PK. Peripheral nerve involvement in Fabry's disease. Arch Neurol 1970; 22: 81-88.

Krishnan N, Singer M. Penetration of peroxidase into peripheral nerve fibres. Am J Anat 1973; 136: 1-14.

Lai C, Watson JB, Bloom FE. Neural protein 1B236/myelin-associated glycoprotein (MAG) defines a subgroup of the immunoglobulin superfamily. Immunol Rev 1987; 100: 129-151.

Lampert P. Mechanism of demyelination in experimental allergic neuritis. Lab Invest 1969; 20: 127-138.

Lampert PW, Schochet SSJr. Demyelination and remyelination in lead neuropathy-electron microscopic studies. J Neuropathol Exp Neurol 1968; 27: 527-545.

Lemke G, Axel R. Isolation and sequence of a cDNA encoding the major structural protein of peripheral myelin. Cell 1985; 40: 501-508.

Letourneau PC, Shattuck TA, Roche FK, Takeichi M, Lemmon V. Nerve growth cone migration onto Schwann cells involves the calcium-dependent adhesion molecules, N-cadherin. Dev Biol 1990; 138: 430-442.

Letourneau PC, Roche FK, Shattuck TA, Lemmon V, Takeichi M. Interactions of Schwann cells with neurites and with other Schwann cells involove the calcium-dependent adhesion molecule, N-cadherin. J Neurobiol 1990; 22: 707-720.

Li H, Terenghi G, Hall SM. Effects of delayed re-innervation on the expression of c-erbB receptors by chronically denervated rat Schwann cells in vivo. Glia 1997; 20: 333-347.

Lipski J, Martin-Body RL. Morphological properties of respiratory intercostal motoneurons in cats as revealed by intracellular injection of horseradish peroxidase. J Comp Neurol 1987; 260: 423-434.

Llewelyn, J.G., Gilbey, S.G., Thomas, P.K., King, R.H.M., Muddle, J.R., and Watkins, P.J. (1991) Sural nerve morphometry in diabetic autonomic and painful sensory neuropathy, a clinical study. Brain, 114:867-892.

MacKinnon SE, Dellon AL, Hudson AR, Hunter DA. Chronic human nerve compression – a histological assessment. Neuropathol Appl Neurobiol 1986; 12: 547-565.

Marchionni MA, Goodearl ADJ, Chen MS, Bermingham-McDonogh O, Kirk C, Hendricks M, Danehy F, Misumi D, Sudhalter J, Kobayashi K, Wroblewski D, Lynch C, Baldassare M, Hiles I, Davis JB, Hsuan JJ, Totty NF, Otsu M, McBurney RN, Waterfield MD, Stroobant P, Gwynne D. Glial growth factors are alternatively spliced erbB2 ligands expressed in the nervous system. Nature 1993; 362: 312-318.

Martini R. Expression and functional roles of neural cell surface molecules and extracellular matrix components during development and regeneration of peripheral nerves. J Neurocytol 1994; 23: 1-28.

Ochs S, Brimijoin WS. Axonal transport. In: Dyck PJ, Thomas PK, Lambert EH, Bunge, RP, editors. Peripheral Neuropathy, 3rd edition. Philadelphia: WB Saunders, 1993: 331-360.

Ohnishi A, Schilling K, Brimijoin WS, Lambert EH, Fairbanks VF, Dyck PJ. Lead neuropathy. J Neuropathol Exp Neurol 1977; 36: 499-518.

Olson WH. Peripheral nerve compound action potentials and fiber diameter histograms. PhD thesis. Ann Arbor MI, University of Michigan, 1973. Cit in: Schellens RLLA, Veen BKV, Gabreëls-Festen AAWM, Notermans SLH, Hof MAV, Stegeman DS. A statistical approach to fibre diameter distribution in human sural nerve. Muscle Nerve 1993; 16: 1342-1350.

O'Neil JH, Jacobs JM, Gilliatt RW, Baba M. Changes in the compact myelin of single internodes during axonal atrophy. Acta Neuropathol (Berl) 1984; 63: 313-318.

O'Neil JH, Gilliatt RW. Adaptation of the myelin sheath during axonal atrophy. Acta Neuropathol (Berl) 1987; 74: 62-66.

O'Sullivan DJ, Swallow M. The fiber size and content of the radial and sural nerves. J Neurol Neurosurg Psychiat 1968; 31: 464-470.

Ouvrier RA, McLeod JG, Pollard JD. Peripheral neuropathy in childhood. New York: Raven Press, 1990: 13-20.

Pareek S, Suter U, Snipes GJ, Welcher AA, Shoote EM, Murphy RA. Detection and processing of peripheral myelin protein PMP22 in cultured Schwann cells. J Biol Chem 1993; 268: 10372-10379

Pellegrino RG, Politis MJ, Ritshie JM, Spencer PS. Events in degenerating cat peripheral nerve: Induction of Schwann cell S phase and its relation to nerve fibre degeneration. J Neurocytol 1986; 15: 17-28.

Pellegrino RG, Spencer PS. Schwann cell mitosis in response to regenerating peripheral axons in vivo. Brain Res 1985; 341:16-25.

Pollard JD, King RHM, Thomas PK. Recurrent experimental allergic neuritis. An electron microscope study. J Neurol Sci 1975; 24: 365-383.

Pollock M, Nukada H, Taylor P, Donaldson I, Carroll G. Comparison between fascicular and whole sural nerve biopsy. Ann Neurol 1983; 13: 65-68.

Prineas JW, McLeod JG. Chronic relapsing polyneuritis. J Neurol Sci 1976; 27: 427-458.

Prineas JW. Acute idiopathic polyneuritis. An electron microscope study. Lab Invest 1972; 26: 133-147.

Poduslo JF. Regulation of Schwann cell expression of myelin-specific glycoconjugate. Adv Biosci 1986; 61: 311-321.

Ranvier L. Traité technique d'Histologie 1875. Savy: Paris. Cit. In: Behse F. Morphometric studies on the human sural nerve. Acta Neurol Scand 1990; 82(suppl 132): 4-38.

Reichardt LF. Extracellular matrix molecules and their receptors: functions on neural development. Annu Rev Neurosci 1991; 14: 531-70.

Ross MH, Romrell LT, Kaye GI. Histology: a text book, 3rd editors. Baltimore, Williams & Wilkins, 1995.

Roytta M, Salonen V. Long-term endoneurial changes after nerve transection. Acta Neuropathol 1988; 76: 35-45.

Russell JW, Karnes JL, Dyck PJ. Sural nerve myelinated fibre density differences associated with meaningful changes in clinical and electrophysiologic measurements. J Neurol Sci 1996; 135: 114-117.

Rutishauser U, Jessell TM. Cell adhesion molecules in vertebrate neural development. Physiol Rev 1988; 68: 819-857.

Sadoul R, Fahrig T, Bartsch U, Schachner M. Binding properties of liposomes containing the myelin-axxociated glyprotein MAG to neural cell cultures. J Neurosci Res 1990; 25: 1-13.

Said G, Slama G, Salva J. Progressive centripetal degeneration of axons in small fibre diabetic polyneuropathy. Brain 1983; 106: 791-807.

Salzer JL. Mechanisms of adhesion between axons and glial cells. In: Waxman SG, Kocsis JD, Stys PK, editors. The axon. Structure, function and pathophysiology. Oxford University Press, 1995: 164-184.

Saxod R, Torch S, Vila A, Laurent A, Stoebner P. The density of myelinated fibres is related to the fascicle diameter in human superficial peroneal nerve. J Neurol Sci 1985; 71: 49-64.

Schaumburg H, Kaplan J, Winderbank A, Vick N, Rasmus S, Pleasure D, Brown MJ. Sensory neuropathy from pyridoxine abuse. A new megavitamin syndrome, N Engl J Med 1983; 309: 445-448.

Schellens RLLA, Veen BKV, Gabreëls-Festen, AAWM, Notermans SLH, Hof MAV, Stegeman DS. A statistical approach to fibre diameter distribution in human sural nerve. Muscle Nerve 1993; 16:1342-1350.

Schmitt FO, Bear RS. The optical properties of vertebrate nerve axons as related to fibre size. J Cell Comp Physiol 1937; 9:261-273. Cit. In: Thomas PK, Landon DN, King RHM. Diseases of the peripheral nerves. In: Graham DI, Lantos PL, editors. Greenfield's Neuropathology, 6th edition. London: Edward Arnold, 1997: 367-487.

Schoonhoven R, Schellens RLLA, Stegeman DF, Gabreëls-Festen AAWM. Sensory potentials and sural nerve biopsy: A model evaluation. Muscle Nerve 1987; 10: 246-262.

Schröder JM. Altered ratio between axon diameter and myelin sheath thickness in regemerated nerve fibres. Brain Res 1972; 45: 49-65.

Schröder JM, Bohl J, Brodda K. Changes of the ratio between myelin thickness and axon diameter in the human developing sural nerve. Acta Neuropathol (Berl) 1978; 43:169-178.

Service FJ, Rizza RA, Daube JR. Improved nerve conduction and vibration sensation in diambetic neuropathy. Diabetologia 1985; 28: 722-727.

Shield LK, King RHM, Thomas PK. A morphometric study of human fetal sural nerve. Acta Neuropathol (Berl) 1986; 70: 60-70.

Siperstein MN, Norton W, Unger RH. Muscle capillary basement membrane. Trans Assoc Am Physicians 1966; 79: 330-347.

Siperstein MN, Unger RH, Madison LL. Studies of muscle capillary basement membrane. J Clin Invest 1968; 47: 1973-1999.

Smith KJ, Blakemore WF, Murray JA, Patterson RC. Internodal myelin volume and axon surface area. A relationship determining myelin sheath thickness. J Neurol Sci 1982; 55: 231-246.

Spencer PS, Schaumburg HH. Ultrastructural studies of the dying-back process. III. The evolution of experimental peripheral giant axonal degeneration. J Neuropathol Exp Neurol 1977; 36: 276-299.

Sugimura K, Dyck PJ. Multifocal loss in proximal sciatic nerve in symmetric distal neuropathy. J Neurol Sci 1982; 53: 501-509.

Swallow M. Fibre size and content of the anterior tibial nerve of the foot. J Neurol Neurosurg Psychiat 1966; 29: 205-213

Tang DB, Ebbesson SOE. A comparison of a systematic sampling method with complete random sampling for estimating total numbers of nerve fibers. Anat Rec 1972; 174: 495-502.

Taniuchi M, Clark HB, Schweitzer JB, Johnson EM. Expression of nerve growth factor receptors by Schwann cells of axotomized peripheral nerve: Ultrastructural location, supression by axonal contact, and binding properties. J Neurosci 1988; 8: 664-681.

Timperley WR, Ward JD, Preston FE, Duckworth T, O'Malley BC. Clinical and histological studies in diabetes neuropathy. Diabetologia 1976; 12: 237-243.

Tohgi H, Tsukagoshi H, Toyokura Y. Quantitative changes in sural nerves in various neurological diseases. Acta Neuropath (Berl) 1977a; 38: 95-101.

Tohgi H, Tsukagoshi H, Toyokura Y. Quantitative changes with age in normal sural nerves, Acta Neuropath (Berl) 1977b; 38: 213-220.

Thomas PK. The connective tissue of peripheral nerve: an electron microscope study. J Anat 1963; 97: 35-44.

Thomas PK, Jones DG. The cellular response to nerve injury. II. Regeneration of the perineurium after nerve section. J Anat 1967; 101: 45-55.

Thomas PK. The quantitation of nerve biopsy findings. J Neurol Sci 1970a; 11: 285-295.

Thomas PK. The cellular response to nerve injury: 3. The effect of repeated crush injuries. J Anat 1970b; 106: 463-470.

Thomas PK, Hollinrake K, Lascelles RG, O'Sullivan DJ, Baillod RA, Moorhead JF, Mackenzie JC. The polyneuropathy of chronic renal failure. Brain 1971; 94: 761-780.

Thomas PK, Walker RWH, Rudge P, Morgan-Hughes JA, King RHM, Jacobs JM, Mills KR, Ormerod IEC, Murray NMF, McDonald WI. Chronic demyelinating peripheral neuropathy associated with multifocal central nervous system demyelination. Brain 1987; 110: 53-76.

Thomas PK, Landon DN, King RHM. Diseases of the peripheral nerves. In: Adams JH, Duchen LW, editors. Greenfield's Neuropathology, 5th edition. London: Edward Arnold, 1992: 1116-1245.

Thomas PK, Berthold CH, Ochoa J. Microscopic anatomy of peripheral nervous system. In: Dyck PJ, Thomas PK, Lambert EH, Bunge RP, editors. Peripheral Neuropathy, 3rd edition. Philadelphia: WB Saunders, 1993: 28-91.

Thomas PK, Landon DN, King RHM. Diseases of the peripheral nerves. In: Graham DI, Lantos PL, editors. Greenfield's Neuropathology, 6th edition. London: Edward Arnold, 1997: 367-487.

Tomanek RJ, Tipton CM. Influence of exercise and tenotomy on the morphology of a muscle nerve. Anat Rec 1967; 159: 105-114.

Torch S, Stoebner P, Usson Y, D'Aubigny GD, Saxod R. There is no simple adequate sampling scheme for estimating the myelinated fibre size distribution in human peripheral nerve: a statistical ultrastructural study. J Neurosci Methods 1989a; 27: 149-164.

Torch S, Usson Y, Saxod R. Automated morphometric study of human peripheral nerves by image analysis. Path Res Pract 1989b; 185: 567-571.

Trapp BD. Distribution of the myelin-associated glycoprotein and P_0 protein during myelin compaction in quaking mouse peripheral nerve. J Cell Biol 1988; 107: 675-685.

Trapp BD, Andrews SB, Wong A, O'Connell M, Griffin JW. Co-localization of the myelin-associated glycoprotein and the microfilament components, F-actin and spectrin, in Schwann cells of myelinated nerve fibres. J Neurocytol 1989; 18: 47-60.

Trapp BD, Quarles RH, Suzuki K. Immunocytochemical studies of quaking mice support a role for the myelin associated glycoprotein in forming and maintaining the periaxonal

space and periaxonal cytoplasmic collar of myelinating Schwann cells. J Cell Biol 1984; 99: 594-606.

Trapp BD, Quarles RH. Presence of the myelin-associated glycoprotein correlates with alterations in the periodicity of peripheral myelin. J Cell Biol 1982; 92: 877-882.

Usson Y, Torch S, Drout d'Aubigny G. A method for automatic classification of large and small myelinated fibre populations in peripheral nerves. J Neurosci Methods 1987; 20: 237-245.

Vita G, SantoroM, Trombetta G, Leonardi L, Messina CA. A computer-assisted automatic method for myelinated nerve fibre morphometry. Acta Neurol Scand 1992; 85: 18-22.

Vital A, Vital C, Brechenmacher C, Serise JM, Callen S, Nicolau H, Videau J. Qauntitative, histological and ultrastructural studies of peripheral nerve in arteriosclerotic non-diabetic patients. Clin Neuropathol 1986; 5: 224-229.

Vital A, Vital C, Rigal B, Decamps A, Emeriau JP, Galley P. Morphological study of the aging human peripheral nerve. Clin Neuropathol 1990; 9(1): 10-15.

Voyvodic JT. Target size regulates caliber and myelination of sympathetic axons. Nature 1989; 342: 430-433.

Walsh JC. The peripheral nervous system in lymphoma and multiple myeloloma, M.D. Thesis, University of Sydney, 1971. Cit in: Prineas JW, McLeod JG. Chronic relapsing polyneuritis. J Neurol Sci 1976; 27: 427-458.

Waxman SG. Structure and function of the myelinated fiber. In: Vinken PJ, Bruyn GW, Klawans HL, Editors. Handbook of Clinical Neurology, 1985; 47: 1-28.

Webster HE, Schröder JM, Asbury AK, Adams RD. The role of Schwann cells in the formation of onion bulbs found in chronic neuropathies. J Neuropathol Exp Neurol 1967; 26: 276-299.

Weinberg HJ, Spencer PS. Studies on the control of myelinogenesis. II. Evidence for neuronal regulation of myelin production. Brain Res 1976; 113: 363-378.

Weinberg HJ, Spencer PS. The fate of Schwann cells isolated from axonal contact. J Neurocytol 1978; 7: 555-569.

Weller RO, Cervós-Navarro J. Pathology of peripheral nerves. Butterworths, 1978: 30-60.

Williams AF, Barclay AN. the immunoglobulin superfamily—domains for cell surface recognition. Ann Rev Immunol 1988; 6: 381-405.

Williams E, Timperley WR, Ward JD. Electron microscopic studies of vessels in diabetic peripheral neuropathy. Clin Pathol 1980; 33: 462-470.

Williams PL, Kashef R. Asymmetry of the node of Ranvier. J Cell Sci 1968; 3: 341

Williams PL, Wendell-Smith CP. Some additional parametric variations between peripheral nerve fibre populations. J Anat 1971; 109: 505-526.

Windebank AJ, Low PA, Blexrud MD, Schmelzer JD, Schaumberg HH. Pyridoxine neuropathy in rats: specific degeneration of sensory axons. Neurosurg 1985; 35: 1617-1622.

Windebank AJ, Blexrud MD, Dyck PJ, Duabe JR, Karnes JL. The syndrome of acute sensory neuropathy: clinical features and electrophysiologic and pathologic changes. Neurology 1990; 40: 584-591.

Wisniewski H, Terry RD, Whitaker JN. Landry-Guillain-Barré syndrome. A primary demyelinating disease. Arch Neurol 1969; 21: 269-276.

Wood PM, Bunge RP. Evidence that sensory axons are mitogenic for Schwann cells. Nature 1975; 256: 662-664.

Xu Y, Siadky JT, Brown MJ. Dose-dependent expression of neuronopathy after experimental pyridoxine intoxication. Neurology 1989; 39:1077-1083.

Yee WC, Hahn AF, Gilbert JJ. Adult onset scapuloperoneal myopathy: diagnostic value of nerve morphometry and multiple muscle biopsies. J Neurol Neurosurg Psychiatr 1988; 51: 808-813.

Yoshikawa H, Dyck PJ, Poduslo JF, Giannini C. Polyglucosan body axonal enlargement increases myelin sheath spiral length but not lamellar number. J Neurol Sci 1990; 98: 107-117.

Younger DS, Rosoklija G, Hays AP, Trojaborg W, Latov N. Diabetic peripheral neuropathy: a clinicopathologic and immunohistochemical analysis of sural nerve biopsies. Muscle Nerve 1996; 19: 722-727.

Zimmerman IR, Karnes JL, O'Brien PC, Dyck PJ. Imaging system for nerve and fibre tract morphometry: components, approaches, performance, and results. J Neuropathol Exp Neurol 1980; 39:409-419.

Appendix A
Illustrations of Histological Features

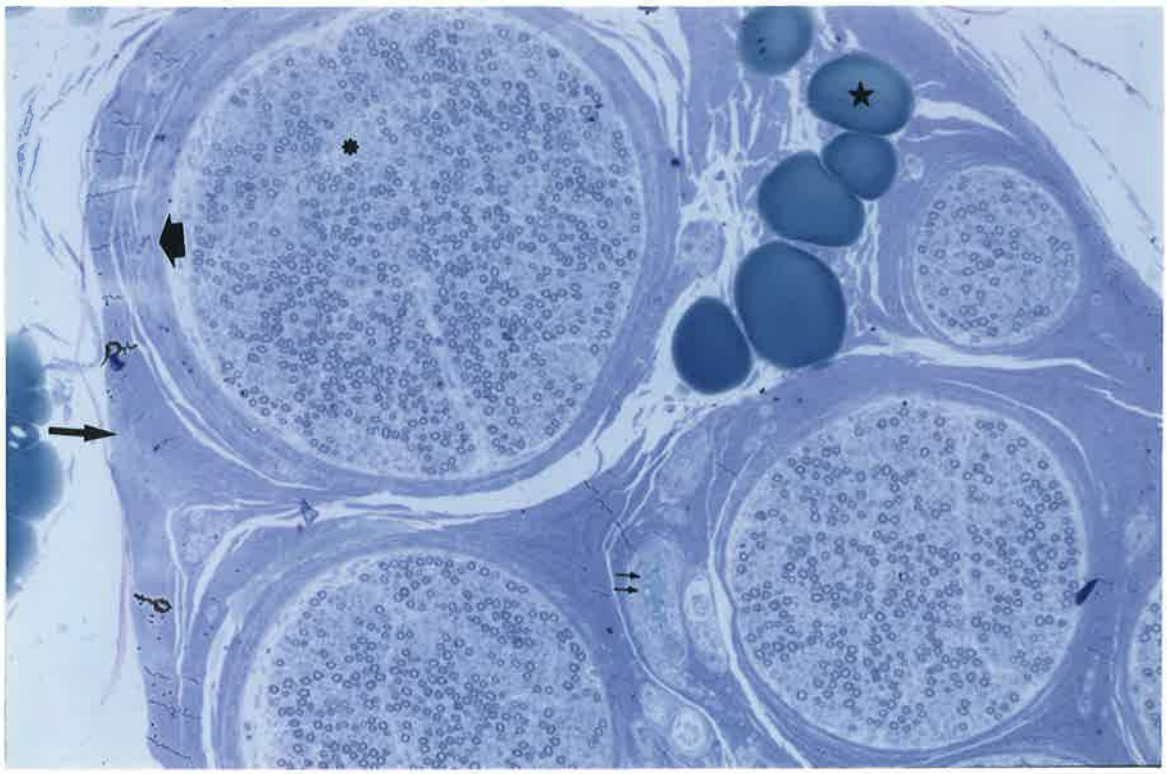

Figure 1: Upper part shows part of the cross section of a control sural nerve (nerve No.2, toluidine blue stained, ×100). Epineurium (arrow), perineurium (arrowhead), endoneurium (asterisk), blood vessels (double arrow), adipose (star) and 3 complete fascicles (1st, largest; 2nd, middle; and 7th, smallest) in this picture. On visual inspection, the spatial distribution of myelinated fibres in each fascicle is heterogeneous. Myelinated fibre density is 5785/mm^2 for the whole nerve, 6386/mm^2 for the 1st fascicle, 5130/mm^2 for the 2nd fascicle and 5210/mm^2 for 7th fascicle(see p84). Lower part shows high magnification (×200) of the 1st fascicle. It is obvious that the spatial distribution of myelinated fibres is non-uniform in the fascicle.

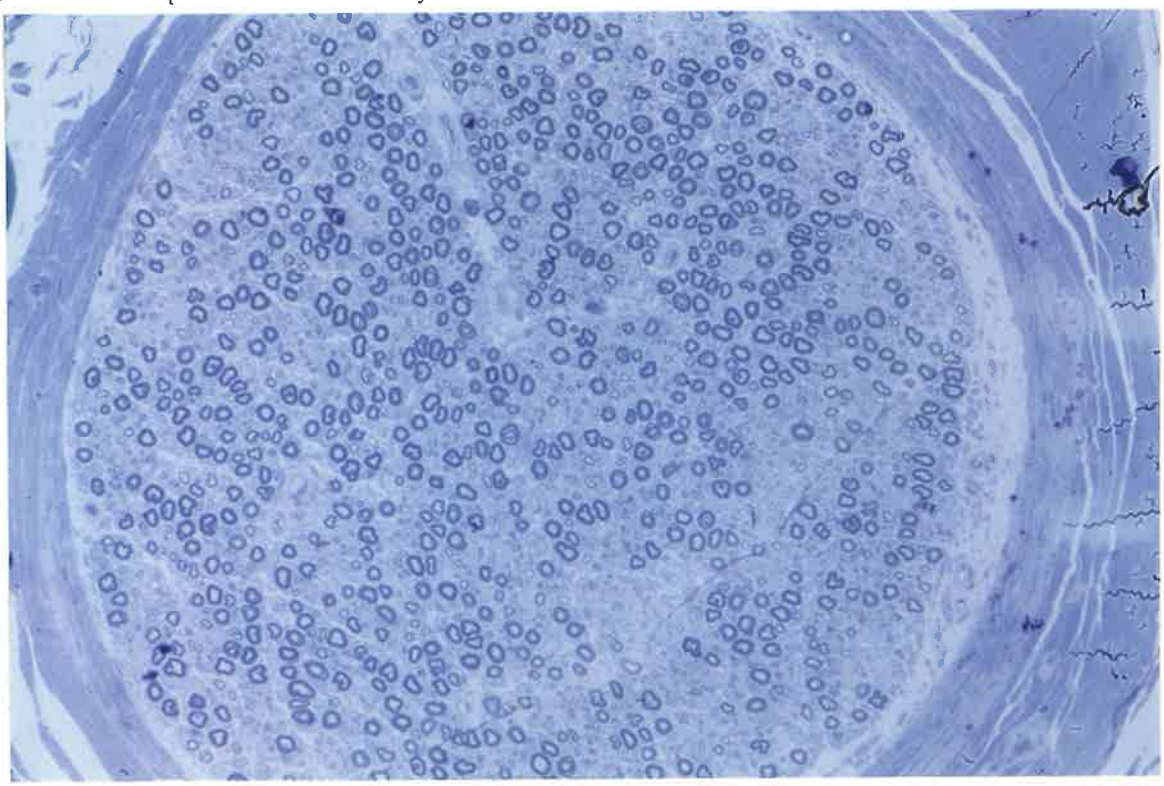

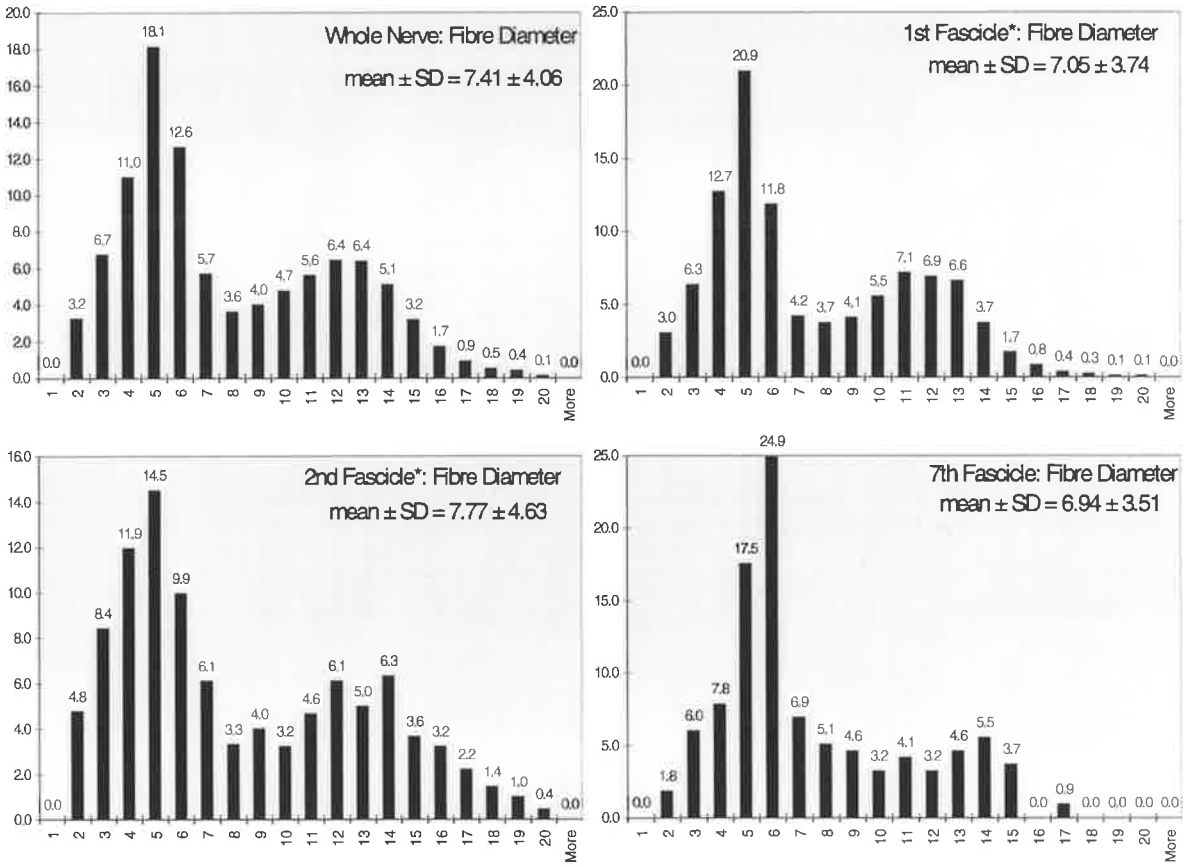

Figure 2: Fibre diameter frequency distributions of the whole myelinated fibre population in nerve No.2 and in the 1st, 2nd and 7th fascicle (Figure 1). Fibre diameter (micron) is displayed on the abscissa, and the percentage of the total myelinated fibre count is displayed on the ordinate. Fibre diameter mean values and frequency distributions in the three fascicles are different from that of the whole nerve.

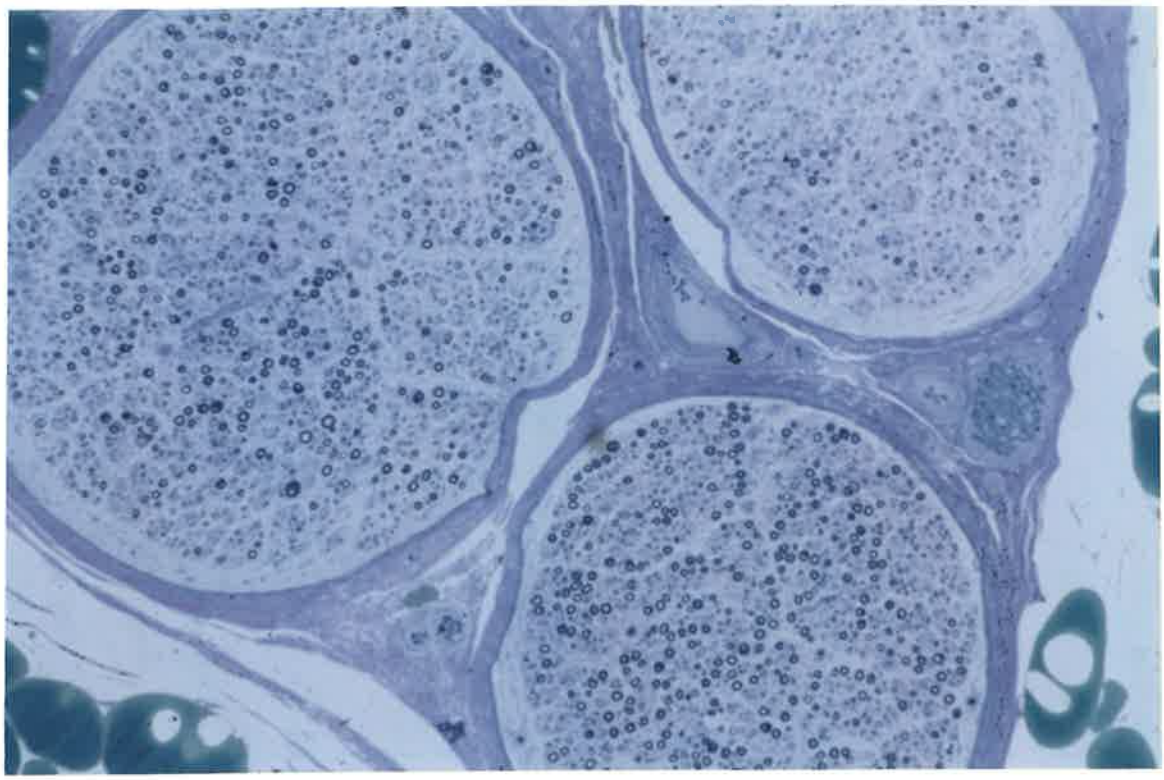

Figure 3: Upper part shows three fascicles (6th, upper right; 7th lower right; and 8th, left) in nerve No.7 (toluidine blue, ×100). Loss of myelinated fibres is uneven within and between fascicles. Myelinated fibre density is 3006/mm^2 for the whole nerve, 2084/mm^2 for the 6th fascicle, 3717/mm^2 for the 7th fascicle and 2590/mm^2 for 8th fascicle (see p87). Lower part shows the fibre diameter (Ds) frequency distribution in the whole nerve and the three fascicles. Ds is displayed on the abscissa, and percentage of total myelinated fibre count is displayed on the ordinate. It is obvious that the mean value of Ds and the graphic curve of Ds frequency distribution of the 6th fascicle are different to those of the whole nerve. The mean value of Ds of the 7th fascicle is similar to that of the whole nerve, but Ds frequency distribution is obviously bimodal in the 7th fascicle and looks like unimodal in the whole nerve. Kolmogorov-Smirnov goodness-of-fit test proved Ds frequency distributions are significantly different in the whole nerve and the 7th fascicle. The mean value and the frequency distribution of Ds in the 8th fascicle are similar to those of the whole nerve.

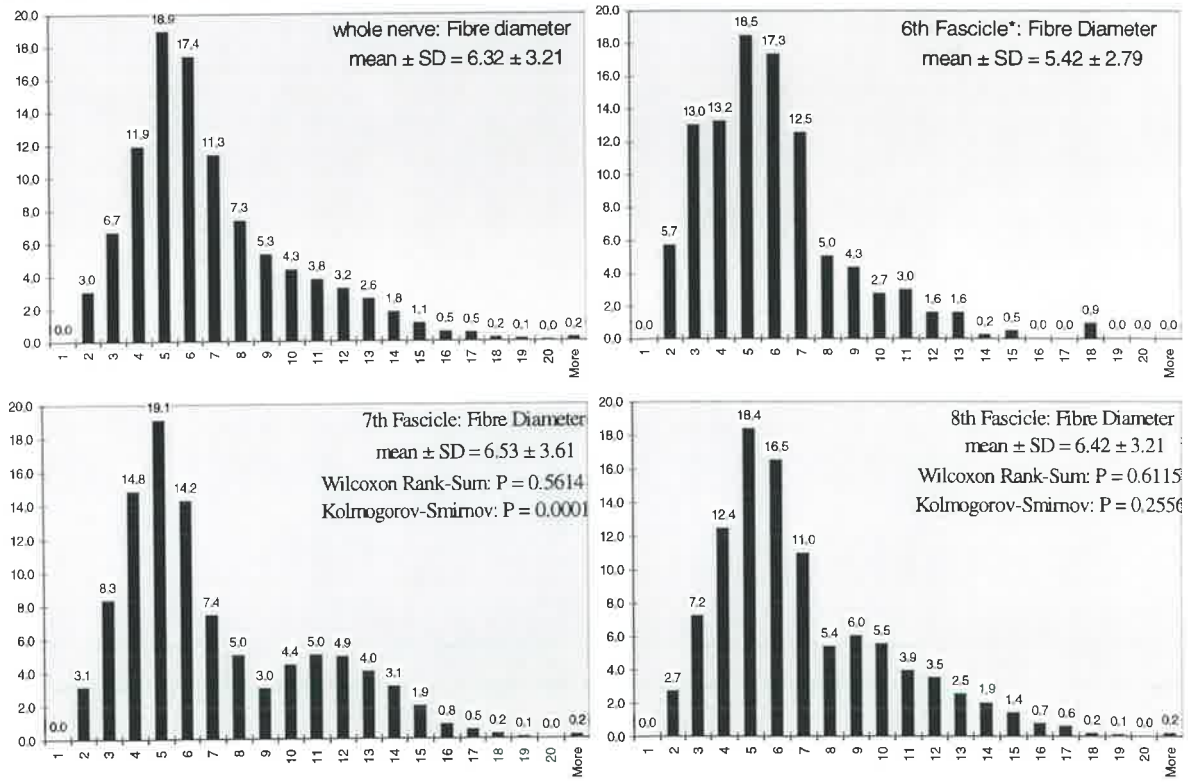

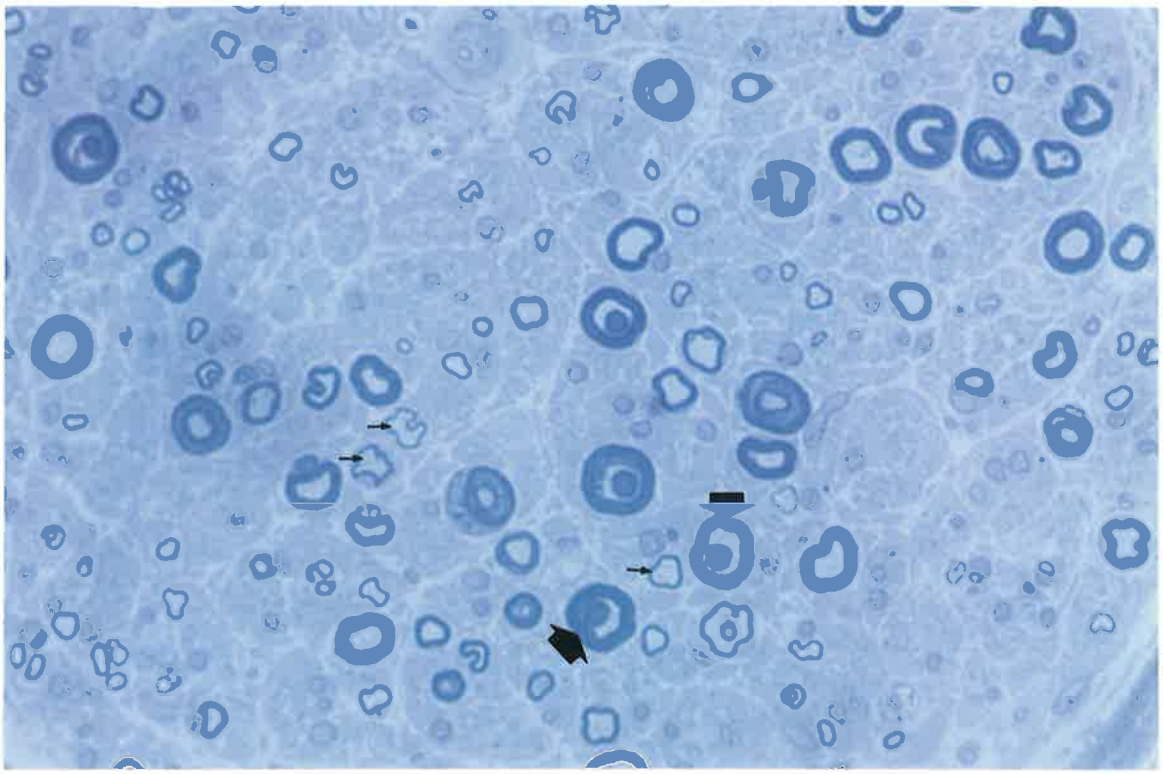

Figure 4: Pathological changes in a sural nerve (No. 17, toluidine blue stained, ×400). Disproportionately thin myelin sheaths for axonal diameter indicative of remyelination (arrow). Fibres showing myelin infolding are also present (arrowhead).

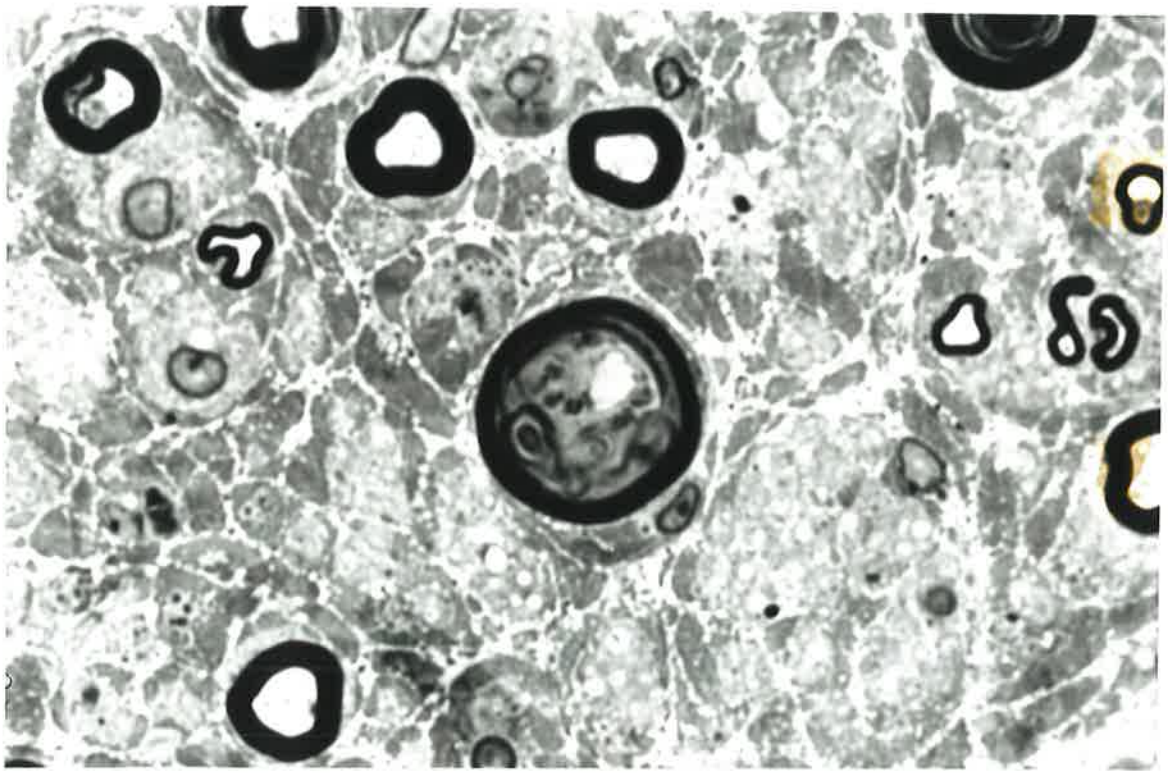

Figure 5: Axonal degeneration (center, nerve No.18, toluidine blue stained, ×1000)

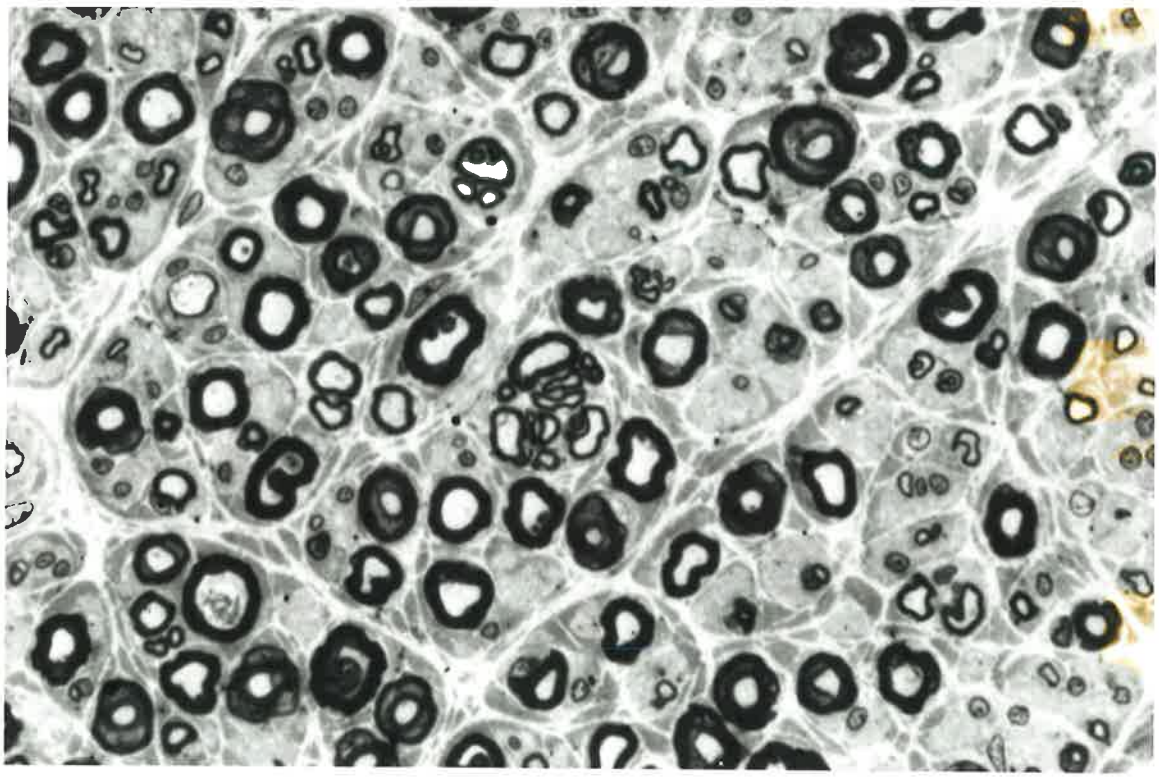

Figure 6: Cluster of regenerating fibres (in the center, toluidine blue stained, ×400)

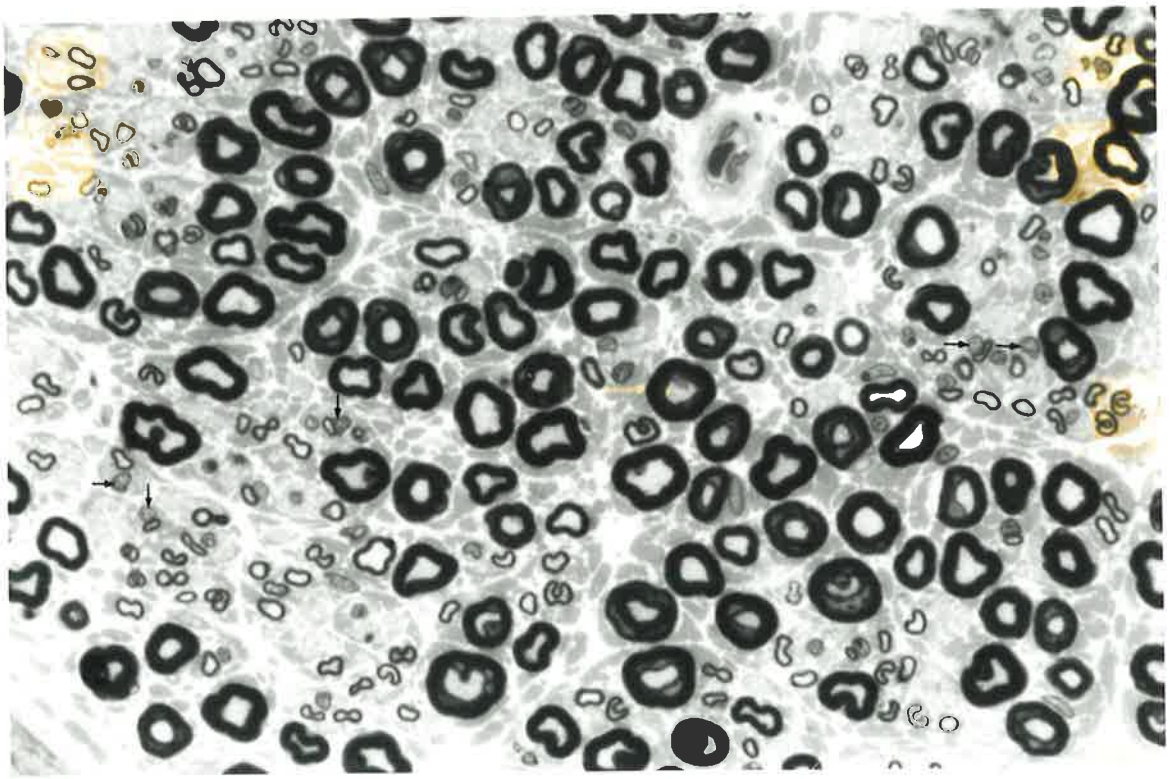

Figure 7: Comparison of toluidine blue and aqueous osmium tetroxide stained sections (×400). Upper part shows toluidine blue stained cross section. Schwann cell nuclei (arrow) are obvious and may be recognized as myelinated fibres or part of a fibre when quantitating myelinated fibres on such sections using image analysis system. Lower part shows the aqueous osmium tetroxide stained section. Only myelin sheaths are clear here.

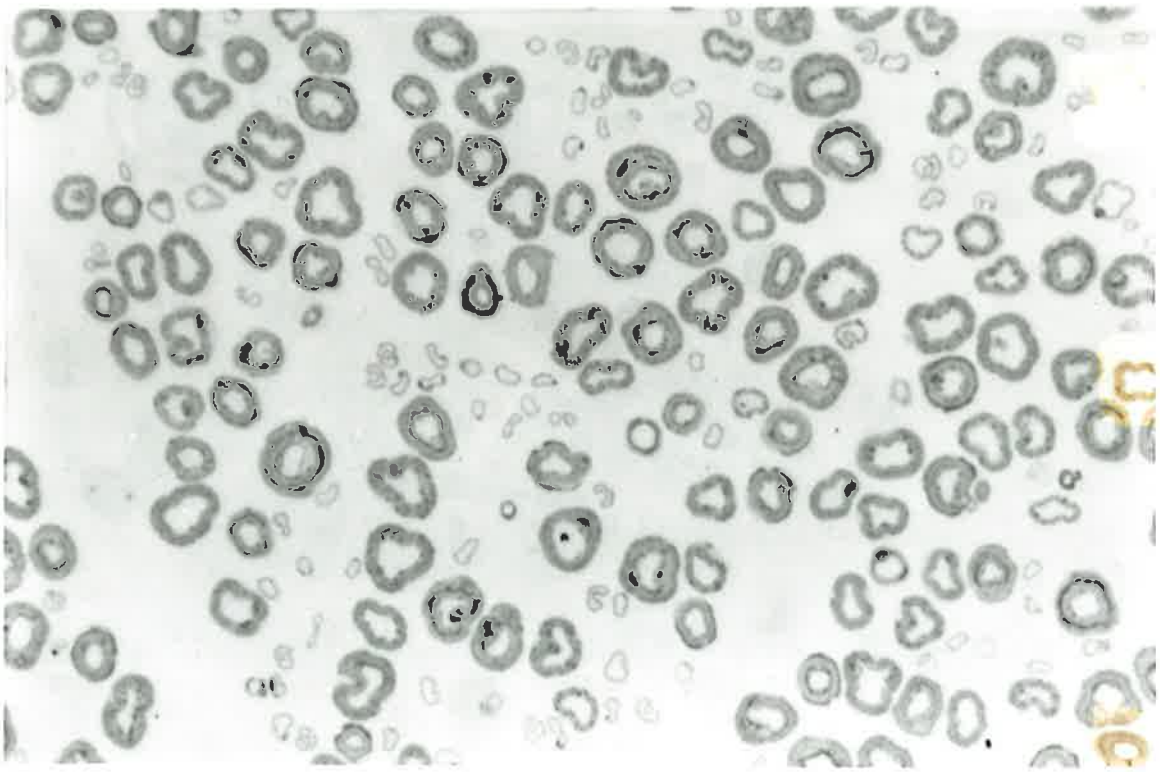

Appendix B

Module for extracting data from every nth field to form systematic samples and for calculating fibre diameter, axonal diameter and the number of myelinated fibres per measuring frame

```
Sub sample()

For var1 = 2 To 10
row1 = 1
row2 = 1
counter = 1
Sheets.Add after:=Sheets("Sheet1")
ActiveSheet.Name = "Every " + var1
var2 = ActiveSheet.Name
Cells(1, 1).Select
Sheets("Sheet1").Select
Columns("c").Find("2").Select
ActiveCell.Offset(0, -1).Select
Do While ActiveCell <> Empty
    Do Until ActiveCell.Value <> ActiveCell.Offset(1, 0) _
  Or ActiveCell.Value = Empty
    row1 = ActiveCell.Row
    Do While ActiveCell.Offset(0, 1) = ActiveCell.Offset(1, 1)
    ActiveCell.Offset(1, 0).Select
    Loop
    row2 = ActiveCell.Row
  Range(Cells(row1, 1), Cells(row2, 7)).Select
  Selection.Copy
  Sheets(var2).Activate
  Cells(counter, 1).Select
  ActiveSheet.Paste
  counter = counter + ((row2 + 1) - row1)
  Sheets("Sheet1").Select
  Cells(row2, 2).Select
```

```
    var3 = ActiveCell.Offset(0, 1)
      Do Until ActiveCell.Offset(0, 1) = var3 + var1 _
      Or ActiveCell.Offset(0, 1) < var3
      If ActiveCell.Value = Empty Then Exit Do
      ActiveCell.Offset(1, 0).Select
      Loop
      Do While ActiveCell.Offset(0, 1) = "1"
      ActiveCell.Offset(1, 0).Select
      Loop
    Loop
Loop
Next var1

End Sub

Sub analyse()

    Cells(1, 1).Select
    Rows(1).Insert
    Cells(1, 1).Select
    ActiveCell.Value = "Filename"
    ActiveCell.Offset(0, 1) = "Fascicle"
    ActiveCell.Offset(0, 2) = "Field"
    ActiveCell.Offset(0, 3) = "Area"
    ActiveCell.Offset(0, 4) = "Length"
    ActiveCell.Offset(0, 5) = "Breadth"
    ActiveCell.Offset(0, 6) = "Perimeter"
    ActiveCell.Offset(0, 7) = "Fibre Diameter"
    ActiveCell.Offset(0, 8) = "Axon Diameter"
    Cells(2, 8).Select
    Do Until ActiveCell.Offset(0, -1) = Empty
    ActiveCell.Formula = 0.11 * (((0.5 * ActiveCell.Offset(0, -1)) + _
    (2 * 3.1416 * ActiveCell.Offset(0, -4) / ActiveCell.Offset(0, -1))) / 3.1416)
    ActiveCell.Offset(1, 0).Select
    Loop
```

```
Cells(2, 9).Select
Do Until ActiveCell.Offset(0, -2) = Empty
ActiveCell.Formula = 0.11 * (((0.5 * ActiveCell.Offset(0, -2)) - _
(2 * 3.1416 * ActiveCell.Offset(0, -5) / ActiveCell.Offset(0, -2))) / 3.1416)
ActiveCell.Offset(1, 0).Select
Loop
Cells(2, 10).Select
Cells(1, 10).Value = "Case"
Cells(1, 11).Value = ActiveCell.Offset(0, -9)
Cells(2, 10).Value = "Fascicles"
Columns("b").Find(Empty).Select
var1 = ActiveCell.Offset(-1, 0)
Cells(2, 11).Value = var1
Cells(1, 12).Value = "Fascicle"
Cells(1, 13).Value = "Field"
Cells(1, 14).Value = "Fibres in Field"
Cells(1, 15).Value = "Myelin in Field"
Cells(2, 3).Select
Do While ActiveCell.Offset(0, -1) <> Empty
field_num = 1
myelin = 0
Do While ActiveCell.Value = ActiveCell.Offset(1, 0) _
And ActiveCell.Offset(0, -1) = ActiveCell.Offset(1, -1)
field_num = field_num + 1
myelin = myelin + ActiveCell.Offset(0, 1) * (0.11 * 0.11)
ActiveCell.Offset(1, 0).Select

Loop
rownum = ActiveCell.Row
Range(Cells(rownum, 2), Cells(rownum, 3)).Copy
Columns(12).Find(Empty).Select
ActiveSheet.Paste
ActiveCell.Offset(0, 2).Value = field_num
ActiveCell.Offset(0, 3).Value = myelin
Cells(rownum + 1, 3).Select
```

```
    Loop
    Cells(1, 1).Select
    Exit Sub
    For i = 1 To 20
    Cells(i, 10).Select
    ActiveCell.FormulaR1C1 = i
    Next i
    Application.ExecuteExcel4Macro String:= _
    "HISTOGRAM([nerve.xls]!C8,  [nerve.xls]!R1C11,[nerve.xls]!R1C10:R20C10,
FALSE,  FALSE,  FALSE,  TRUE)"
    Stop
    Application.ExecuteExcel4Macro String:= _
       "HISTOGRAM([nerve.xls]Sheet1!C9,  [nerve.xls]Sheet1!R1C13,
[nerve.xls]Sheet1!R1C10:R20C10,  FALSE,  FALSE,  FALSE,  TRUE)"
    Range("K1:L22").Select
    Charts.Add
    ActiveSheet.Name = var1 + "(Fibre)"
    ActiveChart.ChartWizard Source:=Sheets(var1).Range("K1:L22"), _
       Gallery:=xlColumn, Format:=1, PlotBy:=xlColumns, _
       CategoryLabels:=1, SeriesLabels:=1, HasLegend:=0, Title:="Fibre Diameter"
    Sheets("Sheet1").Select
    Range("M1:N22").Select
    Charts.Add
    ActiveSheet.Name = var1 + "(Axon)"
    ActiveChart.ChartWizard Source:=Sheets(var1).Range("M1:N22"), _
       Gallery:=xlColumn, Format:=1, PlotBy:=xlColumns, _
       CategoryLabels:=1, SeriesLabels:=1, HasLegend:=0, Title:="Axon Diameter"


End Sub
```

Appendix C

Intra- and inter- observer variation: The following table and histograms illustrate the results obtained by the author from measurements on two separate occasions of the myelinated fibre content within the first fascicle of nerve No.2. A further series of measurements were conducted by another observer (3rd measurement) demonstrating essentially the same result, and therefore low inter-observer variability. Comparisons between the mean fibre density (MFD), the numbers of MF in each measuring frame, and fibre and axonal diameter were undertaken using the Wilcoxon Rank-Sum test for the mean sample values and the Kolmogorov-Smirnov goodness-of-fit test for the frequency distribution of fibres. Three way analysis of variance (ANOVA) compared the MFD, Ds and Da of the first and second measurements by the author and the third measurement by another observer. There is no significant difference among the results of the three measurements.

Table: TFA, NMF, MFD, Ds and Da for the 1st fascicle of nerve No.2. Two consecutive measurements by the author and a third by another observer with comparisons of inter and intra observer variability are shown.

Data	TFA(mm^2)	NMF	MFD(/mm^2)	Ds(μm)	Da(μm)
1st measurement	0.3112	1987	6386±1942	7.05±3.74	4.92±2.43
2nd measurement	0.3087	1923	6229±1901	7.02±3.80	5.02±2.56
*Wilcoxon Rank-Sum test			0.3996	0.6618	0.2578
*Kolmogorov-Smirnov goodness-of-fit test			0.7965	0.3539	0.2919
**3rd measurement	0.3087	1920	6220±2014	6.98±3.80	5.02±2.59
*Wilcoxon Rank-Sum test			0.3073	0.4345	0.3898
*Kolmogorov-Smirnov goodness-of-fit test			0.6942	0.7383	0.3259
ANOVA			0.7487	0.8620	0.3284

TFA: transverse fascicular area

NMF: number of myelinated fibres

MFD: myelinated fibre density

Ds: fibre diameter

Da: axonal diameter

* compared to the results of the 1st measurement

** another observer

Figure: Histograms show frequency distributions of Ds and Da. Ds and Da are displayed on the abscissa, and the percentage of the total fibre count is displayed on the ordinate.

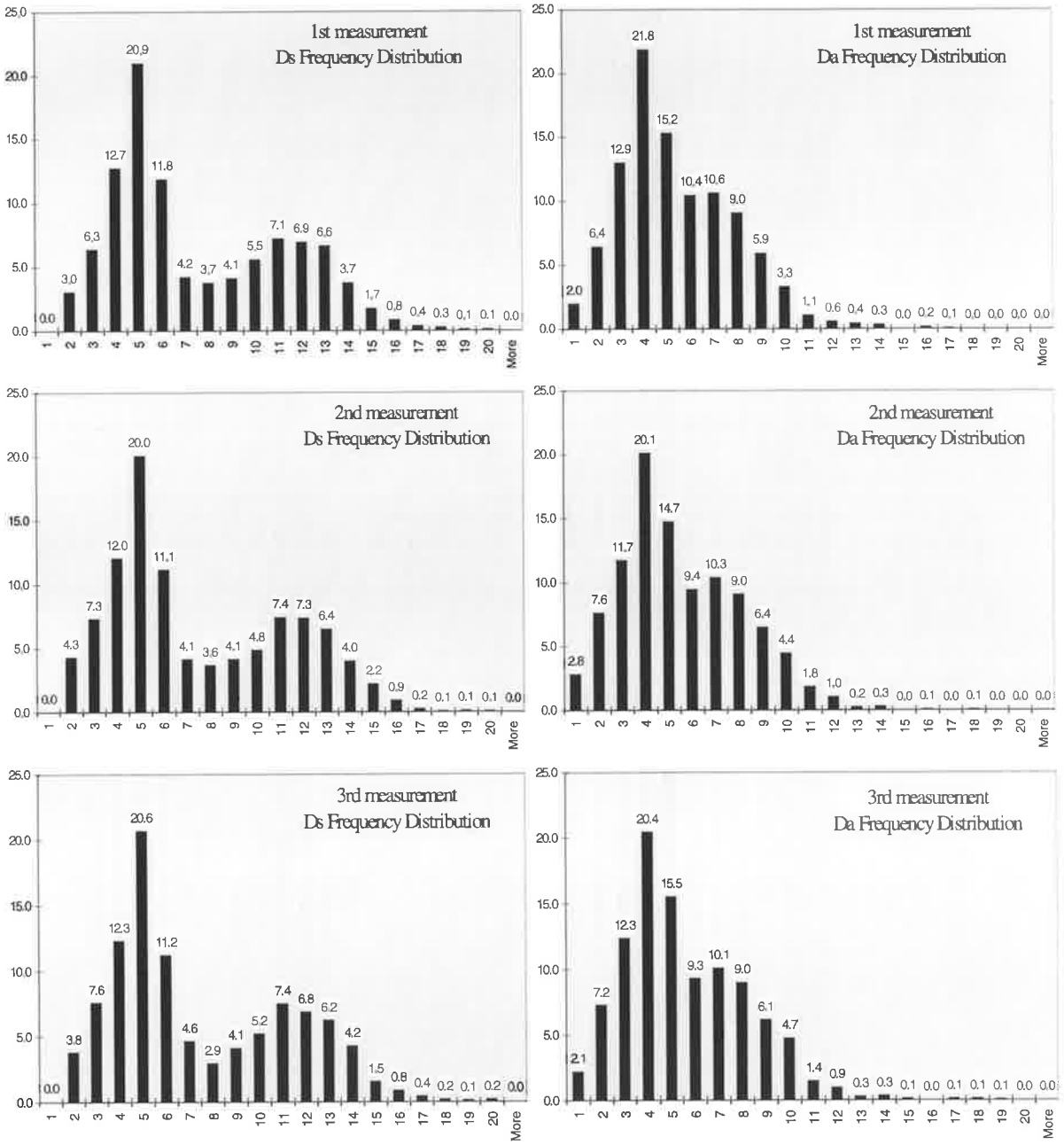

ADDENDUM

Page	line	
6	12	"21 weeks" should be "15-21 weeks"
10	2	"conventiona" should be "convention"
	11	"daimeter" should be "diameter"
15	4	"arteries veins" should be "arteries and veins"
15	20	"in to" should be "into"
27	22	"at 15-16 weeks" should be "at 15-21 weeks"
31	2	"lower peakupper peak" should be "lower peak upper peak"
37	14	"In the development" should be "In development"
41	10	"many" should be "many pixels."
45		The line between line 12 and 13 should be between line 13 and 14.
51		"following legionella pneumonia" should be "sensorimotor neuropathy post Legionella pneumonia"
53	6	"23%demyel." should be "23% demyel."
57	10	"On" should be "One"
98	11	"*enery 2nd*" should be "*every 2nd*"
130	24	"cell" should be "Cell"
133	13	"merve" should be "nerve"
	30	"dimentions" should be "dimensions"
136	18	"involove" should be "involve"
139	15	"myelin-axxociated" should be "myelin-associated"
141		Thomas references should been placed after Taniuchi et al. in page 140.

Wilcoxon Rank-Sum test compares the medians, not mean values, between samples.